

Joao Felix Nolasco, José Antonio Jardini,  
and Elilson Ribeiro

## Contents

### Section 1: Electric Parameters of Overhead AC Transmission Lines

4.1	Electrical Characteristics.....	48
4.1.1	Introduction .....	48
4.1.2	Resistance .....	49
4.1.3	Inductance .....	49
4.1.4	Capacitance .....	50
4.1.5	Negative and Zero Sequence Parameters .....	50
4.1.6	Representation of Lines.....	51
4.1.7	General Overhead Transmission Line Models .....	55
4.2	Surge Impedance and Surge Impedance Loading (Natural Power) .....	68
4.2.1	Methods for Increasing SIL of Overhead Lines.....	69
4.2.2	Compact Lines.....	69
4.2.3	Bundle Expansion.....	71
4.3	Stability .....	71
4.4	Thermal Limit and Voltage Drop .....	72
4.5	Capability of a Line.....	74
4.6	Reactive Power Compensation.....	74
4.7	Electromagnetic Unbalance - Transposition .....	75
4.8	Losses.....	75
4.8.1	Losses by Joule Heating Effect ( $RI^2$ ) in the Conductors .....	75
4.8.2	Dielectric Losses: Corona Losses, Insulator and Hardware Losses .....	75
4.8.3	Losses by Induced Currents .....	76
4.9	Reliability and Availability .....	76
4.10	Overvoltages .....	77
4.10.1	Fast-front Overvoltages (Lightning Overvoltages) .....	77
4.10.2	Temporary (Sustained) Overvoltage.....	114
4.10.3	Slow-Front Overvoltages (Switching Surges).....	116

---

Originally published by Cigré, 2014, under the ISBN 978-2-85873-284-5. Republished by Springer International Publishing Switzerland with kind permission.

J.F. Nolasco (✉) • J.A. Jardini • E. Ribeiro  
Florianópolis, Brazil  
e-mail: [nolascojf@gmail.com](mailto:nolascojf@gmail.com)

4.11	Insulation Coordination.....	119
4.11.1	General .....	119
4.11.2	Statistical Behavior of the Insulation .....	120
4.11.3	Insulation Coordination Procedure.....	122
4.11.4	Withstand Capability of Self Restoring Insulation.....	127
4.12	Electric and Magnetic Fields, Corona Effect .....	128
4.12.1	Corona Effects .....	132
4.12.2	Fields .....	140
<b>Section 2: DC Transmission Lines</b>		
4.13	Overvoltages and Insulation Coordination.....	143
4.13.1	Overvoltages.....	143
4.13.2	Insulation Coordination.....	147
4.14	Pole Spacing Determination.....	156
4.14.1	Case of I-Strings.....	156
4.14.2	Case of V-Strings.....	157
4.15	Conductor Current Carrying Capability and Sags .....	159
4.16	Tower Height.....	160
4.17	Lightning Performance .....	161
4.18	Right-of-Way Requirements for Insulation.....	163
4.18.1	Line with I-Strings.....	164
4.18.2	Line with V-Strings .....	164
4.19	Corona effects .....	165
4.19.1	Conductor Surface Gradient and onset Gradient.....	165
4.19.2	Corona Loss.....	168
4.19.3	Radio Interference and Audible Noise .....	171
4.20	Electric and Magnetic Field .....	174
4.20.1	Ground-Level Electric Field and Ion Current .....	174
4.20.2	Magnetic Field.....	182
4.21	Hybrid Corridor or Tower .....	183
4.21.1	Conductor Surface Gradient.....	183
4.21.2	Radio Interference .....	184
4.21.3	Audible Noise.....	185
4.21.4	Corona Losses .....	185
4.21.5	Electric and Magnetic Fields.....	186
References to 4.1–4.12.....		186
References to 4.13–4.21.....		188

---

## 4.1 Electrical Characteristics

### 4.1.1 Introduction

Electrical parameters of transmission lines or otherwise referred to as line constants, resistance, inductance and capacitance ( $R, L, C$ ) are used to evaluate the electrical behavior of the power system. Depending on the phenomena to be studied a different set of parameters is required. For load flow and electromechanical transients the parameters used are the positive sequence. In the short-circuit calculation the positive/negative/zero sequence parameters and for electromagnetic transients the phase parameters and its frequency-dependent parameters.

For the former case, normally, the line is considered full transposed and there are simple equations to determine the parameters. For others cases digital programs are used like the ATP. The various procedures of calculation are discussed here-in-after, starting with straight forward calculation for positive sequence model and completing with a general calculation.

### 4.1.2 Resistance

The resistance of conductors  $R$  is found in the manufacturers catalog. The values of resistance in  $\Omega/\text{km}$  for dc current at  $20^\circ\text{C}$  and sometimes for ac (50 or 60 Hz) are given as function of the conductor cross section.

$R$  - the resistance of the bundle- is then the one sub-conductor resistance divided by the number of them in a bundle.

It should be noted that manufacturers' catalog indicate, normally, conductor resistance ( $R_{20}$ ) for dc at  $20^\circ\text{C}$ . For other temperature ( $R_t$ ) a correction shall be applied:

$$R_t = R_{20} [1 + \beta(t - 20)] \quad (4.1)$$

where  $t$  is the conductor temperature and  $\beta$  the resistance temperature coefficient equal to 0.00403 for Aluminum and 0.00393 for copper. Aluminum Association provides specific values of  $\beta$  for every conductor section in the ranges  $25\text{-}50^\circ\text{C}$  and  $50\text{-}75^\circ\text{C}$ .

Example: for the conductor ACSR 954 MCM (45/7), extracting the individual resistances from a Catalogue ([Aluminum Association Handbook](#)) and making the calculation of  $\beta$  coefficients, Table 4.1 is obtained:

### 4.1.3 Inductance

The inductive reactance of the transmission line is calculated by (Stevenson 1962):

$$X_l = 2w10^{-4} \ln\left(\frac{GMD}{GMR}\right) (\Omega / \text{km}) / \text{phase} \quad (4.2)$$

**Table 4.1** Examples of coefficients of resistance variation according to temperatures

ACSR 954 MCM (Rail)			
	t(°C)		
Unit	25	50	75
$\Omega/\text{Mi}$	0.099	0.109	0.118
$\Omega/\text{km}$	0.061778	0.067744	0.073337
$\beta_{(25-50)}$	0.003863		
$\beta_{(50-75)}$	0.003303		

$$w = 2\pi f \quad (4.3)$$

$f$  is the frequency.

GMD and  $GMR$  are the geometric mean distance and geometric mean radius.

For a single circuit fully transposed:

$$GMD = \sqrt[3]{d_{ab}d_{ac}d_{bc}} \quad (4.4)$$

$d_{ab}$   $d_{ac}$   $d_{bc}$  are the phase distances.

For bundle of  $n$  sub-conductors located in a circle of radius  $R$  and being  $a$  the equal spacing between adjacent sub-conductors the equivalent radius of the bundle or the  $GMR$  is:

$$GMR = R^n \sqrt[n]{\frac{nrk}{R}} \quad (4.5)$$

$r$  is the sub conductor radius

$$R = \frac{a}{2 \sin(\pi/n)} \quad (4.6)$$

$k$  is a correction factor

#### 4.1.4 Capacitance

The capacitance of a full transposed three phase line is calculated by:

$$C = \frac{0.05556}{\ln\left(k_1 \frac{GMD}{GMR_c}\right)} \mu F / km \quad (4.7)$$

$$GMR_c = R^n \sqrt[n]{\frac{nr}{R}} \quad (4.8)$$

$k_1$  depends on distances between conductors and conductors to images in the soil (equal to 0.95-1.0 for 138 kV and 0.85-0.9 for 400 kV and higher voltages).

#### 4.1.5 Negative and Zero Sequence Parameters

Negative sequence parameters are equal to the positive parameters for transmission lines.

There are straight forward equations also for the calculation of the zero sequence parameters, however it is recommended to use the procedures described in (Stevenson 1962; Happoldt and Oeding 1978; Kiessling et al. 2003).

### 4.1.6 Representation of Lines

In this section formulae will be presented for calculating voltage, current and power at any point of a transmission line, provided such values are known at one point. Loads are usually specified by their voltage, power and power factor, for which current can be calculated for use in the equations.

Normally transmission lines are operated with balanced three-phase loads. Even if they are not spaced equilaterally and may not be transposed, the resulting dissymmetry is slight, and the phases are considered to be balanced.

The equivalent circuit of a short line is represented by a series reactance only, which are concentrated or lumped parameters not uniformly distributed along the line. As the shunt admittance is neglected for short lines, it makes no difference, as far as measurements at the ends of the line are concerned, whether the parameters are lumped or uniformly distributed.

The shunt admittance, generally pure capacitance, is included in the calculations for a line of medium length. The nominal  $\Pi$  circuit, shown in Figure 4.1 below, is often used to represent medium-length lines.

In this circuit, the total shunt admittance is divided into two equal parts placed at the sending and receiving ends of the line.

The voltage and current relationships used in electrical calculations under this approach are:

$$V_S = \left( \frac{ZY}{2} + 1 \right) V_R + ZI_R \tag{4.9}$$

$$I_S = Y \left( \frac{ZY}{4} + 1 \right) V_R + \left( \frac{ZY}{2} + 1 \right) I_R \tag{4.10}$$

Neglecting the capacitance for short lines, the above equations become the well-known simple relationships:

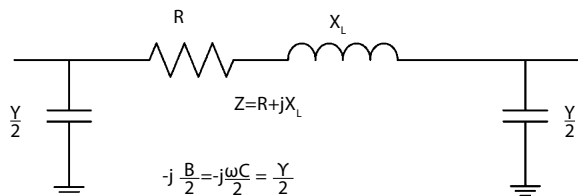
$$V_S = V_R + ZI_R \tag{4.11}$$

$$I_S = I_R \tag{4.12}$$

The magnitude of the voltage regulation (%Reg) for the case of medium lines is:

$$\%Reg = 100 \frac{|V_S| - |V_R|}{|V_R|} \tag{4.13}$$

**Figure 4.1** Nominal  $\Pi$  circuit of a line.



#### 4.1.6.1 Long Transmission Lines

As impedance and admittance are uniformly distributed along the line, the exact solution of any transmission line is required for a high degree of accuracy in calculating long lines (for instance longer than 100 km); distributed parameters should be used in this case.

The following nomenclature is used:

- $z$  = series impedance per unit length, per phase
- $y$  = shunt admittance per unit length, per phase to neutral
- $l$  = line length
- $Z = zl$  = total series impedance per phase
- $Y = yl$  = total shunt admittance per phase to neutral

The following equations can be deduced:

$$V = \frac{V_R + I_R Z_C}{2} e^{\gamma x} + \frac{V_R - I_R Z_C}{2} e^{-\gamma x} \quad (4.14)$$

$$I = \frac{V_R + I_R Z_C}{2Z_C} e^{\gamma x} + \frac{V_R - I_R Z_C}{2Z_C} e^{-\gamma x} \quad (4.15)$$

$$Z_C = \sqrt{\frac{z}{y}} \quad (4.16)$$

and the propagation constant is:

$$\gamma = \sqrt{zy} \quad (4.17)$$

Both  $\gamma$  and  $Z_C$  are complex quantities. The real part of the propagation constant  $\gamma$  is called the attenuation constant  $\alpha$ , while the quadrature part is called phase constant  $\beta$ .

Thus:  $\gamma = \alpha + j\beta$ . The above equations for voltage and current for defining  $V$  and  $I$  turn out into:

$$V = \frac{V_R + I_R Z_C}{2} e^{\alpha x} e^{j\beta x} + \frac{V_R - I_R Z_C}{2} e^{-\alpha x} e^{-j\beta x} \quad (4.18)$$

$$I = \frac{V_R + I_R Z_C}{2Z_C} e^{\gamma x} + \frac{V_R - I_R Z_C}{2Z_C} e^{-\gamma x} \quad (4.19)$$

A deep analysis, beyond the scope of these highlights, will prove that the first terms of the above equations are the incident voltage (or current), while the second term is the reflected voltage (or current). Observe that a line terminated in its characteristic impedance  $Z_C$  has  $V_R = I_R Z_C$  and therefore has no reflected wave.

Such a line is called flat line or infinite line, the latter designation arising from the fact that a line of infinite length cannot have a reflected wave. Usually power

**Table 4.2** Typical line parameters and line constants for a 500 kV Line

4 × ACAR 1300 MCM (30/7)			Ling length → 365 km		$\beta^{(b)}$
Parameter	R( $\Omega$ /km)	$X_L$ ( $\Omega$ /km)	$X_C$ ( $\Omega$ *km)	B( $\mu$ S/km))	0,001276
$Z_1$ unit	0.013172	0.220388	135411	7,385	$\gamma$
$Z_0$ unit	0.15317	1.00965	326807	$B_0$ ( $\mu$ S/km))	0,001277
Eq. LT	R( $\Omega$ )	$X_L$ ( $\Omega$ )	B/2( $\mu$ S)	3,060	$\lambda$ (km)
“ $\Pi$ ”nom $Z_1$	4.808	80.442	1347.7	$Z_C$ ( $\Omega$ )	4923
“ $\Pi$ ”equiv	4.466	77.576	1372.64	172,9	
“ $\Pi$ ”nom $Z_0$	55.906	368.521	558.43	$\alpha$	v(km/s)
E/ $E_0$	0.785	SIL(MW)	1447	3,81 E-05	295373

Notes: a) 1 MCM = 0.5067 mm<sup>2</sup> b) This column refers to line constants

Line data used for the calculation above:

- voltage → 500 kV Tower type → Guyed cross rope
- phase bundle conductor → 4 × ACAR 1300 MCM (~4 × 653 mm<sup>2</sup>).
- diameter → 3.325 cm Stranding: 30/7
- sub-conductor spacing → 120,0 cm (Expanded bundle)
- phase spacing → 6.41 m
- conductor height at tower → 28.3 (average) m
- minimum distance conductor to ground → 12.0 m
- conductor sag → 22.5 m
- shield wires EHS → 3/8” and OPGW 14.4 mm S. wires spacing → 28.1 m
- shield wire height at tower → 38.0 m shield wire sag 16.5 m
- soil resistivity → 1000  $\Omega$  m

lines are not terminated in their characteristic impedance, but communication lines are frequently so terminated in order to eliminate the reflected wave. A typical value of  $Z_C$  is 400  $\Omega$  for a single conductor line. For conductor bundles between 2 and 6, see typical values in Table 4.2. The phase angle of  $Z_C$  is usually between 0 and  $-15^\circ$ .  $Z_C$  is also called surge impedance in power lines.

Surge impedance loading (SIL) of a line is the power delivered by a line to a purely resistive load equal to its surge impedance.

#### 4.1.6.2 Lumped Representation of Lines

The exact representation of a transmission line is usually made through the use of hyperbolic functions that can treat the line with distributed electric parameters of resistance, inductance and capacitance.

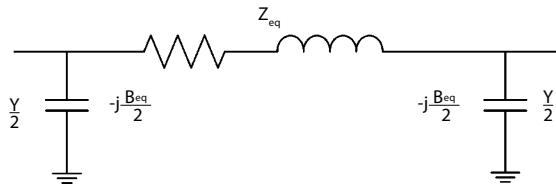
Such functions are equated in terms of the incident and reflected waves of voltage and current, being summarized as follows:

$$V_S = V_R \cosh \gamma l + I_R Z_C \sinh \gamma l \quad (4.20)$$

$$I_S = I_R \cosh \gamma l + \frac{V_R}{Z_C} \sinh \gamma l \quad (4.21)$$

$$V_R = V_S \cosh \gamma l - I_S Z_C \sinh \gamma l \quad (4.22)$$

**Figure 4.2** Equivalent circuit of a long line (Equivalent  $\Pi$ ).



$$I_R = I_S \cosh \gamma l - \frac{V_S}{Z_C} \sinh \gamma l \quad (4.23)$$

However for the case of short or medium-length lines, equivalent circuits of transmission lines have been simplified by calculating equivalent series resistance and reactance, which are shown as concentrated or lumped parameters and not distributed along the line. The distributed capacitances are also represented by one or two lumped parameters.

This simple circuit having the shape of the Greek letter  $\Pi$  is named as nominal  $\Pi$ . The nominal  $\Pi$  does not represent a transmission line exactly because it does not account for the parameters of the line being uniformly distributed.

The discrepancy between the nominal  $\Pi$  and the actual line becomes larger as the length of the line increases. It is possible, however, to find the equivalent circuit of a long transmission line composed of lumped parameters so that voltage and current relations at both ends are accurate. In view of that, the true line representation that is really a hyperbolic function can be replaced by a simplified Line Representation having the shape of the so called Equivalent  $\Pi$  as shown in Figure 4.2. The values of the equivalent parameters,  $R_{eq}$ ,  $X_{eq}$  and  $B_{eq}$  are determined so that the voltages and currents are the same at the sending-end and receiving-end terminals. The calculation formulas state below.

$$Z_C \sin \gamma l = z \frac{\sinh \gamma l}{\gamma l} \quad (4.24)$$

$$\frac{B_{eq}}{2} = \frac{1}{Z_C} \frac{\tanh \gamma l}{2} = \frac{B}{2} \frac{\tanh (\gamma l / 2)}{\gamma l} \quad (4.25)$$

Therefore, starting from the nominal  $\Pi$  parameters and using the circuit constants, it is possible to calculate the equivalent  $\Pi$  values.

$$Z_{eq} = R_{eq} + jX_{eq} \quad (4.26)$$

For short lines and low voltage lines, capacitance  $C$  is neglected and a simplified model neglecting the capacitance can be used instead. Such simplification could be applied to lines below 72.5 kV and for lengths below 30 to 40 km.

An example of calculation of the main parameters and line constant is shown in Table 4.2 for a 500 kV overhead line.



Line data used for the calculation above:

- voltage = 500 kV Tower type = Guyed cross rope
- phase bundle conductor =  $4 \times \text{ACAR 1300 MCM}$  ( $\sim 4 \times 653 \text{ mm}^2$ ).
- diameter = 3.325 cm Stranding: 30/7
- sub-conductor spacing = 120.0 cm (Expanded bundle)
- phase spacing = 6.41 m
- conductor height at tower = 28.3 (average) m
- minimum distance conductor to ground = 12.0 m
- conductor sag = 22.5 m
- shield wires EHS = 3/8" and OPGW 14.4 mm s. wires spacing = 28.1 m
- shield wire height at tower = 38.0 m shield wire sag 16.5 m
- soil resistivity =  $1000 \Omega \text{ m}$ .

### 4.1.7 General Overhead Transmission Line Models

Overhead transmission lines are modeled by electric circuit based on their parameters (resistance, inductance and capacitance) and length.

The relation between voltage to ground ( $V$ ), incremental length voltage drop along the line ( $\Delta V / \Delta x$ ), and current ( $I$ ) or charge ( $Q$ ) are (Dommel 1986):

- Electromagnetic phenomena

$$[\Delta V / \Delta x] = [Z][I] \tag{4.27}$$

- Electrostatic phenomena

$$[V] = [H][Q] \tag{4.28}$$

For AC system, matrixes  $Z$  and  $H$  have one line and one column for each conductor and shield wire. For instance, for an AC line with three phases (sub index  $p$ ) and two shield wires (sub index  $s$ ) they look like:

$Z_{pp}$				
				$Z_{ps}$
			$Z_{ss}$	
	$Z_{sp}$			

For bipolar DC systems the matrixes are similar however with  $p=2$ .

#### 4.1.7.1 Electromagnetic and Electrostatic Line Equations

The terms of the impedance matrix  $Z$  in ( $\Omega/\text{km}$ ) are:

$$Z_{ii} = (R_{ii} + \Delta R_{ii}) + j(X_{ii} + \Delta X_{ii}) \quad (4.29)$$

$$Z_{ij} = (\Delta R_{ij}) + j(X_{ij} + \Delta X_{ij}) \quad (4.30)$$

$R_{ii}$  is the AC resistance of the bundle (one sub-conductor resistance divided by the number of them in a bundle)

$$X_{ii} = 2w10^{-4} \ln \left( \frac{1}{R_{eqz_{ii}}} \right) \quad (4.31)$$

$$X_{ij} = 2w10^{-4} \ln \left( \frac{1}{d_{ij}} \right) \quad (4.32)$$

$\Delta R_{ii}$ ,  $\Delta R_{ij}$ ,  $\Delta X_{ii}$ ,  $\Delta X_{ij}$ , are additional parcels (Carlson correction) for which resistance and reactance initial term of the series are:

$$\Delta R_{ij} = 4w10^{-4} \left[ \frac{1.5708}{4} - \frac{0.0026492(h_i + h_j)\sqrt{f l \rho}}{4} + \dots \right] \quad (4.33)$$

$$\Delta X_{ij} = 4w10^{-4} \left[ \frac{2}{4} \ln \left( \frac{658.8}{\sqrt{f l \rho}} \right) + \frac{0.0026492(h_i + h_j)\sqrt{f l \rho}}{4} + \dots \right] \quad (4.34)$$

for ii terms use  $h_i$  in place of  $h_j$

For bundle of  $n$  sub-conductors located in a circle of radius  $R$  and being  $a$  the spacing between adjacent sub-conductors the equivalent radius of the bundle is:

$$R_{eqz_{ii}} = R \sqrt{\frac{nrk}{R}} \quad (4.35)$$

$r$  is the sub conductor radius

$$R = \frac{a}{2 \sin(\pi/n)} \quad (4.36)$$

$k$ =correction factor

$d_{ij}$ =distance between the center of the bundles  $i$  and  $j$

$h_i$ =average conductor  $i$  height (height at mid span plus 1/3 of the sag)

$f$ =frequency

$\rho$ =soil resistivity in  $\Omega \text{ m}$

The terms of the potential matrix  $H$  in ( $\text{km}/\mu\text{F}$ ) are:

$$H_{ii} = 17.976 \ln \left( \frac{D_{ii}}{R_{eqc_{ii}}} \right) \quad (4.37)$$

$$H_{ij} = 17.976 \ln \left( \frac{D_{ij}}{d_{ij}} \right) \quad (4.38)$$

$$R_{eqc_{ii}} = R \sqrt[n]{\frac{nr}{R}} \quad (4.39)$$

$D_{ij}$  = distance from bundle  $i$  to the image of bundle  $j$ .

The inverse  $H_{-1}$  is the bus admittance matrix  $Y$  divided by  $w$  and includes the line capacitances.

Therefore for the line parameters calculation the tower geometry has to be known.

Notes:

- Shield wire may be grounded ( $\Delta V_s = 0$ ), and their rows and columns can then be eliminated (Gauss's elimination) as shown by the equation below, and hence their effects are included in the others lines and rows.

$$Z_{ij}^{new} = Z_{ij} - \frac{Z_{ik} Z_{kj}}{Z_{kk}} \quad (4.40)$$

- for  $k=4,5$  and  $i,j=1,2,3$  in the example above.
- For isolated shield wire ( $I_s=0$ ) their lines and columns are deleted.
- For asymmetrical bundle every sub-conductor has one line and one column in the matrix  $Z$  for instance. As the sub-conductors in the same bundle have the same voltage drop the lines and columns of one is maintained, and the others lines and columns are substituted by the difference of their values and the corresponding of the remained lines and columns. Now for the modified sub-conductors  $\Delta V = 0$ ,  $I_t = \Sigma I_c$ , and can be eliminated like the shield wires, and their effect is kept in the remaining one (Dommel 1986).
- If the line has phase transpositions the terms of the matrixes  $Z, H$  can be averaged by its section length.
- Finally matrices  $Z, H$  remain with the number of lines/columns equal to the number of phases.
- For DC line the same applies being the remaining lines/columns equal to the number of poles.
- The Electromagnetic Transients Programs that are available have routines to perform the necessary calculations.

#### 4.1.7.2 Line Models

The equations indicated before, for a short line of length  $L$  are:

$$[\Delta V] = [Z_u][I] = [Z][I] \quad (4.41)$$

$$[I] = jw[H]^{-1}[V] \quad (4.42)$$

- Symmetrical components (AC lines)

$Z$  and  $Y$  matrixes terms are all non zeros, and  $\Delta V$ ,  $V$ ,  $I$  are phase quantities. To simplify the calculation the equations above may be transformed for instance,  $Z$ , into symmetrical components (positive, negative and zero sequences, or 1, 2, 0) by:

$$[\Delta V_{012}] = [T]^{-1}[Z][T][I_{012}] \quad (4.43)$$

Hence the symmetrical component impedance matrix is:

$$[Z_{012}] = [T]^{-1}[Z][T] \quad (4.44)$$

If the line has a complete transposition of phases in equal sections then the symmetrical component matrix  $Z_{012}$  has only the diagonal terms (the sequential impedances,  $Z_0$ ,  $Z_1$ ,  $Z_2$ )

Now for the calculation, given one set of phase values, they are transformed into symmetrical components, and the calculation is carried using the equation above. After that, the calculated sequence components values have to be changed back to phase components. The transformation matrix  $T$  is:

$$T = \frac{1}{\sqrt{3}} \begin{bmatrix} 1 & 1 & 1 \\ 1 & a & a^2 \\ 1 & a^2 & a \end{bmatrix} \quad (4.45)$$

With  $a = e^{j120}$ .

Note that the phase components are:

$$Z = \begin{bmatrix} Z_{aa} & Z_{ab} & Z_{ac} \\ Z_{ba} & Z_{bb} & Z_{bc} \\ Z_{ca} & Z_{cb} & Z_{cc} \end{bmatrix} \quad (4.46)$$

The matrix  $Z$  is symmetric (Ex.:  $Z_{ab} = Z_{ba}$ ). Also, if the phases have the same configuration and they have complete phase transposition, then:

$$Z = \begin{bmatrix} Z_s & Z_m & Z_m \\ Z_m & Z_s & Z_m \\ Z_m & Z_m & Z_s \end{bmatrix} \quad (4.47)$$

$$Z_{aa} = Z_{bb} = Z_{cc} = Z_s \quad (4.48)$$

$$Z_{ab} = Z_{ac} = Z_{bc} = Z_m \quad (4.49)$$

And

$$Z_1 = Z_2 = Z_s - Z_m \quad (4.50)$$

$$Z_0 = Z_s + 2Z_m \tag{4.51}$$

Note: If the line is a double circuit (w,y) then Z matrix can be partitioned into four 3×3 sub-matrices  $Z_{ww}$ ;  $Z_{yy}$ ;  $Z_{wy}$  and the same equations can be applicable, provided there is a complete transposition, obtaining the sequence self parameters of circuit w, y and the mutual wy.

Therefore for two circuits w and y close together considering complete transposition the matrix has the following type.

$Z_{ws}$	$Z_{wm}$	$Z_{wm}$	$Z_{wys}$	$Z_{wym}$	$Z_{wym}$
	$Z_{ws}$	$Z_{wm}$	$Z_{wym}$	$Z_{wys}$	$Z_{wym}$
		$Z_{ws}$	$Z_{wym}$	$Z_{wym}$	$Z_{wys}$
			$Z_{ys}$	$Z_{ym}$	$Z_{ym}$
				$Z_{ys}$	$Z_{ym}$
					$Z_{ys}$

And the self impedances of circuit w are:

$$\begin{aligned} Z_{w1} = Z_{w2} &= Z_{ws} - Z_{wm} \\ Z_{w0} &= Z_{ws} + 2Z_{wm} \end{aligned} \tag{4.52}$$

The mutual impedances of circuit w and y are:

$$\begin{aligned} Z_{wy1} = Z_{wy2} &= Z_{wys} - Z_{wym} \\ Z_{wy0} &= Z_{wys} + 2Z_{wym} \end{aligned} \tag{4.53}$$

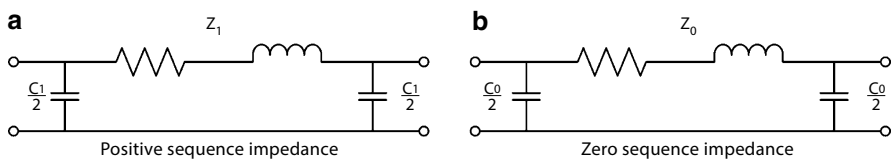
Similar considerations apply to the second equation and Y matrix. As example, for single circuit being:

$$C_1 = \frac{1}{H_s - H_m} \tag{4.54}$$

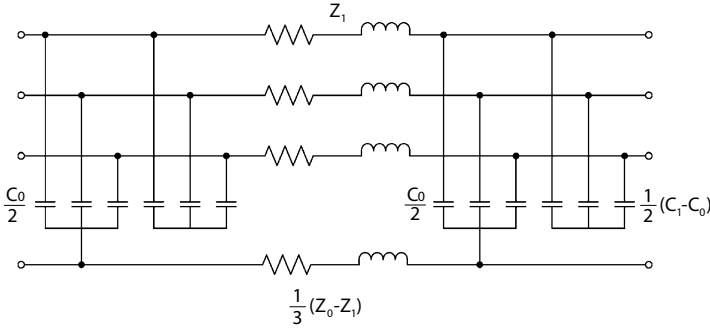
$$C_0 = \frac{1}{H_s + 2H_m} \tag{4.55}$$

Once obtained the sequence impedances the line/cable can be modeled using lumped circuits,  $\pi$  sections like in Figure 4.3.

For short lines ( $\leq 50$  km) the above impedances are obtained by multiplying the unit impedance with the line length. For long lines a factor  $< 1$  shall be included as indicated before.



**Figure 4.3** AC line model, single phase  $\pi$  for positive/negative sequences a) and zero sequence b).



**Figure 4.4** Three phase,  $\pi$ -model.

A three phase model can also be established and was useful for TNA calculation (Figure 4.4).

For DC lines, similarly to the symmetrical component transformation, the matrix  $T$  is:

$$T = \frac{1}{\sqrt{2}} \begin{bmatrix} 1 & 1 \\ 1 & -1 \end{bmatrix} \tag{4.56}$$

That leads to two modes: ground and aerial or metallic modes (0 and 1 respectively).

Similarly for the AC equations, it results:

$$Z_1 = Z_{11} - Z_{12} \tag{4.57}$$

$$Z_0 = Z_{11} + Z_{12} \tag{4.58}$$

$$C_1 = \frac{1}{H_s - H_m} \tag{4.59}$$

$$C_0 = \frac{1}{H_s + H_m} \tag{4.60}$$

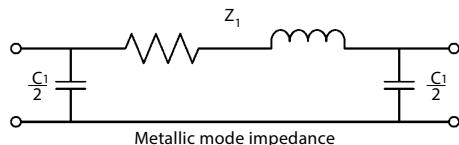
The corresponding  $\pi$  circuit for aerial mode is (Figure 4.5):

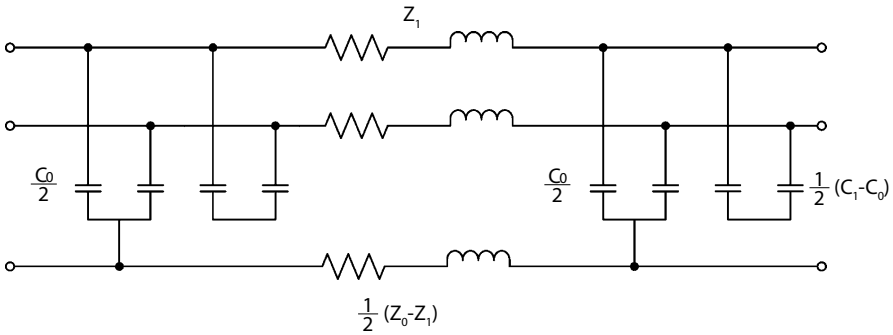
The two poles model is that of Figure 4.6.

- For electromagnetic calculations the following equations applies

$$[\partial V / \partial x] = [Z][I] \tag{4.61}$$

**Figure 4.5** Aerial/  
Metallic mode circuit; for  
ground mode change  $Z_1, C_1$   
by  $Z_0, C_0$ .





**Figure 4.6** Two poles circuit.

$$[\partial I / \partial x] = j\omega[H]^{-1}[V] = [Y][V] \tag{4.62}$$

and

$$[\partial^2 V / \partial x^2] = [Z][Y][V] \tag{4.63}$$

Now it is necessary to transform into diagonal matrix the product  $[Z][Y]$ . This is obtained by searching for the eigenvalues and eigenvector of it (modal analysis) (Dommel 1986).

### 4.1.7.3 Electrical Studies and Their Line Models

The following studies are applicable for AC and DC systems.

- Steady-state (load flow and short circuit)
- Electromechanical transients (stability, power frequency overvoltage due to load rejection, and line/cable energization/reclosing)
- Electromagnetic transient (transient part of short-circuits, switching surge over-voltages, DC converters commutation failure).
- Harmonic performance
- Relay protection and control coordination.

The overhead transmission line models may vary depending on the study.

- Steady state.  
For load-flow calculation, the overhead AC lines and cables are represented by  $-\pi$  sections based on positive sequence parameters. Overhead DC lines are represented by their resistance only.  
For short circuit calculations transposed symmetrical components parameters should be used for AC lines. For DC lines this type of calculation is not completely valid unless the converter station control action is simulated.
- Electromechanical transients

AC and DC lines are represented using the same above mentioned modelling for load flow analysis. However, for power-frequency over-voltages (rated frequency  $\pm 10\%$ ) the variation of the parameters (reactance:  $\omega L$  and  $1/\omega C$ ) with the frequency shall be simulated (note that this does not refer to line frequency dependence of parameters).

- Electromagnetic transients  
AC and DC lines are represented by distributed parameter or a cascade of  $-\pi$  sections. Now, overhead DC lines model considers frequency dependant parameters. Modal decomposition analysis is normally used in the calculation together with non transposed  $Z$ ,  $H-I$ , matrixes. This line model applies when calculating the initial transient of a short circuit in DC and AC lines.
- Harmonic performance  
AC and DC overhead lines are represented as  $-\pi$  sections using transposed parameters at the specific harmonic frequency taking into account the parameters as a function of frequency.
- Relay protection and control  
The same modeling used for electromagnetic studies applies in this case when the transient part of the overcurrent/overvoltage phenomena is important.

#### 4.1.7.4 Examples of Calculation DC Line

Calculations were done using ATP/EMTP-RV for the line on Figure 4.7 and are reported below. The data for the example (arbitrarily chosen (Cigré 2009)).

- voltage =  $\pm 500$  kV
- pole conductor =  $3 \times 1590$  MCM ( $\sim 806$  mm<sup>2</sup>)
- economic conductor for 1300 MW bipole
- diameter = 3.822 cm
- pole spacing = 13 m
- sub-conductor spacing = 45 cm
- minimum distance conductor to ground = 12.5 m
- conductor sag = 20.5 m (conductor height at tower 33 m)
- shield wires = EHS 3/8"
- shield wires spacing = 11 m
- shield wire sag = 20.5 m
- shield wire height at tower = 41 m
- soil resistivity = 500  $\Omega$  m.

The results using EMTP-RV are shown below (Figures 4.8, and 4.9):

After bundling (left) and elimination of the shield wires (right) the matrixes are (Figures 4.10, 4.11, and 4.12):

or

$$I_+ = \omega 1.12E-08 V_+ + \omega (-1.69E-09) V_-$$

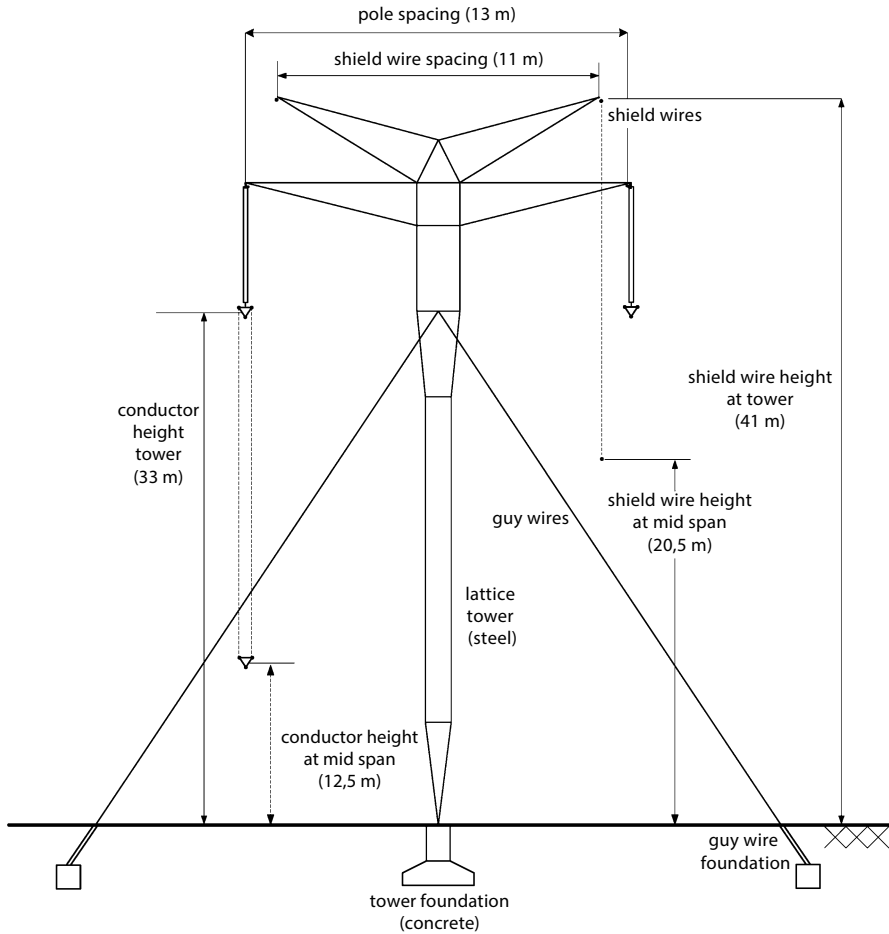
$$\omega = 2\pi f = 1 \text{ as } f = 1/2\pi$$

$$C_0 = 1.12E-08 - 1.69E-09 \Rightarrow 9.51 \mu\text{F}$$

$$C_1 = 1.12E-08 + 1.69E-09 \Rightarrow 12.89 \mu\text{F}$$

Therefore





**Figure 4.7** Line geometry.

$$Z_0 = (1.21 \text{ E-}02 + 1.58 \text{ E-}04) + j (2.49 \text{ E-}03 + 1.59 \text{ E-}03) = 0.0122 + j 0.00408 \ \Omega$$

( $\omega = 1 \text{ rad/s}$ )

$$Z_1 = (1.21 \text{ E-}02 - 1.58 \text{ E-}04) + j (2.49 \text{ E-}03 - 1.59 \text{ E-}03) = 0.0120 + j 0.0009 \ \Omega$$

( $\omega = 1 \text{ rad/s}$ ).

**AC Line**

Calculations were done using ATP/EMTP-RV for the line on Figure 4.13 and are reported below. The data for the example are.

- voltage = 500 kV
- phase bundle conductor =  $4 \times 954 \text{ MCM}$  ( $\sim 483 \text{ mm}^2$ )
- diameter = 2.961 cm
- sub-conductor spacing = 45.7 cm.

INPUT DATA									
Line conductor card.	(skin)	(resistance)	(group) (rep.)	(rep.) (model)	(outer diameter)	(X)	(Ytower)	(Ymin)	
3.750E-01	3.596E-02	4	10.3750.035959	4	3.822	6.7285	33.1319	12.6319	
3.750E-01	3.596E-02	4	10.3750.035959	4	3.822	6.2715	33.1319	12.6319	POLE 1
3.750E-01	3.596E-02	4	10.3750.035959	4	3.822	6.5	32.7362	12.2362	
3.750E-01	3.596E-02	4	20.3750.035959	4	3.822	-6.7285	33.1319	12.6319	POLE 2
3.750E-01	3.596E-02	4	20.3750.035959	4	3.822	-6.2715	33.1319	12.6319	
3.750E-01	3.596E-02	4	20.3750.035959	4	3.822	-6.5	32.7362	12.2362	
5.000E-01	3.282E+00	4	3.0.5	3.28153	0.953	5.5	41.	20.5	SHIELD WIRES
5.000E-01	3.282E+00	4	4.0.5	3.28153	0.953	-5.5	41.	20.5	
Blank card terminating conductor cards.									
BLANK CARD ENDING CONDUCTOR CARDS									
Frequency card.	5.000E+02	1.592E-01	1.000E+00	500.0.15915494	000110	110000	0	1.	44

INPUT PRINTOUT										
Line conductor table after sorting and initial processing.	Table	Phase	Skin effect	Resistance	Reactance data	specification	Diameter	Horizontal	Avg height	Name
Row	Number	R-type	R (ohm/km)	X-type	X(ohm/km)	or GMR	(cm)	X (mtrs)	Y (mtrs)	
1	1	.37500	.03596	4	.000000	.000000	3.82200	6.728	19.465	
2	2	.37500	.03596	4	.000000	.000000	3.82200	-6.728	19.465	
3	3	.37500	.03596	4	.000000	.000000	3.82200	6.271	19.465	
4	1	.37500	.03596	4	.000000	.000000	3.82200	6.500	19.070	
5	2	.37500	.03596	4	.000000	.000000	3.82200	-6.271	19.465	
6	2	.37500	.03596	4	.000000	.000000	3.82200	-6.500	19.070	
7	0	.50000	3.28153	4	.000000	.000000	.95300	5.500	27.333	
8	0	.50000	3.28153	4	.000000	.000000	.95300	-5.500	27.333	

Matrices are for earth resistivity = 5.00000000E+02 ohm-meters and frequency 1.59154940E-01 Hz. Correction factor = 1.00000000E-06

Figure 4.8 Input data of line geometry.

1,29E-02										
-1,58E-04	1,29E-02									
-4,59E-03	-1,86E-04	1,29E-02								
-4,60E-03	-1,70E-04	-4,59E-03	1,29E-02							
-1,86E-04	-4,59E-03	-2,22E-04	-2,03E-04	1,29E-02						
-1,70E-04	-4,60E-03	-2,03E-04	-1,89E-04	-4,59E-03	1,29E-02					
-6,16E-04	-2,69E-04	-6,16E-04	-5,14E-04	-3,00E-04	-2,58E-04	6,52E-03				
-2,69E-04	-6,16E-04	-3,00E-04	-2,58E-04	-6,16E-04	-5,14E-04	-7,51E-04	6,52E-03			

**Figure 4.9** Susceptance matrix, in units of [mhos/km] for the system of physical conductors. Rows and columns proceed in the same order as the sorted input.

1,12E-08										
-1,69E-09	1,12E-08									
-1,75E-09	-8,27E-10	6,52E-09								
-8,27E-10	-1,75E-09	-7,51E-10	6,52E-09							

**Figure 4.10** Susceptance matrix, in units of [mhos/km] for the system of equivalent phase conductors. Rows and columns proceed in the same order as the sorted input.

3,61E-02										
2,94E-03										
1,57E-04	3,61E-02									
1,58E-03	2,94E-03									
1,57E-04	1,57E-04	3,61E-02								
2,26E-03	1,59E-03	2,94E-03								
1,57E-04	1,57E-04	1,57E-04	3,61E-02							
2,26E-03	1,59E-03	2,26E-03	2,94E-03							
1,57E-04	1,57E-04	1,57E-04	1,57E-04	3,61E-02						
1,59E-03	2,26E-03	1,60E-03	1,59E-03	2,94E-03						
1,57E-04	1,57E-04	1,57E-04	1,57E-04	1,57E-04	3,61E-02					
1,59E-03	2,26E-03	1,59E-03	1,59E-03	2,26E-03	2,94E-03					
1,57E-04	1,57E-04	1,57E-04	1,57E-04	1,57E-04	1,57E-04	3,28E+00				
1,69E-03	1,57E-03	1,69E-03	1,68E-03	1,57E-03	1,57E-03	3,22E-03				
1,57E-04	1,57E-04	1,57E-04	1,57E-04	1,57E-04	1,57E-04	1,57E-04	3,28E+00			
1,57E-03	1,69E-03	1,57E-03	1,57E-03	1,69E-03	1,68E-03	1,62E-03	3,22E-03			

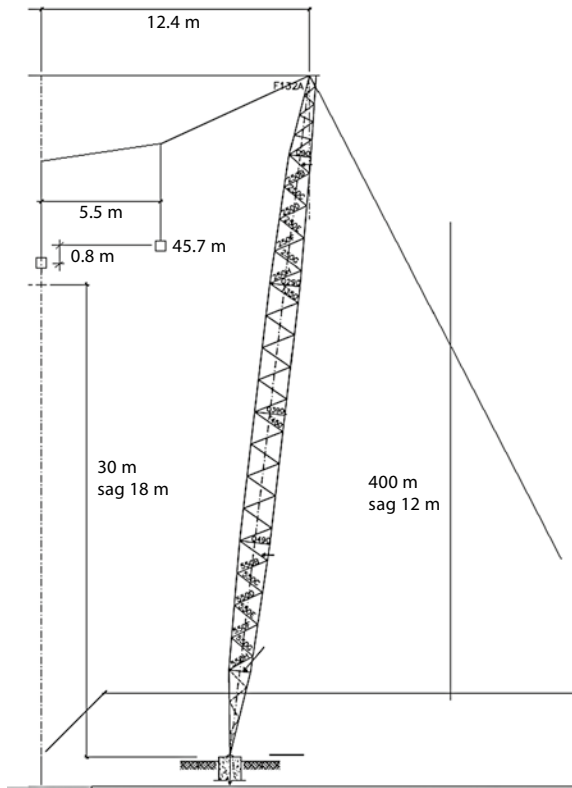
**Figure 4.11** Impedance matrix, in units of [ $\Omega$ /km] for the system of physical conductors. Rows and columns proceed in the same order as the sorted input.

<b>1,21E-02</b>					
<b>2,49E-03</b>					
<b>1,57E-04</b>	<b>1,21E-02</b>				
<b>1,59E-03</b>	<b>2,49E-03</b>				
<b>1,57E-04</b>	<b>1,57E-04</b>	<b>3,28E+00</b>			
<b>1,69E-03</b>	<b>1,57E-03</b>	<b>3,22E-03</b>			
<b>1,57E-04</b>	<b>1,57E-04</b>	<b>1,57E-04</b>	<b>3,28E+00</b>		
<b>1,57E-03</b>	<b>1,69E-03</b>	<b>1,62E-03</b>	<b>3,22E-03</b>		

<b>1,21E-02</b>
<b>2,49E-03</b>
<b>1,58E-04</b> <b>1,21E-02</b>
<b>1,59E-03</b> <b>2,49E-03</b>

**Figure 4.12** Impedance matrix, in units of [ $\Omega/\text{km}$ ] for the system of equivalent phase conductors. Rows and columns proceed in the same order as the sorted input.

**Figure 4.13** AC 500 kV line.



- phase spacing = 11 m
- conductor height at tower = 30.0 and 30.8 m
- minimum distance conductor to ground = 12.0 m
- conductor sag = 18.0 m
- shield wires EHS = 3/8".

- shield wires spacing = 24.8 m
- shield wire height at tower = 40.0 m shield wire sag 12.0 m
- soil resistivity = 500 Ω m.

INPUT DATA	(skin)	(resistance)	(group)(rep.)	(rep.) (mode)	(outer diameter)	(s)	(Ytower)	(Ymin)	(Ytower)	(Ymin)	
Line conductor card.	5.000E-01	6.000E-02	4	1 0.5 0.06 4	2.961	-5.5	30.8	12.8	45.7	45.5	4
Line conductor card.	5.000E-01	6.000E-02	4	2 0.5 0.06 4	2.961	0.0	30.	12.	45.7	45.5	4
Line conductor card.	5.000E-01	6.000E-02	4	3 0.5 0.06 4	2.961	5.5	30.8	12.8	45.7	45.5	4
Line conductor card.	5.000E-01	3.282E+00	4	0 0.5 3.28153 4	0.9525	-12.4	40.	28.	0.0	0.0	1
Line conductor card.	5.000E-01	3.282E+00	4	1 0 0.5 3.28153 4	0.9525	12.4	40.	28.	0.0	0.0	1
Blank card terminating conductor cards.				BLANK CARD ENDING CONDUCTOR CARDS							
Frequency card.	5.000E+02	6.000E+01	1.000E+00	500. 60.	000111	111000	0	1.		44	

INPUT PRINTOUT

Line conductor table after sorting and initial processing.

Table Row	Phase Number	Skin effect	Resistance R-type	Resistance R (ohm/km)	Reactance X-type	Reactance data specification X(ohm/km) or GMR	Diameter (cm)	Horizontal X (mtrs)	Avg height Y (mtrs)	Name
1	1		.50000	.06000	4	.000000	2.96100	-5.271	18.572	
2	2		.50000	.06000	4	.000000	2.96100	0.229	17.772	
3	3		.50000	.06000	4	.000000	2.96100	5.729	18.572	
4	1		.50000	.06000	4	.000000	2.96100	-5.729	18.572	
5	1		.50000	.06000	4	.000000	2.96100	-5.729	19.029	
6	1		.50000	.06000	4	.000000	2.96100	-5.271	19.029	
7	2		.50000	.06000	4	.000000	2.96100	-0.228	17.772	
8	2		.50000	.06000	4	.000000	2.96100	-0.229	18.229	
9	2		.50000	.06000	4	.000000	2.96100	0.228	18.229	
10	3		.50000	.06000	4	.000000	2.96100	5.271	18.572	
11	3		.50000	.06000	4	.000000	2.96100	5.271	19.029	
12	3		.50000	.06000	4	.000000	2.96100	5.729	19.029	
13	0		.50000	3.28153	4	.000000	.95250	-12.400	32.000	
14	0		.50000	3.28153	4	.000000	.95250	12.400	32.000	

Matrices are for earth resistivity = 5.00000000E+02 ohm-meters and frequency 6.00000000E+01 Hz. Correction factor = 1.00000000E-06

Capacitance matrix, in units of [farads/kmeter] for the system of equivalent phase conductors.

Rows and columns proceed in the same order as the sorted input.

1	1.287220E-08		
2	-3.933361E-09	1.396611E-08	
3	-1.420180E-09	-3.933361E-09	1.287220E-08

Capacitance matrix, in units of [farads/kmeter] for symmetrical components of the equivalent phase conductor

Rows proceed in the sequence (0, 1, 2), (0, 1, 2), etc.; columns proceed in the sequence (0, 2, 1), (0, 2, 1), etc.

0	7.045569E-09		
0	0.000000E+00		
1	2.365456E-10	-1.020045E-09	
-4	0.97090E-10	-1.766769E-09	
2	2.365456E-10	1.633247E-08	-1.020045E-09
4	0.97090E-10	9.996965E-26	1.766769E-09

Impedance matrix, in units of [ohms/kmeter] for the system of equivalent phase conductors.

Rows and columns proceed in the same order as the sorted input.

1	1.273080E-01		
6	4.74170E-01		
2	1.113489E-01	1.265447E-01	
3	3.965905E-01	6.477023E-01	
3	1.115025E-01	1.113489E-01	1.273080E-01
3	4.51484E-01	3.965905E-01	6.474170E-01

Both "r" and "x" are in [ohms]; "c" are in [microFarads].

Impedance matrix, in units of [ohms/kmeter] for symmetrical components of the equivalent phase conductor

Rows proceed in the sequence (0, 1, 2), (0, 1, 2), etc.; columns proceed in the sequence (0, 2, 1), (0, 2, 1), etc.

0	3.498538E-01		
1	1.406398E+00		
1	-1.477963E-02	-2.954170E-02	
-8	8.85908E-03	1.723152E-02	
2	1.508524E-02	1.565342E-02	2.969378E-02
-8	3.56583E-03	2.680689E-01	1.696810E-02

Sequence	Surge impedance magnitude(ohm)	angle(deg.)	Attenuation db/km	velocity km/sec	wavelength km	Resistance ohm/km	Reactance ohm/km	Susceptance mho/km
zero :	7.38668E+02	-6.98464E+00	2.07232E-03	1.93584E+05	3.22640E+03	3.49854E-01	1.40640E+00	2.65612E-06
Positive:	2.08834E+02	-1.67095E+00	3.25669E-04	2.93313E+05	4.88855E+03	1.56534E-02	2.68069E-01	6.15720E-06

Calculated steady state benchmark data for line/cable model

Frequency [Hz]: 6.00000000000000E+0001

Line-voltage [kv]: 5.00000000000000E+0002

Positive and zero-sequence data:

	RO [ohm]	X0 [ohm]	Rp [ohm]	Xp [ohm]	Q0 [MVA]	Qp [MVA]
cir. 1:	0.3501	1.404	0.01594	0.2635	0.664	1.539

## 4.2 Surge Impedance and Surge Impedance Loading (Natural Power)

The energy stored in the electric field of an overhead line can be represented as

$$E_e = \frac{1}{2} CV^2 \quad (4.64)$$

At a similar way, the energy stored in the magnetic field is:

$$E_m = \frac{1}{2} LI^2 \quad (4.65)$$

At the threshold condition of having electric energy equal to the magnetic energy stored in both fields, that is as if  $E_e = E_m$ , it results from the equations above (neglecting resistance):

$$\frac{V}{I} = \sqrt{\frac{L}{C}} = Z_0 \quad (4.66)$$

The ratio above has dimensions of an impedance and is called surge impedance of the line. It can further be deduced

$$Z_0 = \sqrt{\frac{L}{C}} = \sqrt{X_L X_C} \quad (4.67)$$

The surge impedance of a transmission line is also called the characteristic impedance with resistance set equal to zero (i.e.,  $R$  is assumed small compared with the inductive reactance

The power which flows in a lossless transmission line terminated in a resistive load equal to line's surge impedance is denoted as the surge impedance loading (SIL) of the line, being also called natural power.

Under these conditions, the sending end voltage  $E_S$  leads the receiving end voltage  $E_R$  by an angle  $\delta$  corresponding to the travel time of the line.

For a three-phase line:

$$SIL = \frac{V_{\phi\phi}^2}{Z_c} \quad (4.68)$$

Where  $V_{\phi\phi}$  is the phase-to-phase voltage and  $Z_c$  is the surge impedance of the line.

Since  $Z_c$  has no reactive component, there is no reactive power in the line,

$Q_1 + Q_c = 0$ . This indicates that for SIL the reactive losses in the line inductance are exactly offset by the reactive power supplied by the shunt capacitance, or

$$I^2 \omega L = V^2 \omega C \quad (4.69)$$

SIL is a useful measure of transmission line capability even for practical lines with resistance, as it indicates a loading when the line reactive requirements are small. For power transfer significantly above SIL, shunt capacitors may be needed to minimize voltage drop along the line, while for transfer significantly below SIL, shunt reactors may be needed.

**Table 4.3** Surge Impedance Loading of Typical Overhead Lines (MW)

N° of Conductors per phase bundle kV	$Z_0$ ( $\Omega$ )	Operating voltages (kV)					
		69	138	230	345	500	765
1	400	12	48	132	298		
2	320		60	165	372	781	
3	280					893	
4	240					1042	2438
6	162					1550	3613

### 4.2.1 Methods for Increasing SIL of Overhead Lines

An effort that has been made by electric industry nowadays has been directed toward the goal of increasing the SIL of the overhead lines, especially considering the growing difficulties to acquire rights of way for new lines. For increasing the Surge Impedance Loading of an overhead line, the following ways are possible

- Voltage increase
- Reduction of  $Z_0$  through one of the measures:
  - Reducing phase spacing (compaction)
  - Increasing number of conductors per phase bundle
  - Increasing conductor diameter
  - Increasing bundle radius
  - Introducing bundle expansion along the span but keeping the conventional bundle spacing inside and near the tower.

Table 4.3 shows the surge impedance loading of typical overhead lines.

Table 4.3 is only illustrative of loading limits and is useful as an estimating tool. Long lines tend to be stability-limited and give a lower loading limit than shorter lines which tend to be voltage-drop or thermally (conductor ampacity)-limited.

### 4.2.2 Compact Lines

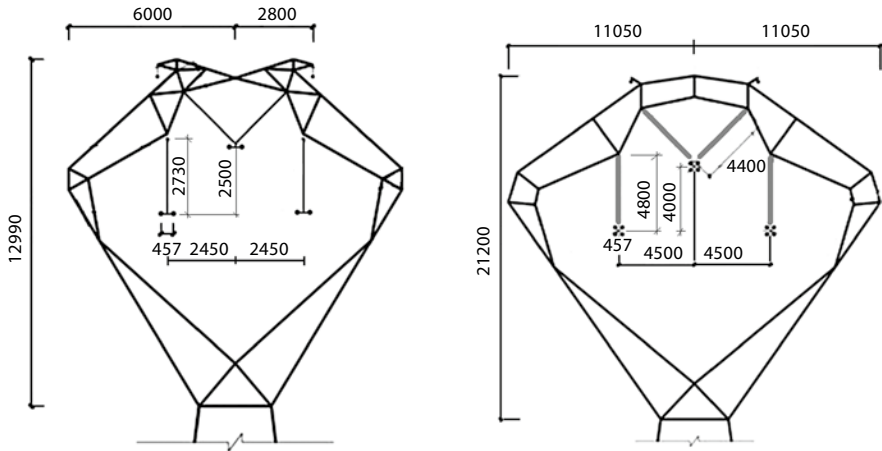
When compacted a Transmission line, the surge impedance loading can be increased. Compaction, in this case, consists of arranging the tower top geometry so that the phases are as close as possible together. As defined by equations below, the SIL reflects the interaction between line parameters, as follows:

$$SIL = \frac{V^2}{Z_1} \quad (4.70)$$

$$Z_1 = Z_s - Z_m \quad (4.71)$$

where:

SIL = Surge Impedance Loading (MW)



**Figure 4.14** Compact Racket Tower 230 kV (left) and Compact Racket Tower 500 kV (right).

- $V$  = Operation voltage (kV)
- $Z_1$  = Positive sequence impedance ( $\Omega$ )
- $Z_s$  = Self impedance ( $\Omega$ )
- $Z_m$  = Mutual impedance ( $\Omega$ ).

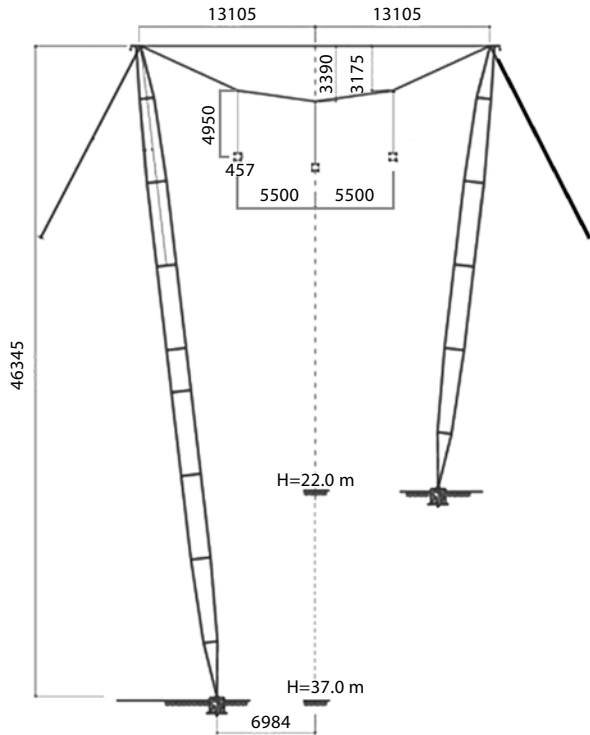
The use of compact lines is one of the most effective methods for obtaining lines with higher surge impedance loading or natural power figures. Reference (Fernandes et al. 2008) shows interesting examples of 500 kV and 230 kV lines adopted by a Utility in Brazil for having their first conventional self-supporting flat-configuration towers which generated High SIL ratings. It was designed in the beginning of the 1980's, but later a more recent development of compact lines was introduced into their system. The big aim of the engineering team consisted in reducing the required series compensation, by means of a high SIL of the lines. This represented a valuable new tool for optimizing the new planned transmission systems

As a first real gain, the use of the compaction technology, associated with the installation of series capacitor banks, could preclude for the transmission of 5000 MW the construction of two additional 500 kV – 800 km long each one – transmission circuits; the adequate use of this technology could simultaneously increase the energy transmission rate through the same corridor ( $\text{MW}/\text{m}^2$ ) and improve the effectiveness of the costs associated thereof ( $\text{MW}/\text{US\$}$ ).

Consequently, the compaction results in an increase of the coupling between phase conductors, so increasing the mutual impedance  $Z_m$  and reducing the positive sequence impedance  $Z_1$ , causing a net increase in the SIL of the line. Such technology can provide a maximum increase of around 20 to 25% in SIL, as a function of some limiting factors as: minimum viable phase spacing able to guarantee adequate insulation coordination, asynchronous swing angles between phase conductors, appropriate limitation of conductor surface gradient. Figure 4.14 shows a compact racket tower for 230 and 500 kV and Figure 4.15 shows a compact cross-rop tower.



**Figure 4.15** Compact Cross-roped Tower 500 kV.



### 4.2.3 Bundle Expansion

This technique consists in designing the bundle radius  $R$  with higher value than normal use. With that, the self impedance  $Z_p$  is reduced therefore decreasing  $Z_1$  and increasing the SIL. Similar effect is obtained by increasing the number of subconductors in the bundle, for the same total phase aluminum area.

## 4.3 Stability

A power system made up of interconnected dynamic elements may be said to have stability if it will remain in stable operation following a system disturbance.

- Steady-state stability is associated with small perturbations such as slow variation on loads or generation. It depends fundamentally on the state of the system, and on the operating conditions at the instant of the perturbation.
- Transient stability is associated with great perturbations (periodic disturbances), such as line faults, loss of a generating unit, sudden application of a big load, fault in equipment.

It strongly depends on the magnitude and size of the perturbation and less on the initial state of the system.

The stability limit is defined as:

$$P = \frac{V_1 V_2}{X_L} \sin \delta \quad (4.72)$$

Where  $P$  is the power in MW,  $V_1$  and  $V_2$  are the voltages at sending end and receiving end terminals respectively;  $\delta$  is the power angle of stability (between  $V_1$  and  $V_2$ ).

As far as dynamic stability is concerned the power angle  $\delta$  is limited to the range 30–45°, depending on the system, for the case of a generator connected to an infinite bus, instead of a theoretical higher value near 90°, to allow stability to be kept following power oscillations resulting from perturbations.

The reduction of the series reactance  $X_L$  is therefore considered by planning engineers as a convenient alternative to increase the power transmitted by the line.

---

#### 4.4 Thermal Limit and Voltage Drop

- As the conductor temperature increases, the following effects take place:
  - The ohmic resistance and therefore the losses increase.
  - The sags increase, reducing conductor-to-ground clearances or, conversely, requiring higher towers.
  - As there is an increase in rating with the increase in conductor temperature, a convenient and economic templating temperature should be chosen for every line.
  - As the conductor temperature reaches values higher than 90 °C (except for HTLS conductor), there is a loss of its mechanical strength. The mechanical strength reduction is cumulative with time and can cause sag increase and the consequent reduction of conductor to ground clearances; due to safety reasons a maximum value of 10% reduction in conductor UTS is usually accepted along the line life.

Design temperature of a conductor is defined as the highest steady-state temperature it can undergo under the worst (from a cooling viewpoint) meteorological conditions (temperature, wind, solar radiation) and current. Regarding to the determination of weather parameters for use in the case of deterministic ratings, see (Cigré TB 299).

It is usually a deterministic value. However, the determination of probabilistic ratings is becoming more and more usual, as often significant savings can be achieved. For more details, see (Stephen 1996) and also Chapter 7.

The actual recommended highest conductor (non HTLS) temperatures for line design and spotting are 75 to 85 °C for steady-state operation and 100 to 150 °C (HTLS conductors excluded) for emergency operation. The line should be spotted considering such temperatures and the relevant clearances to prevent the occurrence of safety problems.

It should be observed that new conductors (HTLS) recently developed or under development stage can be operated continuously at temperatures until 150 °C to 200 °C or even more.

**Table 4.4** Example of Maximum Current Ratings (A) of Some ACSR Conductors and Bundles used in Overhead Lines

Conditions		Steady – State				Emergency
Conductor		Winter		Summer		Summer
N × Section (mm <sup>2</sup> )	Code	Day	Night	Day	Night	Day
170/28	Linnet	505	570	400	495	660
242/40	Hawk	625	715	490	620	825
322/52	Grosbeak	803	892	644	775	1055
403/29	Tern	840	965	647	840	1100
564/40	Bluejay	1030	1200	780	1045	1370
2 × 403/29	Tern	1680	1930	1290	1680	2200
483/34	Rail	957	1100	737	959	1275
2 × 483/34	Rail	1910	2200	1470	1915	2550
3 × 483/34	Rail	2870	3300	2210	2975	3825
4 × 483/34	Rail	3820	4400	2940	3830	5100
3 × 564/40	Bluejay	3090	3600	2340	3130	4100

Parameters adopted in Table above:

- Ambient temperature: winter: 20 °C  
summer: 30 °C
- Wind speed: 1,0 m/s
- Latitude: 20°
- Solar radiation: winter: Day → 800 W/m<sup>2</sup> Night → 0 W/m<sup>2</sup>  
summer: Day → 1000 W/m<sup>2</sup> Night → 0 W/m<sup>2</sup> Conductor temperature: steady-state: 60 °C (current indicated above) emergency: 100 °C (emergency current above)

Table 4.4 shows an example of thermal limits adopted by some utilities, for steady-state and emergency conditions in lines using ACSR conductors of more widespread use.

Parameters adopted in table above:

- Ambient temperature: winter: 25 °C  
summer: 30 °C
- Wind speed: 0.61 m/s
- Latitude: 20 °C
- Solar radiation: winter: 800 W/m<sup>2</sup>  
summer: 1000 W/m<sup>2</sup>
- Conductor temperature: steady-state: 60 °C  
emergency: 100 °C
- Voltage drop: Radial lines, especially medium and long lines, up-to 138 kV have often their maximum transmitted powers limited by voltage drop or regulation.

The highest limit practically recommended for the line voltage regulation is around 10% for medium voltage lines and around 5% for EHV lines (230 kV and above). Shunt reactive compensation (capacitors or reactors depending on the SIL) are frequently required to reduce the voltage drop in certain cases.

## 4.5 Capability of a Line

It is the degree of power that can be transmitted by a line as a function of its length, considering the limitations imposed by voltage drop, stability and conductor temperature, as well as limitations inherent to substation terminal equipment, such as circuit-breakers, current transformers etc.

The main factors determining the line capability in EHV lines are shown on Table 4.5.

## 4.6 Reactive Power Compensation

There are two basic types of compensation required by an electric system as a consequence of the reactive power requirements, namely:

- Series Compensation, made up of capacitor banks connected in series with the line, offsetting part of the inductive reactance (reduction of electrical length). This compensation may be of fixed or variable value. Its main advantages are following:
  - It improves the steady-state and transient stability
  - It allows a more economical power loading
  - It reduces the voltage drop
  - If a variable type of compensation is used it can be utilized to improve the load distribution between circuits.

When using series compensation, especial attention should be given to other factors affecting technically and economically the system such as, capacitor protection, line protection and sub-synchronous resonance.

- Shunt compensation

The main shunt compensation schemes used in electric systems are:

- Reactors, for long EHV lines for compensating line capacitive powers in hours of light load (Ferranti Effect)
- line connected reactors for line energization
- Capacitors, for voltage control and power factor correction during hours of higher demand load
- Synchronous condensers (rarely used nowadays) that can perform the both functions of reactors or of capacitors, depending on the instantaneous system needs.
- Static compensators that perform the same function of the above synchronous condensers, but have no moving parts.

**Table 4.5** Determinant factors on EHV line capability

Line Length (km)	Governing condition
0-80	Thermal limit
80-320	Voltage drop
> 320	Stability

## 4.7 Electromagnetic Unbalance - Transposition

Transpositions are made for the purpose of reducing the electrostatic and electromagnetic unbalance among the phases which can result in unequal phase voltages for long lines.

Untransposed lines can cause/increase in the following undesirable effects:

- Inductive interference with paralleling wire communication lines.
- Negative sequence currents that heat generator rotors.
- Zero sequence currents that can cause erroneous operation of protection relays.

For carrying out physically the phase transposition of the conductors, some alternatives can be used such as making them in intermediate substations or near dead-end towers through especial conductor and insulator string arrangements or through the utilization of special structures that allow changing phase positions by keeping the necessary clearances to the towers and to earth.

Instead of performing phase transpositions, it is possible to adopt alternatives that preclude them, such as:

- Use of delta or triangular phase configurations
- In rare cases.

---

## 4.8 Losses

The following types of losses have to be considered in overhead transmission lines.

### 4.8.1 Losses by Joule Heating Effect ( $RI^2$ ) in the Conductors

Those are the main losses that occur in the overhead conductors and their correct selection and design are decisive for obtaining an economical line. Losses should be seen as wasteful as they represent consumption of fuels or lowering of water reservoirs without the corresponding generation of useful work.

The power  $RI^2$  spent in the conductors and joints reduce the efficiency of the electric system and its ability to supply new loads while the heat  $RI^2\Delta t$  represents burnt fuel or loss of useful water.

### 4.8.2 Dielectric Losses: Corona Losses, Insulator and Hardware Losses

By careful design and specifications of single or bundle conductors and accessories, maximum conductor gradients may be limited so as to generate minimum Corona losses under fair and foul weather conditions. Similarly a careful design of accessories and insulators can reduce to negligible values the amount of leakage currents and the resulting losses.

### 4.8.3 Losses by Induced Currents

The shield wires of the line are metallic conductors subjected to induced currents by the line conductors and therefore producing losses. There are usually three alternatives for reducing the shield wire losses, consisting basically in insulating them from the towers so that only negligible currents can circulate through them:

- By insulating sections of the shield wires in the towers and just earthing an intermediate point
- By totally insulating the shield wires in the towers, i.e. not grounding them in any point.

Certain utilities have shown that the shield wire insulation has sometimes caused flashovers along the respective insulator, this is usually an insulator with a low flashover capability as it must offer a free conductive path for lightning stroke currents. The current continues to flow in the shield wire until line is opened.

So, in the case the Utility decides to evaluate the economic feasibility of insulating the shield wires for reducing line losses, a compromise must be found between the savings in losses and the additional cost of insulating and maintaining the shield wires and insulators.

---

## 4.9 Reliability and Availability

Consideration of the two important aspects of continuity and quality of supply, together with other relevant elements in the planning, design, control, operation and maintenance of an electric power system network, is usually designated as reliability assessment.

Generally the past performance of a system is calculated according to some performance indices.

SAIFI-System Average Interruption Frequency Index; SAIDI-System Average Interruption Duration Index.

For the transmission lines, the unavailability is measured in terms of hours per year or percent of time while the lines have been out.

Two considerations are more usual, namely:

- Mechanical Unavailability of the weakest component (towers), equal to the inverse of twice the Return Period of the Design Wind Velocity, as per Reference (Nolasco et al. 2002). The unavailability of all other components together usually doesn't exceed 25% of the one for the towers.
- Electrical Unavailability, considered equal to the unsuccessful reclosing operation when a lightning flashover occurs. Generally 65 to 70% of the reclosing operations are successful. Such faults are usually caused by lightning strokes that reach the conductors, towers or shield wires. An index that is generally used for measuring an overhead line. Bush firing may create a similar problem.

- Performance in the last case is the number of outages/100 km/year. The time used for line maintenance (not live) is also part of the index.
- Additionally adverse weather conditions can add about for instance 0.3 events per year with an average duration below 10 hours in general.

---

## 4.10 Overvoltages

The AC system overvoltages stresses are the input of the insulation coordination study for the design of clearances and of the insulator string of transmission line.

The overvoltages can be classified as:

- Sustained voltages: continued power frequency voltages originated from system operation under normal conditions; and temporary sustained overvoltages originating from switching operations such as load rejection, energization and resonance conditions.
- Slow front overvoltages (switching surges): due to faults and switching operations
- Fast front overvoltages: originated mainly from lightning strikes or certain types of switching
- Very fast front overvoltages: mainly related with gas insulated substation equipment switching.

### 4.10.1 Fast-front Overvoltages (Lightning Overvoltages)

An important aspect to be considered in overhead transmission lines is their lightning performance.

Usually, the lightning performance criterion to be considered in the project of a line or in the performance evaluation of an existing line is the maximum number of flashovers, due to lightning, that can occur in the line per 100 km per year.

As the transmission line nominal voltage increases, the overvoltages generated by lightning becomes less important to the specification of its insulation. This is due to the increase in importance of other overvoltages such as switching surges.

Examples of lightning performance of real lines are shown on the Table 4.6. As expected, the flashover rate caused by lightning is greater for lines with the lower nominal voltages.

Lightning strokes to ground near a line or directly on it (on its conductors, towers or ground wires) can generate high over-voltages that cause flashover in their insulation and, consequently, the outage of the line.

Even though it is not the objective of the present item the detailed discussion of lightning phenomenon and the results of studies and researches developed to understand its various aspects (that can be found in Cigré TB 549, 2013), a summary of its most important parameters to the design of an overhead transmission line is presented.

To evaluate the lightning performance of transmission lines it is necessary to considerer many additional aspects, primarily those related to the attachment

**Table 4.6** Examples of transmission line lightning performance (Anderson, 1975)

Nominal Voltage (kV)	Lightning performance (Flashovers/100 km-Year)
11-22	20.3
42	21.9
88	11.9
132	5.0
275	1.9
400	0.6
500	0.5
765	0.3

process of lightning channel to them, the electromagnetic surges generated in the line when impulse currents are injected on them and the overvoltages withstand by their insulation.

#### 4.10.1.1 Lightning Discharge Parameters

The primary lightning parameters are described, in [Cigré TB 549](#), and is summarized here to emphasize the primary aspects relevant to a usual transmission line design ([Cigré TB 549](#)).

Lightning can be defined as a transient, high-current (typically tens of kA) electric discharge in air whose length is measured in kilometers. The lightning discharge in its entirety, whether it strikes ground or not, is usually termed a “lightning flash” or just a “flash.” A lightning discharge that involves an object on ground or in the atmosphere is sometimes referred to as a “lightning strike”. The terms “stroke” or “component stroke” apply only to components of cloud-to-ground discharges. Most lightning flashes are composed of multiple strokes. All strokes other than the “first” are referred to as “subsequent” strokes.

Each lightning stroke is composed of a downward-moving process, termed a “leader”, and an upward-moving process, termed a “return stroke”. The leader creates a conducting path between the cloud charge source region and ground and distributes electric charge from the cloud source along this path, and the return stroke traverses that path moving from ground toward the cloud charge source and neutralizes the leader charge. Thus, both leader and return stroke processes serve to effectively transport electric charge of the same polarity (positive or negative) from the cloud to ground.

The kA-scale impulsive component of the current in a return stroke is often followed by a “continuing current” which has a magnitude of tens to hundreds of amperes and a duration up to hundreds of milliseconds. Continuing currents with duration in excess of 40 ms are traditionally termed “long continuing currents”. These usually occur in subsequent strokes.

The global lightning flash rate is some tens to a hundred flashes per second or so. The majority of lightning flashes, about three-quarters, do not involve ground. These are termed cloud flashes (discharges) and sometimes are referred to as ICs. Cloud discharges include intra cloud, inter cloud, and cloud-to-air discharges.



Lightning discharges between cloud and earth are termed cloud-to-ground discharges and sometimes referred to as CGs. The latter constitute about 25% of global lightning activity.

From the observed polarity of the charge lowered to ground and the direction of propagation of the initial leader, four different types of lightning discharges between cloud and earth have been identified: (a) downward negative lightning (b) upward negative lightning (c) downward positive lightning, and (d) upward positive lightning. Downward flashes exhibit downward branching, while upward flashes are branched upward.

It is believed that downward negative lightning flashes (type a) account for about 90% or more of global cloud-to-ground lightning, and that 10% or less of cloud-to-ground discharges are downward positive lightning flashes (type c). Upward lightning discharges (types b and d) are thought to occur only from tall objects (higher than 100 m or so) or from objects of moderate height located on mountain tops.

As noted above, positive lightning discharges are relatively rare (less than 10% of global cloud-to-ground lightning activity). Positive lightning is typically more energetic and potentially more destructive than negative lightning.

Sometimes both positive and negative charges are transferred to ground during the same flash. Such flashes are referred to as bipolar. Bipolar lightning discharges are usually initiated from tall objects (are of-upward type). It appears that positive and negative charge sources in the cloud are tapped by different upward branches of the lightning channel. Downward bipolar lightning discharges do exist, but appear to be rare.

The ground flash density  $N_g$  (flashes/km<sup>2</sup>/yr) is often viewed as the primary descriptor of lightning incidence. Ground flash density has been estimated from records of lightning flash counters (LFCs) and lightning locating systems (LLSs) and can potentially be estimated from records of satellite-based optical or radio-frequency radiation detectors. It is worth noting that satellite detectors cannot distinguish between cloud and ground discharges and, hence, in order to obtain  $N_g$  maps from satellite observations, a spatial distribution of the fraction of discharges to ground relative to the total number of lightning discharges is needed. IEEE Std 1410-2010 recommends, in the absence of ground-based measurements of  $N_g$ , to assume that  $N_g$  is equal to one-third of the total flash density (including both cloud and ground discharges) based on satellite observations (IEEE Standard 1410-2010).

If no measurements of the ground flash density  $N_g$  for the area in question are available, this parameter can be roughly estimated from the annual number of thunderstorm days  $T_d$ , also called the keraunic level. Apparently the most reliable expression relating  $N_g$  and  $T_d$  is the one proposed by (Anderson et al. 1984):

$$N_g = 0.04T_d^{1.25} \quad (4.73)$$

Another characteristic of lightning activity that can be used for the estimation of  $N_g$  is the annual number of thunderstorm hours  $T_H$ . The relation between  $N_g$  and  $T_H$  proposed by (MacGorman et al. 1984) is:

$$N_g = 0.054T_h^{1.1} \quad (4.74)$$

A typical negative cloud-to-ground flash is composed of 3 to 5 strokes (leader/return stroke sequences), with the geometric mean inter-stroke interval being about 60 ms. Occasionally, two leader/return stroke sequences occur in the same lightning channel with a time interval between them as short as 1 ms or less.

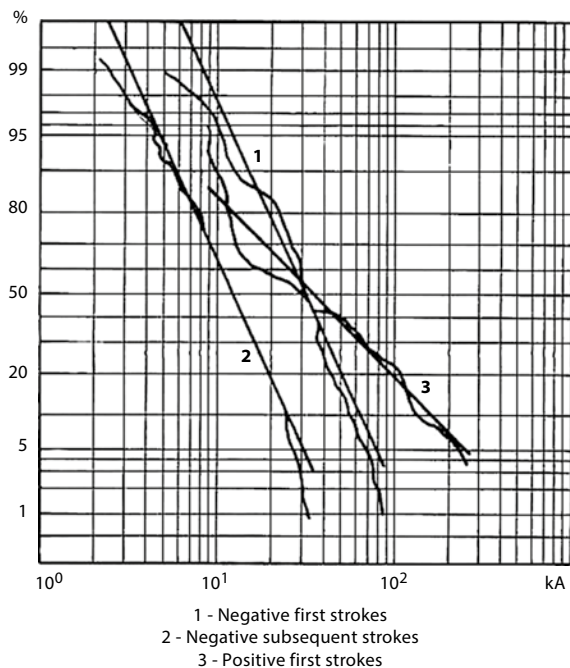
The observed percentage of single-stroke flashes, based on accurate-stroke-count studies is about 20% or less, which is considerably lower than 45% presently recommended by Cigré.

First-stroke current peaks are typically a factor of 2 to 3 larger than subsequent-stroke current peaks. However, about one third of cloud-to-ground flashes contain at least one subsequent stroke with electric field peak, and, by theory, current peak, greater than the first-stroke peak.

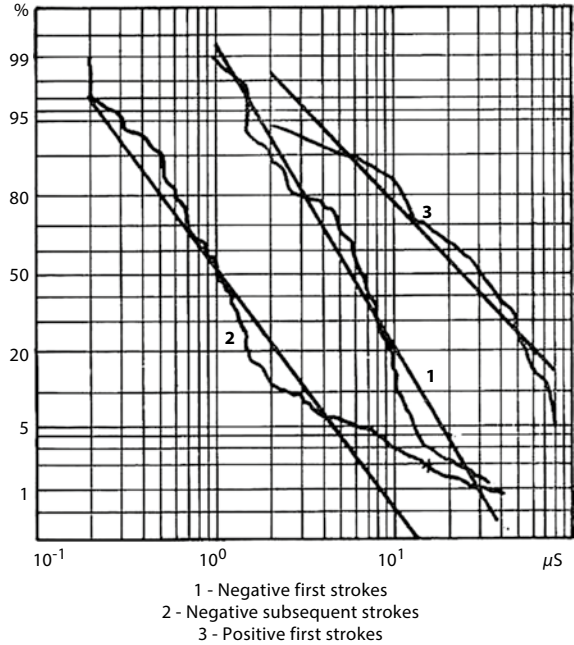
Traditional lightning parameters needed in engineering applications include lightning peak current, maximum current derivative, average current rate of rise, current rise time, current duration, charge transfer, and action integral (specific energy), all derivable from direct current measurements.

Essentially all national and international lightning protection standards (IEEE Standard 1410; IEEE Std 1243; IEC 62305), include a statistical distribution of peak currents for first strokes in negative lightning flashes (including single-stroke flashes). This distribution, which is one of the cornerstones of most lightning protection studies, is largely based on direct lightning current measurements conducted in Switzerland from 1963 to 1971 (Anderson and Eriksson 1980). The cumulative statistical distributions of lightning peak currents for negative first strokes, negative subsequent strokes and positive first strokes are presented in Figures 4.16, 4.17, and 4.18.

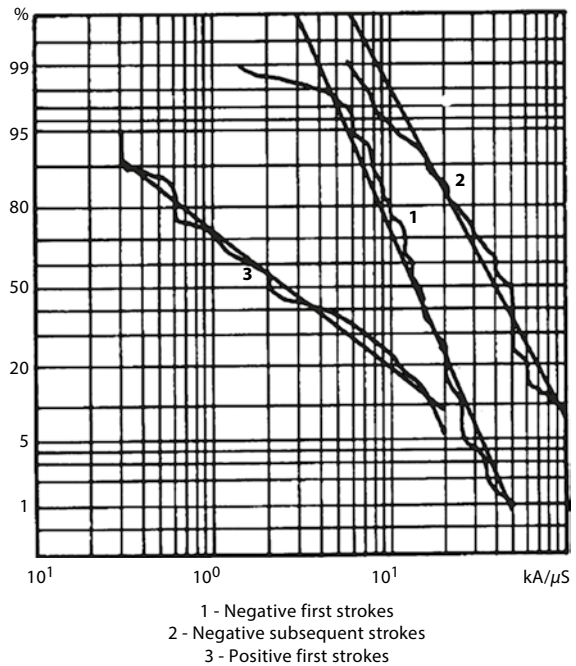
**Figure 4.16** Cumulative statistical distributions of lightning peak currents, giving percent of cases exceeding abscissa value, from direct measurements in Switzerland.



**Figure 4.17** Cumulative statistical distributions of crest time, giving percent of cases exceeding abscissa value, from direct measurements in Switzerland.



**Figure 4.18** Cumulative statistical distributions of current rate of rise, giving percent of cases exceeding abscissa value, from direct measurements in Switzerland (Berger et al. 1975).



The distributions are assumed to be log-normal and give percent of cases exceeding abscissa value.

The log-normal probability density function for peak current  $I$  is given by:

$$f(I) = \frac{1}{\sqrt{2\pi}\beta I} e^{-\left(\frac{z^2}{2}\right)} \quad (4.75)$$

Where:

$$z = \frac{\ln I - \text{Mean}(\ln I)}{\beta} \quad (4.76)$$

and  $\ln I$  is the natural logarithm of  $I$ ,  $\text{Mean}(\ln I)$  is the mean value of  $\ln I$ , and  $\beta = \sigma_{\ln I}$  is the standard deviation of  $\ln I$ .

A log-normal distribution is completely described by two parameters, the median and logarithmic standard deviation of the variable. Logarithmic standard deviations of lightning peak currents are often given for base 10.

$$P(I) = \int_I^{\infty} \frac{1}{\sqrt{2\pi}\beta\lambda} e^{-\left(\frac{z^2}{2}\right)} d\lambda \quad (4.77)$$

Only a few percent of negative first strokes exceed 100 kA, while about 20% of positive strokes have been observed to do so. About 95% of negative first strokes are expected to exceed 14 kA, 50% exceed 30 kA, and 5% exceed 80 kA. The corresponding values for negative subsequent strokes are 4.6, 12, and 30 kA, and 4.6, 35, and 250 kA for positive strokes. Subsequent strokes are typically less severe in terms of peak current and therefore often neglected in lightning protection studies. Slightly more than 5% of lightning peak currents exceed 100 kA, when positive and negative first strokes are combined.

Berger's peak current distribution for negative first strokes shown in Figure 4.18 is based on about 100 direct current measurements. The minimum peak current value included in Berger's distributions is 2 kA.

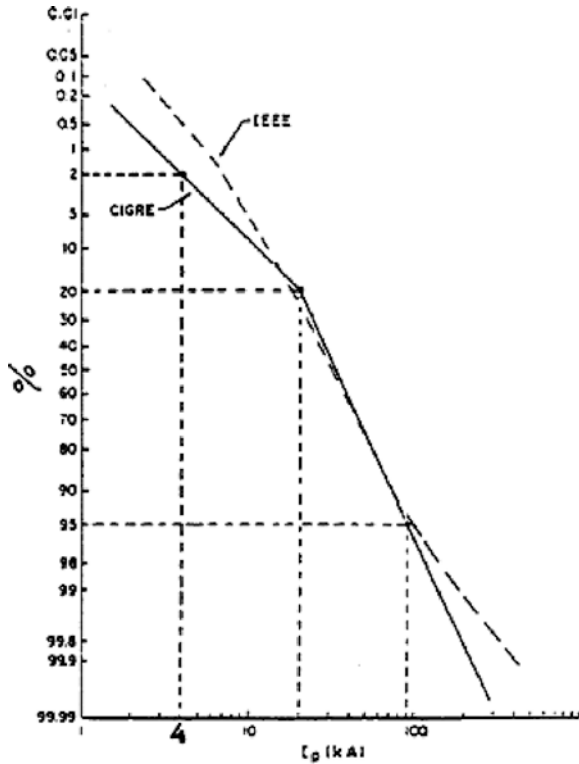
In lightning protection standards, in order to increase the sample size, Berger's data are often supplemented by limited direct current measurements in South Africa and by less accurate indirect lightning current measurements obtained (in different countries) using magnetic links. There are two main distributions of lightning peak currents for negative first strokes adopted by lightning protection standards: the IEEE distribution (IEEE Standard 1410; IEEE Std 1243; Cigré WG 33-04). Both these "global distributions" are presented in Figure 4.19.

For the Cigré distribution, 98% of peak currents exceed 4 kA, 80% exceed 20 kA, and 5% exceed 90 kA.

For the IEEE distribution, the "probability to exceed" values are given by the following equation:

$$P(I) = \frac{1}{1 + \left(\frac{I}{31}\right)^{2.6}} \quad (4.78)$$

**Figure 4.19** Cumulative statistical distributions of peak currents (percent values on the vertical axis should be subtracted from 100% to obtain the probability to exceed).



**Table 4.7** Peak current distributions adopted by IEEE

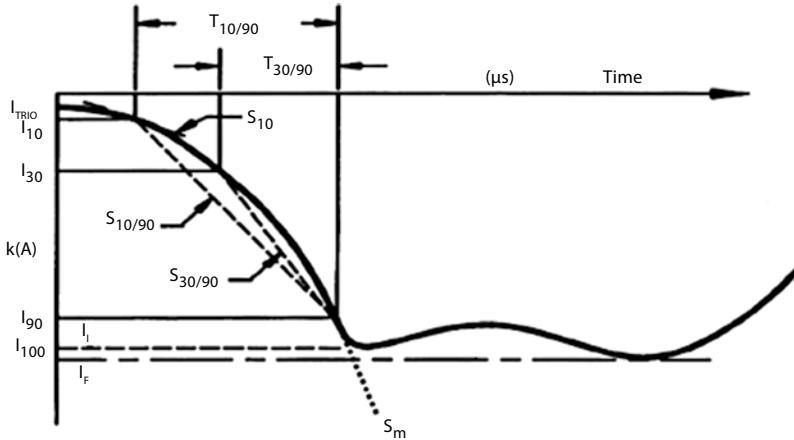
Peak current, I, kA		5	10	20	40	60	80	100	200
Percentage exceeding tabulated value, P(t) 100%	First strokes	99	95	76	34	15	7.8	4.5	0.78
	Subsequent strokes	91	62	20	3.7	1.3	0.59	0.33	0.050

where  $P(I)$  is in per unit and  $I$  is in kA. This equation, usually assumed to be applicable to negative first strokes, is based on data for 624 strokes analyzed by (Popolansky 1972), whose sample included both positive and negative strokes, as well as strokes in the upward direction. This equation applies to values of  $I$  up to 200 kA. Values of  $P(I)$  for  $I$  varying from 5 to 200 kA, computed using the previous equation are given in Table 4.7. The median (50%) peak current value is equal to 31 kA.

In the range of 10 to 100 kA that is well supported by experimental data, the IEEE and Cigré distributions are very close to each other (IEEE Standard 1410).

The peak-current distribution for subsequent strokes adopted is given by:

$$P(I) = \frac{1}{1 + \left(\frac{I}{12}\right)^{2.7}} \tag{4.79}$$



**Figure 4.20** Description of lightning current waveform parameters. The waveform corresponds to the typical negative first return stroke. Adapted from Cigré TB 63 and IEEE Std 1410-2010.

Cigré recommends for negative subsequent stroke peak currents a log-normal distribution with the median of 12.3 kA and  $\beta=0.53$  (Cigré WG 33-04), which is also included in IEEE Std 1410-2010.

In Cigré TB 549, it is discussed what it called “global” distribution of peak current found in most lightning protection standards. Concern is expressed about using imprecise or not homogeneous data (lumped or not in a single sample with data considered more reliable). In this document, recent distributions of lightning peak currents obtained from many individual studies are presented and compared.

A representative double-peaked current waveform of negative first strokes is presented in Figure 4.20, with the definition of its front parameters.

Table 4.8 are lists the values of the lightning current parameters of Figure 4.20 recommended by Cigré and IEEE.

#### 4.10.1.2 Equivalent Impedance of the Lightning Channel

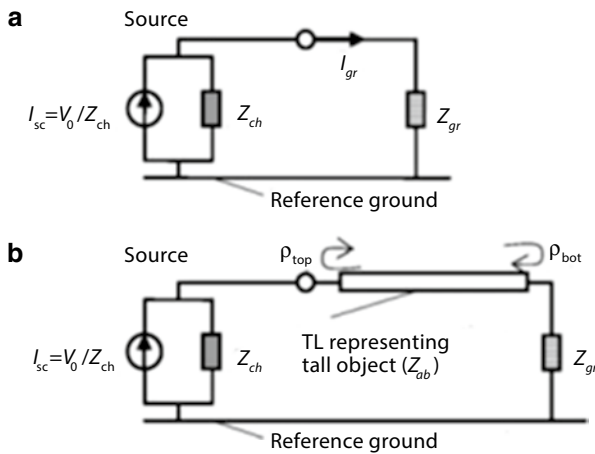
Lightning-channel impedance is an important parameter that can influence the current injected into the object subjected to a strike.

##### *Direct-strike Effects*

Lightning is approximated by a Norton equivalent circuit. This representation includes an ideal current source equal to the lightning current that would be injected into the ground if that ground were perfectly conducting (a short-circuit current,  $I_{sc}$ ) in parallel with a lightning-channel impedance  $Z_{ch}$  assumed to be constant. In the case when the strike object can be represented by lumped grounding impedance,  $Z_{gr}$ , this impedance is a load connected in parallel with the lightning Norton equivalent (Figure 4.21). Thus, the “short-circuit” lightning current  $I_{sc}$  effectively splits between  $Z_{gr}$  and  $Z_{ch}$  so that the current flowing from the lightning-channel base into the

**Table 4.8** Lightning current parameters (based on Berger’s data) recommended by Cigré and IEEE

Parameter	Description
$I_{10}$	10% intercept along the stroke current waveshape
$I_{30}$	30% intercept along the stroke current waveshape
$I_{90}$	90% intercept along the stroke current waveshape
$I_{100}=I_1$	Initial peak of current
$I_F$	Final (global) peak of current (same as peak current without an adjective)
$T_{10/90}$	Time between $I_{10}$ and $I_{90}$ intercepts on the wavefront
$T_{30/90}$	Time between $I_{30}$ and $I_{90}$ intercepts on the wavefront
$S_{10}$	Instantaneous rate-of-rise of current at $I_{10}$
$S_{10/90}$	Average steepness (through $I_{10}$ and $I_{90}$ intercepts)
$S_{30/90}$	Average steepness (through $I_{30}$ and $I_{90}$ intercepts)
$S_m$	Maximum rate-of-rise of current along wavefront, typically at $I_{90}$
$t_{d 10/90}$	Equivalent linear wavefront duration derived from $I_F/S_{10/90}$
$t_{d 30/90}$	Equivalent linear wavefront duration derived from $I_F/S_{30/90}$
$T_m$	Equivalent linear waveform duration derived from $I_F/S_m$
$Q_I$	Impulse charge (time integral of current)



**Figure 4.21** Engineering models of lightning strikes (a) to lumped grounding impedance and (b) to a tall grounded object.

ground is found as  $I_{gr} = I_{sc} Z_{ch} / (Z_{ch} + Z_{gr})$ . Both source characteristics,  $I_{sc}$  and  $Z_{ch}$ , vary from stroke to stroke, and  $Z_{ch}$  is a function of channel current, the latter nonlinearity being in violation of the linearity requirement necessary for obtaining the Norton equivalent circuit. Nevertheless,  $Z_{ch}$ , which is usually referred to as equivalent impedance of the lightning channel, is assumed to be constant.

### **Lightning-Induced Effects**

In studying lightning-induced effects, the distribution of current along the lightning channel is needed for computing electric and magnetic fields (Baba and Rakov).

### **Equivalent Impedance**

The limited estimates of the equivalent impedance of lightning channel from experimental data suggest values ranging from several hundred  $\Omega$  to a few k $\Omega$ .

#### **4.10.1.3 Protection of Power Transmission Lines - Concepts**

Lightning strokes can cause insulation flashover when they strike the conductors, ground wires or even the soil nearby the transmission lines.

- Flashover caused by Induced surges.

Lightning striking to soil nearby a transmission line can induce surge overvoltages on it. Most measurements of induced voltage have been less than 300 kV.

This level of overvoltage can cause flashover in medium voltage lines, but usually is not a concern to high voltage transmission line.

- Flashover caused by direct strokes to conductors.

When a lightning strikes a conductor of a transmission line, a high impulse overvoltage is developed between the conductor and tower (in the insulator strings or air gaps), the conductor and other phase conductors or the conductor and ground. These impulse overvoltages can cause flashover in the line. As the insulation strings are, usually, the elements with the lowest impulse insulation level, they are the element with the greatest probability of occurrence of flashover.

The peak of the impulse overvoltage generated by a direct stroke in a conductor with a surge impedance  $Z$  can be estimated, approximately, by:

$$V_{surge} \cong \frac{Z I_{peak}}{2} \quad (4.80)$$

where  $I_{peak}$  is the peak current of stroke.

Considering a surge impedance  $Z$  of 400  $\Omega$ , it is easy to see that even a low discharge current of 10 kA can generate very high overvoltages in the conductor (2 MV).

So, when a line with high performance is desired, it is necessary to provide some protection to reduce the probability of direct strokes to the conductors that exceed the insulation level of the line.

- Flashover caused by direct strokes to shield wire or tower.

Even installing ground wires in a line, they cannot eliminate the probability of flashover in the line caused by lightning.

High impulse overvoltage can still be generated, especially in the presence of a large peak current.

Related to the lightning stroke hitting the ground wires, as the impulse impedance seen from the point of incidence of the stroke is not low (it is depends on the surge impedance of various elements: ground wires, tower, grounding system,



length of span, etc.), the ground wires voltage can reach very high values. The tower top voltage rises too.

Then, consequently, the insulation of the line is stressed by the large voltage generated between the tower or ground wires and the conductors. If this voltage is high enough, a flashover can occur. This flashover is called back flashover, as it tends to occur from the grounded elements (tower or ground wire) to the energized phase conductors.

### **Induced Surges**

Induced surge by nearby lightning discharge is not a concern to high voltage transmission lines.

In medium voltage lines, some measures can be implemented to improve the performance of the line in respect to flashover caused by nearby strokes.

### **Direct Strokes to Conductors**

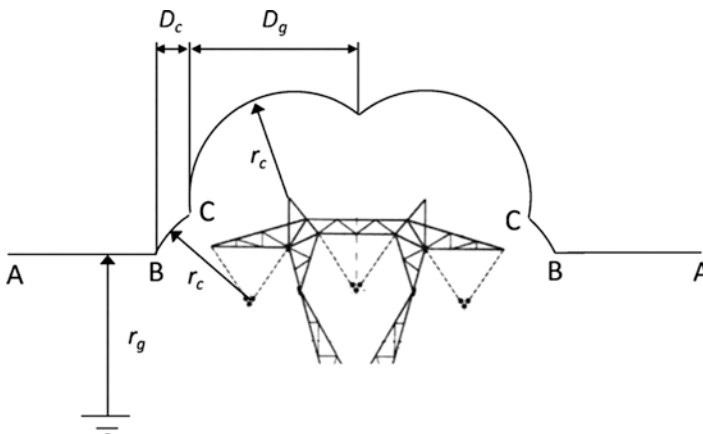
Lightning strokes, with relatively high peak currents, directly to phase conductors can generate very high overvoltages on them, which can cause a line outage in case of flashover.

To reduce the probability of occurrence of such high overvoltages, the most common measure is to install shield wires on the lines. Other measure is the installation of surge arresters. In respect to the installation of shield wires, in a specific line, it is necessary to make a shielding analysis to determine the number and the position relative to the phase conductors.

In both ([Cigré WG 33-04](#)) and ([IEEE Std 1243](#)), the so-called electro-geometric model (EGM) is employed.

The basic concepts involved in this model will be explained using Figure 4.22.

Several researchers have contributed to the electro geometric model (EGM). As the downward leader approaches the earth, a point of discrimination is reached for a final leader step. The EGM portrays this concept with the use of striking distances.



**Figure 4.22** Electrogeometric model representation of conductors and ground wires.

The striking distance is of the form

$$r_{c,g} = AI^b \quad (4.81)$$

Where  $A$  and  $b$  are constants that depend on the object and  $I$  is the stroke current.

Local electric field gradients around conductors are somewhat higher than at ground level, so  $r_c$  is usually considered to be greater than  $r_g$  (the striking distance to ground), resulting in  $r_c \geq r_g$ . Arcs of circles with the radii  $r_c$  are drawn centered at the phase conductor and OHGW. A horizontal line is then drawn at a distance  $r_g$  from earth.

If a downward leader, having a prospective current  $I$ , for which the arcs were drawn, touches the arcs between B and C (Figure 4.22), the leader will strike the phase conductor. If the leader touches the arcs between B's, it will strike the shield wire. If all leaders are considered vertical, the exposure distance for a shielding failure is  $D_c$ .

Since the final jump length in the EGM depends on current, the statistics of the stroke-current distribution will be needed to compute the number of lightning strokes to phase conductors (that depend on  $D_c$ ).

At present, the following striking distance equations are recommended by IEEE (IEEE Std 1243):

$$r_c = 10I^{0.65} \quad (4.82)$$

$$r_g = \begin{cases} \left[ 3.6 + 1.7 \ln(43 - y_c) \right] I^{0.65} & y_c < 40m \\ 5.5I^{0.65} & y_c \geq 40m \end{cases} \quad (4.83)$$

where  $I$  is the stroke current (in kA) and  $y_c$  is the average conductor height, given by the height at the tower minus two-thirds of the sag.

Some researchers of EGM assume all striking distances are equal, while others consider different striking distances to phase conductors, shield wires, and earth. In addition, some researchers do not use a striking distance to earth. Estimates of striking distance sometimes differ by a factor of two. However, this uncertainty has not prevented the design and operation of lines with low lightning outage rates. In particular, when an engineering judgment is made to accept a low but non-zero shielding failure flashover rate (*SFFOR*), most models suggest similar shielding angles.

Figure 4.22 indicates an apparent possibility of perfect shielding: the possibility to install ground wires in a position that makes  $D_c$  null for lightning stroke currents greater than a minimal current necessary to cause flashover when it strikes directly the phase conductors (called critical current  $I_c$ ).

### **Strokes to Shield Wire or Towers**

High impulse overvoltage can be generated in a transmission line when high intensity lightning strikes its ground wires or towers. If the overvoltage stressing the insulation of the line is greater than the voltage that it can withstand, a flashover occurs (in this case, called back-flashover).

To reduce the probability of occurrence of back flashover to an acceptable level, in the design of a transmission line, one important aspect to be considered is the appropriate design of structure grounding systems. It should be considered the necessary value of resistance to achieve the desired lightning performance of the line, but also the fact that the transient response of grounding system cannot be expressed only by its resistance to low frequency and low amplitude currents. For example, a long counterpoise cable can have relatively low resistance to industrial frequency currents, but high impulse impedance (as will be discussed latter. Usually, a number of parallel cables is better than a long counterpoise.

In areas of large flash density and high electrical resistivity of soil, sometimes it is necessary to reduce the resistance to a level that is not possible technically or economically. In these cases, one of the most efficient measures is the installation of surge arresters in the line.

To identify which measures needed to be implemented, it is necessary to evaluate the lightning performance of the line with and without those measures, even if some approximation should be done. The evaluation of lightning performance of transmission lines is then discussed.

#### **4.10.1.4 Evaluating the Lightning Performance of a Power Transmission Line**

To estimate the lightning performance of OHTL the following primary aspects should be considered (information also in 4.10.1.1):

- Ground flash density along the line
- Lightning current parameters (primarily its peak distribution)
- Lightning stroke to the transmission line and to its individual components
- Estimate of insulation stress when lightning strikes the line
- Flashover strength of insulation to the over-voltage
- Estimate the rate of insulation flashover due to lightning striking directly the conductors (shielding flashover) or due to backflashover phenomenon (lighting strokes to ground wires or towers).

In terms of calculation, the fourth aspect in the above list is the most complex, because it involves the estimation of the transient response of relative complex elements that are interconnected: conductors and ground wires (depending on the current front of wave), towers and grounding systems. Usually, many simplifications are done to reduce the complexity of calculation and enable the use of simple computational routines in the lightning performance calculation.

Knowing the current that can reach a component of the line, the comparison of the results of overvoltage stress with the flashover strength of insulation will indicate if the flashover will occur.

In the final the lightning performance of an overhead transmission line can be calculated. Basically, knowing the currents that can reach the line and cause a flashover and its probability of occurrence, it should be determined:

- the shielding failure flashover rate (relative to the lightning strokes directly to conductors);
- the back flashover rate (relative to the lightning strokes on the ground wires or towers);
- overall flashover rate (the sum of the two previous rates).

These rates usually are expressed as number of flashovers per 100 km of line per year.

Two proposed specific procedures for estimating the lighting performance of transmission lines are described in the documents (IEEE Std 1243; Cigré WG 33-04). In the following items the primary aspects involved in the estimation procedures of lightning performance of transmission lines, as recommended by IEEE and Cigré, are characterized, keeping in mind the practical design objective.

### Ground Flash Density

The ground flash density  $N_g$  can be roughly estimated from the annual number of thunderstorm days  $T_D$ , by the equations shown in 4.10.1.1.

### Lightning Current Parameter Considered

Anderson and Eriksson (1980) noted that the two sub-distributions (below and above 20 kA) can be viewed as corresponding to the shielding failure and back-flashover regimes, respectively. A single distribution, also shown in Figure 4.19, was adopted by IEEE guidelines consider a triangular (2  $\mu$ s/50  $\mu$ s) implemented in the software “Flash”.

For the IEEE distribution, the “probability to exceed” value of peak currents from 2 kA to 200 kA are given by the following equation:

$$P(I) = \frac{1}{1 + \left(\frac{I}{31}\right)^{2.6}} \quad (4.84)$$

where  $P(I)$  is in per unit and  $I$  is in kA.

Cigré guidelines consider a concave front current as shown in Figure 4.20, with parameters listed in Tables 4.8 and 4.9.

The log-normal probability density function for peak current  $I$  is given by:

$$f(I) = \frac{1}{\sqrt{2\pi} \beta I} e^{-\left(\frac{z^2}{2}\right)} \quad (4.85)$$

The probability for peak current to exceed a specified value  $I$  is given by:

$$P(I) = \int_I^{\infty} \frac{1}{\sqrt{2\pi} \beta \lambda} e^{-\left(\frac{z^2}{2}\right)} d\lambda \quad (4.86)$$

**Table 4.9** Lightning current parameters (based on Berger’s data) recommended by Cigré and IEEE

Parameter	First stroke		Subsequent stroke	
	M, Median	β, logarithmic (base e) standard deviation	M, Median	β, logarithmic (base e) standard deviation
	Front time (μs)			
$t_{d10/90} = t_{10/90}/0.8$	5.63	0.576	0.75	0.921
$t_{d30/90} = t_{30/90}/0.6$	3.83	0.553	0.67	1.013
$t_m = I_f/S_m$	1.28	0.611	0.308	0.708
	Steepnes (kA/μs)			
$S_m$ , Maximum	24.3	0.599	39.9	0.852
$S_{10}$ , at 10%	2.6	0.921	18.9	1.404
$S_{10/90}$ , 10-90%	5.0	0.645	15.4	0.944
	Peak (Crest) current (A)			
$I_i$ , initial	27.7	0.461	11.8	0.530
$I_f$ , final	31.1	0.484	12.3	0.530
Ratio, $I_i/I_f$	0.9	0.230	0.9	0.207
Other relevant parameters				
Tail time to half value $t_h$ (μs)	77.5	0.577	30.2	0.933
Number of strokes per flash	1	0	2.4	0.96 based on median
				$N_{total} = 3.4$
Stroke charge, $Q_1$ (Coulomb)	4.65	0.882	0.938	0.882
$\int I^2 dt [ (kA)^2 s ]$	0.057	1.373	0.0055	1.366
Interstroke interval (ms)	–	–	35	1.066

**Lightning to the Transmission Line**

NUMBER OF LIGHTNING STROKES THAT HIT THE LINE

IEEE guidelines use the same expression as Cigré to evaluate the number of lightning strokes the hits a transmission line:

$$N_l = \frac{N_g}{10} (28h^{0.6} + b) \tag{4.87}$$

where  $N_g$  is the ground flash density (flashes/km<sup>2</sup>/yr),  $h$  is the tower height (m) and  $b$  is the ground wires separation distance between (m).

LIGHTNING STROKES THAT HIT THE PHASE CONDUCTORS

In IEEE and Cigré procedures, for a line with ground wires, the number of lightning strokes that hit directly the phase conductors are expressed as shielding failure rate (*SFFOR*), calculated by:

$$SFFOR = 2N_g L \int_3^{I_{max}} D_c(I) f(I) dI \quad (4.88)$$

where:

$L$  = length of the line (km)

$D_c(I)$  = exposure length (m) relative to phase conductor, calculated in function of  $I$

$f(I)$  = statistical distribution of  $I$

$I_{max}$  = maximum current (kA) that can hit the phase conductor (current that makes null the distance  $D_c(I)$ ).

The lower limit, 3 kA, recognizes that there is a lower limit to the stroke current.

### Strength of Insulation

To identify if a flashover will occur on an insulator string stressed by an overvoltage generated by a lightning stroke that hits a line, IEEE evaluate the voltage necessary to cause a flashover in an insulator string with the following equations:

$$V_D = \left( 400 + \frac{710}{t^{0.75}} \right) l \quad (0.5\mu s \leq t \leq 16\mu s) \quad (4.89)$$

where  $V_D$  is the impulse flashover voltage in kV,  $t$  is the time to flashover in  $\mu s$  and  $l$  is the insulator string length in m.

For  $t$  greater than 16  $\mu s$ , IEEE recommends the use of 490 kV/m as CFO of insulator strings.

Among other methods that could be used to evaluate the voltage necessary to cause a flashover in an insulator string (Cigré WG 33-04), Cigré recommends the use of a leader propagation model, where the leader propagation velocity is calculated by:

$$v(t) = K_L u(t) \left( \frac{u(t)}{d_g - l_l} - E_o \right) \quad (4.90)$$

where:

$v(t)$  = leader velocity (in m/s)

$u(t)$  = voltage applied to the insulator string (in kV)

$E_o$  = electric field needed to begin the leader considered (kV/m)

$d_g$  = length (in m) of insulator strings or air (at instance  $t=0$ )

$l_l$  = leader length (in m) at an instance  $t$

$K_L$  = constant.

For positive surges in air gaps or insulator strings, Cigré recommends the use of  $E_o$  as 600 kV/m and  $K_L$  as  $0.8 \times 10^{-6}$ . For negative surges, it is recommended  $E_o$  as 670 kV/m and  $K_L$  as  $1 \times 10^{-6}$ .

When voltage/time curve for standard 1.2/50  $\mu s$  lightning impulse is known, the best fitting constants may also be determined by numerical calculations for selected combinations of flashover and time to breakdown.

### **Estimate the Rate of Insulation Flashover**

#### SHIELDING FAILURE FLASHOVER RATE

Shielding failure occurs when a lightning stroke hits directly a phase conductor of a transmission line that has shield wires. When such failure results in flashover, in insulator strings or in air gaps between conductor and metallic grounded components, it is said that a shielding failure flashover occurred.

According to IEEE, the minimal or critical current  $I_c$  required to cause a flashover can be calculated as follows:

$$I_c = \frac{2 \cdot CFO}{Z_{surge}} \quad (4.91)$$

$$Z_{surge} = 60 \sqrt{\ln(2h/r) \ln(2h/R_c)} \quad (4.92)$$

where

$Z_{surge}$  = conductor surge impedance under Corona (Ohms)

$h$  = average conductor height (m)

$r$  = conductor radius (m)

$R_c$  = Corona radius of the conductor under a gradient of 1500 kV/m (m)

$CFO$  = critical flashover voltage (kV), negative polarity, as defined in Item.

According to Cigré procedure,  $I_c$  can be calculated by a similar procedure or by one that considers a more precise transient response of the line (using an electromagnetic transients program, like EMTP-Electromagnetic Transients Program) and the same or other processes of line critical flashover voltage estimation, such as:

- insulation voltage/time curve;
- integration method;
- physical models representing the Corona phase, the streamer propagation
- phase and leader phases along the line insulation.

IEEE and Cigré estimate the shielding failure rate (number of lightning strokes directly to the phase conductors that cause flashover) as:

$$SFFOR = 2N_g L \int_{I_c}^{I_{max}} D_c(I) f(I) dI \quad (4.93)$$

where

$SFFOR$  = shielding failure flashover rate (flashovers/100 km/yr)

$L$  = length of the line (km)

$D_c(I)$  = exposure length (m) relative to phase conductor, calculated in function of  $I$

$f(I)$  = statistical distribution of  $I$

$I_{max}$  = maximum current (kA) that can hit the phase conductor (current that makes null the distance  $D_c(I)$ )

The probability that an individual subsequent stroke current  $I_s$  will exceed  $I_c$  is given approximately by:

$$P(I_c > I_s) = \frac{1}{1 + \left(\frac{I_c}{I_{subs}}\right)^{2.7}} \quad (4.94)$$

where

$I_{subs}$  is taken as 12 kA;  
 $I_c$  is also taken in kA.

The following equation gives  $P_s$ , the probability of flashover on any subsequent stroke, given that no flashover occurs on the previous strokes:

$$P_s = \sum_{n=2}^{n=\infty} P_n \left(1 - [P(I_s > I_c)]^{n-1}\right) \quad (4.95)$$

where  $P_n$  is the probability that there are  $n$  strokes/flash, from data in (Tompson 1980).

The total  $SFFOR$  will be the sum of the first stroke failure rate  $SFFOR$  and the added rate  $SFFOR_s$  obtained from:

$$SFFOR_s = 2N_g L P_s \int_0^{I_c} D_c(I) f_1(I) dI \quad (4.96)$$

If the critical current  $I_c$  is low, most shielding failures will lead to flashover, either from the small first stroke or from the 60-70% chance that there will be a subsequent stroke that exceeds  $I_c$ . If the critical current is higher,  $P_s$  from will be lower ( $P_s=0.4$  for space  $I_c$  of 16 kA).

The extra contribution of subsequent stroke effects to total  $SFFOR$  ensures that perfect shielding ( $SFFOR=0$ ) will rarely be achieved. See next item.

As cited in the previous item, the estimation of shielding failure rate considering only the lighting first strokes (number of lighting first strokes directly to the phase conductors that cause flashover) as:

$$SFFOR = 2N_g L \int_{I_c}^{I_{max}} D_c(I) f(I) dI \quad (4.97)$$

It indicates an apparent possibility of perfect shielding: a shielding angle that makes  $I_{max}=I_c$  (maximum stroke current that can be injected directly to a phase conductor equal to the current necessary to generate an overvoltage in the phase conductor equal to the insulator withstand), but this can be rarely achieved as it can have a contribution of subsequent stroke effects to total  $SFFOR$ .

Considering only lightning first strokes, Cigré procedure presents the following equation to evaluate the shielding angle where  $I_{max}=I_c$ :

$$\alpha_p = 0.5 \left[ \sin^{-1} \left( \frac{r_g - h}{r_c} \right) + \sin^{-1} \left( \frac{r_g - y}{r_c} \right) \right] \quad (4.98)$$



where

$r_g, r_c$  = calculated for the current  $I_c$  (m)

$h$  = average height of ground wire (m)

$y$  = average height of phase conductor (m)

An attempt to achieve a perfect shielding angle may severely handicap an economical design of lines in areas of low flash density ( $N_g < 2$  flashes/km<sup>2</sup>/yr). It is suggested to the designer evaluating the most economical configuration based on the *SFFOR* required. For example, serving a critical load, a design *SFFOR* value of 0.05 flashover/100 km/yr may be suitable, while values of 0.1-0.2 flashover/100 km/yr are recommended for general practice.

#### RATE OF INSULATION FLASHOVER DUE TO BACKFLASHOVER

When a lightning strikes the tower or the overhead ground wire, the current in the tower and ground impedances cause the rise of the tower voltage. A considerable fraction of the tower and shield wire voltage is coupled by mutual surge impedance to the phase conductors. The tower and shield wire voltages are much larger than the phase conductor voltages. If a voltage difference from phase to tower exceeds a critical value, a flashover occurs, called “backflash” or “backflashover”. The corresponding minimum lightning current that produces such a flashover is called “critical current”.

The calculation of the critical current for back-flashover depends, in general order of sensitivity, on the following parameters:

- Amplitude of the lightning current (generally the peak value of the first return stroke);
- Flashover criteria for the insulation and air gaps;
- Presence of surge arresters across some or all insulators;
- Surge impedance coupling among phases and ground wires, evaluated using transmission line models and considering the additional coupling from arrester-protected insulators;
- Steepness ( $di/dt$ ) at the peak of the current wave, which is generally assumed to be the maximum  $di/dt$ ;
- Waveshape, including both time to peak and time to half-peak value
- Footing impedance, influenced by high frequency and soil ionization effects;
- Tower inductance or surge impedance model;
- Representation of nearby towers and grounding systems;
- Representation of nearby power system components (e.g. transformers).

Sometimes, the induction effects of the electromagnetic field of the lightning channel are additionally taken into account for the estimation of the insulator voltage. Induction effects related to current flow in the tower past the phase conductors have been observed and modeled in several ways.

The procedure adopted by Cigré for the calculation of the line backflashover rate (*BFR*), the same as described by (Aileman 1999), is specifically aimed at calculating the critical current and the resultant *BFR* value. In particular, the Cigré procedure analytically estimates the backflashover critical current by making reference to the representation of the travelling wave phenomena that take place for both cases of a lightning strike to a tower or to an overhead ground wire.

The *BFR* is given by the probability of exceeding the critical current multiplied by the number of flashes to the shield wires ( $N_l$ ), taking into account that the crest voltage and the flashover voltage are both functions of the time-to-crest ( $t_f$ ) of the lightning current. Therefore, the *BFR* considering all the possible time-to-crest values is:

$$BFR = 0.6 N_l \int_0^{\infty} \int_{I_c(t_f)}^{\infty} f\left(\frac{1}{t_f}\right) f(t_f) dI dt_f \quad (4.99)$$

(flashovers / 100km / yr)

where  $f(I/t_f)$  is the conditional probability density function of the stroke current given the time-to-crest and  $f(t_f)$  is the probability function of the time-to-crest value. Note that, in order to obtain the *BFR* for strokes to the tower and for stroke to the spans, the *BFR* obtained for strokes to the tower is multiplied by a coefficient, equal to 0.6.

Another, more simplified procedure for the calculation of the *BFR*, is also presented in Cigré procedure as the *BFR* resulting from the application of previous equation using of an equivalent time-to-crest value  $T_e$ . Such a value is approximately the median value of time to crest for the specific critical current. With such a value, since a single equivalent front is used, the *BFR* is reduced to:

$$BFR = 0.6 N_l \int_{I_c}^{\infty} f(I) dI = 0.6 N_l P(I > I_c) \quad (4.100)$$

In these equations,  $I_c$  is the minimum current that leads to insulator backflash in the phase conductor. To consider the system voltage at the striking time, this current can be calculated considering that such voltage is approximated 80% of the nominal voltage.

The approach adopted by the IEEE is based on the estimation of the voltage across the line insulation at two specific time instants namely: a first evaluation of the full impulse-voltage waveshape peak (at 2  $\mu$ s) considering only the stricken tower, and a second evaluation on the tail (at 6  $\mu$ s) considering relevant adjacent towers. In order to estimate the backflash critical current, these values are compared with an estimation of the volt-time curve of the line insulation.

The backflashover rate is computed according to the equation:

$$BFR = N_l \sum_{N_c}^{N_c} (t_i P_i) \quad (4.101)$$

where  $N_c$  is the number of phase conductors and  $t_i$  is the period of time in which each phase is dominant. This concept is related to the system voltage at the different phases when lightning strikes, as well as the different coupling factors between each phase and the shield wire.  $P_i$  is the probability of the lightning current exceeding a backflashover critical value. This is evaluated with respect to each phase, taking into

account the phase shift between the sinusoidal voltages and the different coupling factors between each phase and the ground wire.

Note that the procedures to calculate both rates, *SFFOR* and *BFR*, are based on using the local ground flash density  $N_g$  to determine the number of strikes to the line.

To calculate the  $I_c$ , the minimum current that leads to insulator backflash in the phase conductor, it is necessary to calculate the overvoltage in the insulation of the line and compare with the withstand voltage. In the next items, the most important aspects involved in this calculation are discussed.

The Cigré and IEEE procedures are compared in (Nucci 2010). The main differences, when present, lie in the fact that some approaches/methods proposed so far within Cigré can be considered to be more general than those proposed within IEEE, in that they take into account more variables of the problem. Within the IEEE – thanks in part to the inherently simpler approach – a computer code, called FLASH, has been made available, which can serve either as a professional tool capable of providing an approximate, yet very useful, answer on the lightning performance of typical overhead transmission lines or as a reference for beginner researchers when simple cases are dealt with.

#### 4.10.1.5 Estimate of Insulation Stress Generated by Lightning Strokes in the Line

To estimate the overvoltages generated in the insulation of a transmission line by lightning striking on its conductors, ground wires or towers, it is necessary to model the primary components that are responsible for the transient response of the line.

In the following items the primary aspects involved in such modeling are discussed. The presentation of all the equations involved in the calculation is beyond the scope of the present text.

##### ***Tower Surge Response Model***

In the evaluation of voltages generated at the top of tower during a lightning discharge, it is necessary to consider the response of the tower to electromagnetic transients. Usually, the tower is modeled with distributed parameters, characterized by a surge impedance associated with an electromagnetic wave travel time. In Table 4.10 are listed equations that enable the evaluation of these parameters for some self-supporting towers.

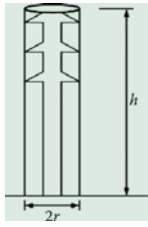
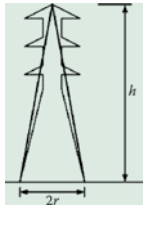
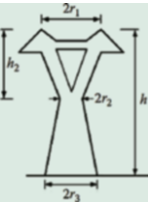
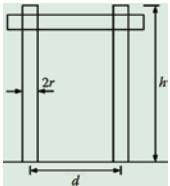
Common experience with practical structures yields typical values for tower surge impedances in the range 150-250  $\Omega$ .

For tower with guy wires, Cigré presents a simplified approach where the mutual coupling of guy-wires is not taken into account.

Basically, the process is:

- Evaluate the guy-wire surge impedance and travel time;
- Evaluate the equivalent inductance of all guy-wires;
- Evaluate the inductance parallel of guy-wires inductance with the tower inductance;
- Evaluate the equivalent surge impedance and travel time.

**Table 4.10** Tower model (impedance and travel time) (IEEE Std 1243-1997)

Cylindrical	Conical
	
$Z = 60 \left[ \ln \left( \sqrt{2} \frac{2h}{r} \right) - 1 \right]$ $\tau = \frac{h}{0.85c}$	$Z = 60 \ln \left( \sqrt{2} \sqrt{\frac{h^2 + r^2}{r^2}} \right)$ $\tau = \frac{h}{0.85c}$
Waist	H-Frame
	
$Z = \sqrt{\frac{\pi}{4}} 60 \left[ \ln \left( \cot \frac{\tan^{-1}(r/h)}{2} \right) - \ln \sqrt{2} \right]$ $r = \frac{r_1 h_2 + r_2 h + r_3 (h - h_2)}{h}$ $\tau = \frac{h}{0.85c}$	$Z_1 = 60 \left( \ln \left( 2\sqrt{2} \frac{h}{r} \right) - 1 \right)$ $Z_2 = \frac{60 d \ln \left( 2 \frac{h}{r} \right) + h Z_1}{h + d}$ $Z = \frac{Z_1 Z_2}{Z_1 + Z_2}$ $\tau = \frac{1}{cZ} \frac{h Z_1 (d + h) Z_2}{h Z_1 + (d + h) Z_3}$

Note (1): For tower of conical type, IEEE uses  $h/(0.85.c)$  as travel time instead of  $h/c$  indicated by Cigré Document 63 (1991).

To evaluate the parameters cited the following equations can be used:

$$Z_{guy} = 60 \left[ \ln(2h/r) - 1 \right] \quad (4.102)$$

$$\tau_{guy} = l_{guy} / c \quad (4.103)$$

$$L_{guy} = L_{guy} \tau_{guy} \quad (4.104)$$

$$L_{equiv\_guy\_wires} = L_{guy} / n \quad (4.105)$$

where:

$h$  = guy-wire height (m)

$r$  = guy-wire radius (m)

$l_{guy}$  = guy-wire length (m)

$c$  = light velocity

$n$  = number of parallel guy-wires

$L_{guy}$  = inductance of a guy-wire ( $H$ )

$L_{equiv\_guy\_wires}$  = inductance of  $n$  guy-wires ( $H$ ).

Finally, for item (d), the following equations can be used:

$$L_{tower} = Z_{tower} \tau_{tower} \quad (4.106)$$

$$L_{equiv\_tower+guy\_wires} = \frac{L_{equiv\_guy\_wires} L_{tower}}{L_{equiv\_guy\_wires} + L_{tower}} \quad (4.107)$$

$$Z_{equiv\_tower+guy\_wires} = \frac{cL_{equiv\_tower+guy\_wires}}{H_T} \quad (4.108)$$

$$\tau_{equiv\_tower+guy\_wires} = H_T / c \quad (4.109)$$

where:

$Z_{tower}$  = surge impedance of tower only ( $\Omega$ )

$\tau_{tower}$  = travel time in the tower only (s)

$L_{tower}$  = inductance of tower only (H)

$H_T$  = tower height (m)

$L_{equiv\_tower+guy\_wires}$  = inductance of the tower and guy wires ( $H$ ).

It is important to note that several approaches have been presented in the recent literature addressing tower models.

### **Tower Footing Resistance**

In the IEEE and Cigré procedures the tower grounding system behavior is characterized by a lumped resistance (the tower footing resistance).

In IEEE procedure this resistance is constant. In Cigré procedure, the effect of soil ionization is taken into account, using the following equation when the lightning current amplitude exceeds the critical value  $I_g$ :

$$R_i = \frac{R_0}{\sqrt{1 + \frac{I}{I_g}}} \quad (4.110)$$

where:

$R_0$  = is the low frequency non-ionized soil resistance;

$I_g$  = is the critical value of the lightning current.

$I_g$  = is estimated considering the soil ionization threshold field  $E_g$ , using the equation:

$$I_g = \frac{E_g \rho}{2\pi R_0^2} \quad (4.111)$$

Where:

$\rho$  = is the electrical resistivity of the soil ( $\Omega$  m)

$E_g$  = is the soil ionization threshold field, considered to be, approximately, 400 kV/m for most common soils (Cigré TB 63, 1991).

In both evaluation procedures, of IEEE and Cigré, except the soil ionization, no reference is made explicit to the transient response of structure grounding systems or to the fact that the soil parameters vary with frequency.

Relative to these aspects, many researchers have been done. For example, the main factors that influence the grounding behavior have been analyzed in (Visacro and Alípio 2012), the current-dependent response of electrodes is addressed in (Sekioka et al. 2005) and the effect of the frequency-dependent soil parameters on this response is addressed in (Visacro and Alípio 2012).

### **Transmission Line Modeling**

In both procedures, of IEEE and Cigré, the effects of occurrence of Corona in ground wires are considered.

The surge impedance of each conductor or ground wire and the mutual impedance between them are calculated considering as infinite the electrical conductivity of soil and the cables in their mean height.

In IEEE procedure the wave travel time in the phase conductors and ground wires is calculated considering an electromagnetic traveling wave velocity as 90% of velocity of light.

To evaluate the voltage on the top of a tower where a lightning strikes, usually it is not necessary to model more than three spans and towers on each side of the tower.

#### **4.10.1.6 Improving Lightning Performance**

As discussed in more details in IEEE Std 1243-1997, the following special methods, among others, can improve lightning performance of a line:

- Installation of additional ground wires under conductors:  
Basically used to increase the common-mode coupling of voltage surges on the ground wires to the phase conductors, and cause a reduction on the insulator voltage at the tower.
- Installation of guy wire on the towers:  
Fitting new or additional guy wires from tower to rock or soil anchors can reduce the tower surge impedance and the grounding resistance (the latter because new guy anchor will behave as an additional ground electrode).
- Ground wires in separated structures:  
OHGWs may be supported by separate outboard towers or poles instead of being assembled on the same structure that supports the phase conductors. This arrangement may give extreme negative shielding angles, which minimize induction losses and provide excellent security from shielding failures.  
Tower height and wind loading may also be reduced. While an expensive option, OHGWs on separate structures may result in excellent lightning performance. Connections can be made from the OHGWs to towers, if required for ac fault-current management, should be designed to have a high impedance to lightning through long interconnection length to minimize risk of backflash over.
- Installation of surge arresters:  
With the installation of surge arresters in parallel to the insulator strings the over-voltage on them will be reduced to acceptable levels.  
The number of surge arresters can be optimized, i.e., it is not necessary to install them in all towers and in all phases.  
The use of surge arresters is covered by [Cigré TB 440 \(Cigré TB 440\)](#).

#### 4.10.1.7 Grounding

Grounding systems are installed in the structures of a transmission line with the following primary objectives:

- to provide a preferential path to earth for currents generated by faults in the line;
- to provide a grounding system with a resistance low enough to enable the over-current protection to detect a ground fault in the line.
- to provide a preferential path to earth to lightning discharge currents;
- in urban areas, to control the step and touch voltages generated during ground faults in the line;
- to reduce the structure ground potential rise during a lightning discharge and, consequently, reduce the probability of occurrence of backflashover on the line.

In the following items, the primary practical aspects involved in the design of the grounding system of the transmission line structures are discussed.

#### ***Measuring the Electrical Resistivity of Soil***

To design a grounding system it is necessary to measure the electrical resistivity of the soil where it will be installed.

As the soil resistivity may vary considerably over the surface and depth, it is necessary to perform measurements at various locations throughout the area

occupied by the grounding system using a process that enables the identification of the variation of the resistivity with depth.

To design the grounding systems of transmission lines structures, measurements should be done with electrodes driven along an axis coincident or near the axis of the line and centered at the installation point of each structure. In addition to this axis, some companies specify measurements on axes near the edges of the right-of-way of the line. In this case, measurements made on three axes: one in the center of the right-of-way and the other two near their limits. The final resistivity considered for each distance “ $a$ ” (between measuring probes) is the mean value of all the measurements done with that distance, except that ones those have great discrepancies from the mean value, which are neglected.

One of the most widely used methods of measuring electrical resistivity of soil is the *Wenner four-pin method* (Dawalibi and Barbeito 1991).

### Soil Stratification

Usually, modeling the soil with a model of stratified horizontal layers, where each layer has a specific resistivity and thickness, is used in grounding system design. This can be done as most of the real soils are not homogeneous, but composed of several layers of different electrical resistivity and thickness. These layers, due to the geological formation, in general, are fairly horizontal and parallel to the ground surface.

From the results of resistivity measurement, it is possible to find the parameters of the model (of a soil stratified in two or more horizontal layers).

Considering a two-layer soil model (Figure 4.23), its structure can be characterized by:

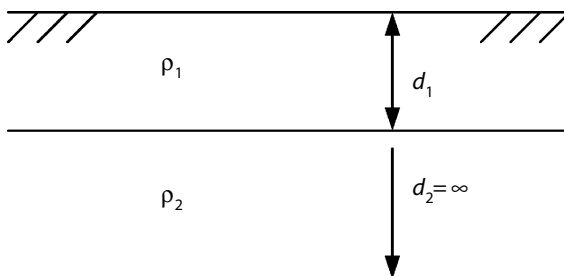
- a first layer with resistivity  $\rho_1$  and thickness  $d_1$
- a second layer with resistivity  $\rho_2$  and infinite thickness.

The stratification of the soil can be carried out by a curve fitting process, where  $\rho_1$ ,  $\rho_2$  and  $d_1$  are determined.

As an example, it will be shown the results of a stratification process done with a specific set of measured resistivity values obtained with the Wenner four-pin method, that are presented in Table 4.11.

The two-layer soil parameters are shown Table 4.11. In Figure 4.24 are shown the measured values and the curve  $\rho$  over  $a$  generated with the values of  $\rho_1$ ,  $\rho_2$  and  $d_1$  shown on Table 4.11.

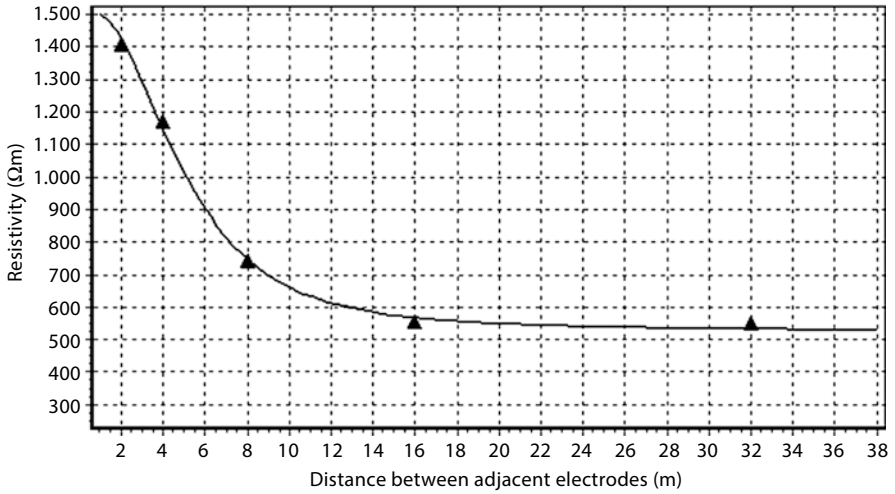
**Figure 4.23** Structure of a soil stratified in two-layer of different resistivities.





**Table 4.11** Measured value of apparent resistivity of soil obtained with the Wenner four-pin method

Resistivity in $\Omega$ m for distance $a$ between electrodes					
$a$	2 m	4 m	8 m	16 m	32 m
$\rho_a$	1405	1173	743	553	549
Two-layer soil stratification					
		$\rho_1$ ( $\Omega$ m)	$\rho_2$ ( $\Omega$ m)	$d1$ (m)	
		1515	525	3.2	



**Figure 4.24** Measured resistivity for distance  $a$  and curve calculated with the parameters of the two-layer soil structure obtained in the stratification process.

In this example, the deviations between measured and calculated values of resistivity are small, indicating that the real soil can effectively be approximated by a two-layer soil model.

In many practical situations, the soils cannot be perfectly stratified in two layers as the one shown here. In such cases, conservative approximations should be done or multi-layer layer soil model should be used.







**Resistance Calculation**

The resistance of a grounding system can be estimated knowing its geometry and the resistivity of the soil where it will be installed (Table 4.12).

Usually, simplified equations are used to calculate the resistance of single electrodes or simple grounding systems. In most case, they consider uniform soil with a resistivity called the apparent resistivity. Such apparent resistivity can be evaluated, approximately, from the stratification of the soil and the dimensions of the grounding system.

Reference (Hepppe 1979) presents the equations necessary to calculate the induction coefficients and the potential generated in each point of the soil by the currents

**Table 4.12** Examples of simplified equations that can be used to calculate the resistance of electrodes installed in a uniform soil of resistivity  $\rho$  (IEEE Std 142)

Electrode		Grounding Resistance
	Vertical ground rod	$R = \frac{\rho}{2\pi L} \left( \ln \frac{4L}{a} - 1 \right)$
	Single counterpoise	$R = \frac{\rho}{\pi L} \left( \ln \frac{2L}{\sqrt{2ad}} - 1 \right)$
	Three point star	$R = \frac{\rho}{6\pi L} \left( \ln \frac{2L}{a} + \ln \frac{2L}{s} + 1.071 - 0.209 \frac{s}{L} + 0.238 \frac{s^2}{L^2} - 0.054 \frac{s^4}{L^4} \dots \right)$
	Four point star	$R = \frac{\rho}{8\pi L} \left( \ln \frac{2L}{a} + \ln \frac{2L}{s} + 2.912 - 1.071 \frac{s}{L} + 0.645 \frac{s^2}{L^2} - 0.145 \frac{s^4}{L^4} \dots \right)$
	Six point star	$R = \frac{\rho}{126\pi L} \left( \ln \frac{2L}{a} + \ln \frac{2L}{s} + 6.851 - 3.128 \frac{s}{L} + 1.758 \frac{s^2}{L^2} - 0.490 \frac{s^4}{L^4} \dots \right)$
	Eight point star	$R = \frac{\rho}{16\pi L} \left( \ln \frac{2L}{a} + \ln \frac{2L}{s} + 10.98 - 5.51 \frac{s}{L} + 3.26 \frac{s^2}{L^2} - 1.17 \frac{s^4}{L^4} \dots \right)$

Dimensions: Rod or wire radius  $\rightarrow a$  ; Length  $\rightarrow L$  ; Depth  $\rightarrow d = s/2$

injected through the segments of conductors in which the grounding system was subdivided. These equations were derived considering a two-layer soil.

To calculate the grounding system resistance, it is assumed that all segments of conductor are metallicly interconnected and the calculations done at power frequency. Then, it can be assumed that all the segments are at the same potential  $V_m$ . For an arbitrary value of  $V_m$ , for example 1.0 V, the current injected in earth by each segment of conductor can be calculated. Then, the grounding resistance can be calculated as:

$$R_{grounding} = \frac{V_m}{\sum_{i=1} I_i} \quad (4.112)$$

To calculate the potentials generated in the soil during the occurrence of ground fault in the transmission line, it is necessary to estimate the ground potential rise of the grounding system  $V_m$ , in the desired situation, and with it to calculate the real currents that will be injected into the soil.

### **Resistance and Impedance**

For low frequency currents, the behavior of typical grounding systems that are installed in structures of transmission lines can be characterized by a resistance.

For greater frequencies, especially the frequencies that are present in lightning currents (ranging from 100 Hz to 4 MHz), the capacitance and inductance of grounding systems are significant in their behavior (Visacro et al. 2011).

For such high frequencies, the relation between voltage (ground potential rise) and current injected in the grounding system cannot be characterized by a constant (the resistance). To be more precise, this relation should be described as an impedance that varies with frequency:

$$Z(\omega) = \frac{V(\omega)}{I(\omega)} \tag{4.113}$$

The variation of the soil resistivity and permittivity with frequency is another important aspect to be considered when high precision is required, especially for grounding systems installed in high resistivity soils.

In the literature, some expressions are presented to describe the variation of resistivity and permittivity with frequency. They are curve-fitting expressions that are based on experimental results.

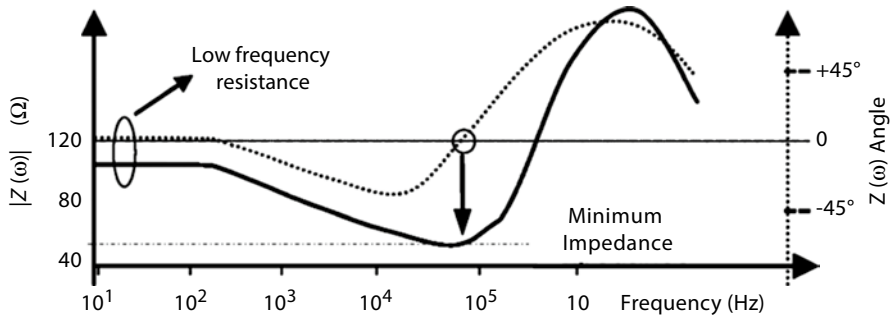
The following expressions were proposed in (Visacro and Alípio 2012):

$$\rho = \rho_0 / \left\{ 1 + 1.2E^{-6} \rho_0^{0.73} (f - 100)^{0.65} \right\} \tag{4.114}$$

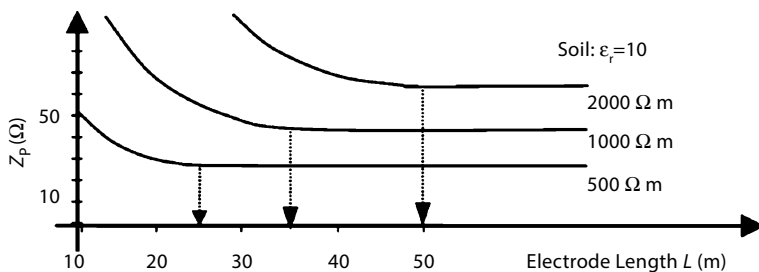
$$\epsilon_r = 7.6E^3 f^{-0.4} + 1.3 \tag{4.115}$$

where  $\rho_0$  is the soil resistivity at 100 Hz,  $\rho$  (in  $\Omega$ ,m) and  $\epsilon_r$  are the soil resistivity and relative permittivity at frequency  $f$  (in Hz), respectively. The equation of  $\rho$  is valid for frequencies between 100 Hz and 4 MHz, while the equation of  $\epsilon_r$  is valid for frequencies between 10 kHz and 4 MHz (below 10 kHz, it is suggested to use the value of relative permittivity calculated at 10 kHz).

In Figure 4.25, the impedance  $Z(\omega)$  is shown for a counterpoise of 50 m in length, buried in 2500  $\Omega$  m soil. It considers the frequency variation of the soil parameters. As can be seen, immediately after power frequency,  $Z(\omega)$  reduces with increasing frequencies. For even greater frequencies, it increases again, until exceeding the low frequency resistance value.



**Figure 4.25** Impedance of a counterpoise of 50 m buried in a 2500  $\Omega$ m soil. Continuous line: modulus of impedance. Dotted line: impedance angles.



**Figure 4.26** Calculated Impedance of a counterpoise buried in a uniform soil. For each soil the effective length is indicated.

**Table 4.13** Effective counterpoise length  $L_{eff}$  (Visacro 2007)

Resistivity of Soil ( $\Omega$ m)	$L_{eff}$ (m) for fast current waves 1.2/50 $\mu$ s
100	14
500	23
1000	34
2000	50

For impulse waves, primarily in lightning analysis, the behavior of a grounding system is, usually, described by its impulse grounding impedance  $Z_p$ , defined as the ratio between the voltage and current peaks developed at the current injection point:

$$Z_p = \frac{V_p}{I_p} \quad (4.116)$$

For a specific grounding system, the impulse grounding impedance  $Z_p$  is a function of resistivity of soil and the current waveform, primarily its front-time parameter.

Figure 4.26 shows calculated curves  $Z_p$  over  $L$ , where  $Z_p$  is the impulse impedance of a counterpoise of length  $L$  installed in a uniform soil. In this same figure is indicated the effective length of counterpoise, defined as that length beyond it  $Z_p$  no longer reduces which the increase of  $L$ . These curves were calculated considering the soil parameters constant with frequency.

Table 4.13 shows values of effective counterpoise length for current waves of 1.2/50  $\mu$ s (Visacro 2007). For current waves of 4.5/60  $\mu$ s, the effective length for these same cases are, approximately, 40% greater than for 1.2/50  $\mu$ s.

The results of Figure 4.26 and Table 4.13 were obtained considering constant the soil parameters  $\rho$  and  $\epsilon$ ; Soil ionization were not considered. In recent works, it was identified lower values of  $Z_p$  and greater values of effective length, primarily for high soil resistivity (as 3000  $\Omega$  m) and for impulse current waves representative to lightning first strokes wave.

Even though the precision of the values of effective length can be an object of discussion it clearly shows that too long counterpoises should not be used with the

objective of reducing its impulse impedance. Using a continuous counterpoise, for example, is clearly a mistake.

As a design criterion, it is suggested not to install counterpoise with length much greater than the effective length calculated with the 4.5/60  $\mu$ s current wave form.

One interesting parameter that can be used to analyze the impulse behavior of a grounding system is the impulse coefficient, defined as the relation between the impulse impedance  $Z_p$  and the low frequency resistance  $RLF$  of the grounding system, usually called  $I_c$ .

Soil ionization occurs primarily when high current is discharged into concentrated electrodes. Usually the ionization process starts when the electric field in the soil reaches a critical value (approximately 300 kV/m for typical soils (Mousa 1994)), and tends to reduce the ground system resistance.

In large grounding systems, as the ones used in a high voltage transmission line constructed in high resistivity soil, which can be composed by long counterpoises, reduction in their resistance by soil ionization occurs only for very high lightning currents injected on them.

Although some studies have been done and simplified methodologies have been proposed to consider the soil ionization in grounding system analyses (Mousa 1994), in practical power transmission line grounding system design, usually, the soil ionization has not been considered explicitly.

### ***Measuring the Structure Grounding Resistance***

After the installation of the grounding system in a structure of a transmission line, it is recommended to measure its resistance. In the following paragraphs, a basic procedure that is widely used to do this measurement is described.

Some utilities have specification for this procedure.

In rural areas, usually, horizontal counterpoise wires, radially disposed from the structures, with or without ground rods, are used as tower grounding system.

Usual variations done in the grounding system geometries are:

- installation of additional small wire or cables from tower (to reduce the grounding system surge impedance)
- installation of a wire or cable in a form of rectangular ring around the tower base or around guy-wires foundation
- preclusion of the cables that interconnect the guy-wires to the central mast, in guyed tower
- installation of ground rods with or without the counterpoise cables
- installation of continuous counterpoise cables, i.e., interconnecting the counterpoises of adjacent towers (this procedure is not recommended as reported before)
- installation of deep grounding well
- use of low resistivity materials in substitution of some portion of the local soil: use of bentonite, for example.

Grounding systems with greater number of counterpoises or ground rods in parallel from the points of connection to tower have lower impulse impedances.

### **Determining the Ground System to Install in each Tower**

As mentioned before, the geometry of the grounding system to install in a structure depends on the value and distribution of the soil resistivity, the desired maximum resistance to be obtained and the extension of the area available to install it.

When the transmission line has a large number of structures, it is common to define basic geometries of grounding systems to be used. Usually, they are called grounding stages as one geometry can be viewed as an extension of the previous one. Then, the grounding stage to be installed in a specific structure is identified by calculations or measurements.

In regions with soil of high resistivity where, even with the last stage of grounding system it may occur that the desired maximum resistance is not reached. In this case, the installation of special grounding system should be considered.

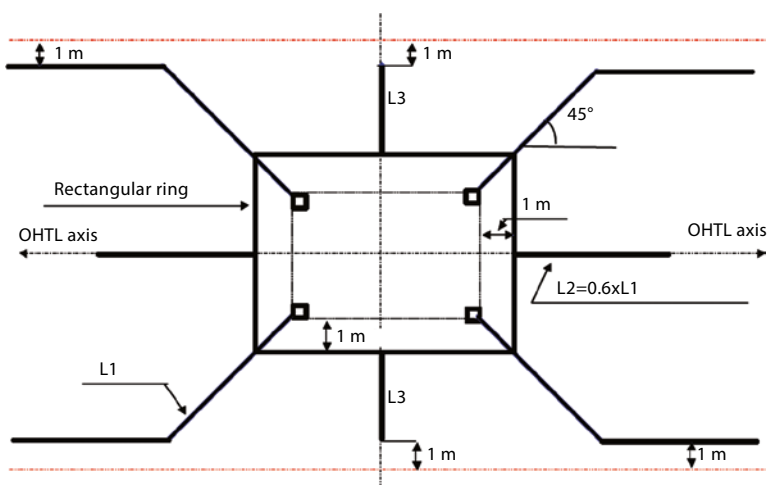
Depending on the soil resistivity, it can be considered the installation of a larger number of horizontal radial counterpoises, ground rods, deep grounding well and the use of low resistivity materials, like bentonite, for example.

In Figure 4.27 an example is shown of special grounding system geometry designed to be used in very high resistivity soils, with the objective of reduction of the tower grounding impulse impedance.

In urban areas, the structures can be in regions with high traffic of people. In this case, to guarantee the public safety, it may be necessary to design specific grounding systems to control the touch and step voltage generated, primarily, during faults on the transmission line.

### **Touch and Step Voltage Limits**

As discussed in (IEEE Std 80-2000), the touch and step voltages generated at the grounding system should not exceed the limits calculated with the following equations:



**Figure 4.27** Example of grounding system designed to reduce the grounding impulse impedance of a tower.

$$V_{\max\_step} = (R_{ch} + R_{2Fs}) I_{ch} \quad (4.117)$$

$$V_{\max\_touch} = (R_{ch} + R_{2Fp}) I_{ch} \quad (4.118)$$

where:

$R_{ch}$  = human body resistance (of order of 1000  $\Omega$ );

$R_{2Fs}$  = resistance of the two human feet in series;

$R_{2Fp}$  = resistance of the two human feet in parallel;

$I_{ch}$  = maximum allowable current in the human body.

The current  $I_{ch}$  can be estimated as (for 50 kg person):

$$I_{ch} = \frac{0.116}{\sqrt{t}} [A] \quad (4.119)$$

where  $t$  is the exposition time to the current.

The resistances  $R_{2Fs}$  and  $R_{2Fp}$  can be estimated by the following equations:

$$R_{2Fs} = 6C_s \rho_s \quad (4.120)$$

$$R_{2Fp} = 1.5C_s \rho_s \quad (4.121)$$

where  $\rho_s$  is the soil surface resistivity and  $C_s$  is a function of  $\rho_s$ , its thickness  $h_s$  and the resistivity of the soil immediately below  $\rho_s$ . In a natural soil  $\rho_s$  is equal to  $\rho_t$  and  $C_s$  is equal to 1. If the natural soil is covered with a high resistivity material, as a layer of gravel, asphalt or stones,  $\rho_s$  will be the resistivity of this material and  $C_s$  can be calculated as:

$$C_s = 1 - \frac{0.09 \left( 1 - \frac{\rho_1}{\rho_s} \right)}{2h_s + 0.09} \quad (4.122)$$

With the installation of a layer of high resistivity material the step and touch voltage generated by the grounding system can be greater, lowering its complexity and cost or providing a greater safety margin. Another advantage is that it gives some protection to the grounding system against thieves and vandalism.

As an example, in Table 4.14 the step and touch voltage limits are shown for a natural soil with resistivity 500  $\Omega$  m, with or without a thin layer of high resistivity material: granite stones or asphalt (the installation of gravel is not recommended as it is easy to be stolen). The time of exposure  $t$  to the current was considered equal to 1.0 s.

The step and touch voltages generated at the grounding system of a structure will depend on the characteristics of the electrical system (basically its short-circuit current and fault clearing time), the characteristics of the transmission line, the electrical resistivity of soil and the geometry of the grounding system. In case of proximity of the structure with a substation, the influence of its grounding mat should be considered.

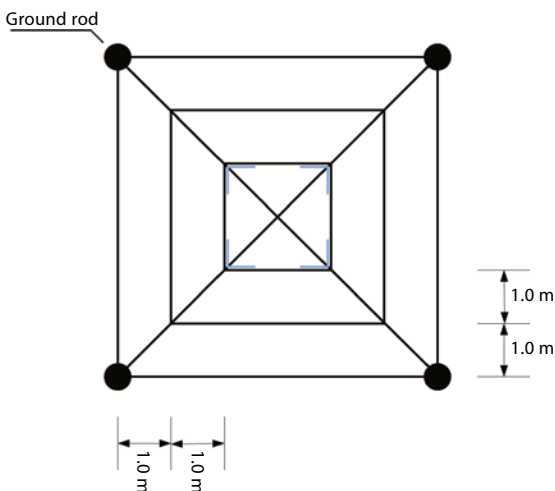
Typical geometries of grounding systems installed in urban areas are shown in Figure 4.28. Basically, they are composed by ground rods and cables installed as

**Table 4.14** Step and touch voltage limits

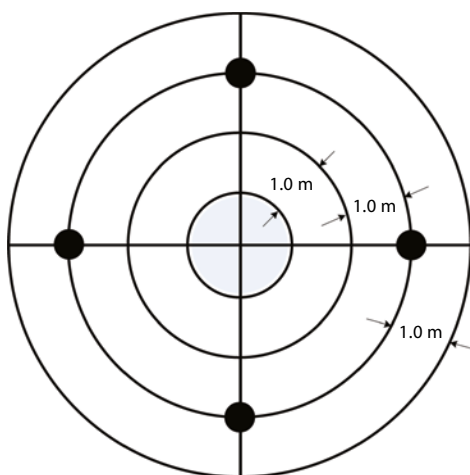
Short duration step and touch voltage limits (V)					
Natural soil ( $500 \Omega \text{ m}$ )		Thin layer of granite stones ( $\rho_s : 5000 \Omega \text{ m}$ ; thickness: 10 cm)		Thin layer of asphalt ( $\rho_s : 10000 \Omega \text{ m}$ ; thickness: 10 cm)	
$V_{\text{touch}}$	$V_{\text{step}}$	$V_{\text{touch}}$	$V_{\text{step}}$	$V_{\text{touch}}$	$V_{\text{step}}$
203	464	742	2621	1073	3944

Note: Except for natural soil, all the other resistivities are for wet materials.

**Figure 4.28** Typical grounding system geometry for structures in areas where it is necessary to control the step and touch voltages.



Four ground rods and three wires/cables installed as rectangular rings around the base of a metallic structure at a depth of 0.5 m.



Four ground rods and wires/cables installed as circular rings around the base of a concrete structure, at a depth of 0.5 m, except the last ring, that is at 1.0 m.



rectangular or circular rings, around the feet of the structure, with 1 m apart. The installation depth of the outer ring may be greater in order to control the step voltage in the border of the grounding rings.

In addition to the grounding system itself, usually it is necessary to install a thin layer of high electrical resistivity material over the natural soil to increase the maximum allowable step and touch voltages and also to protect the grounding system. Examples are parallelepipeds of granite with sides, at least, 10 cm in length or a layer of asphalt, with a thickness of 5 cm.

### **Example of Design**

As an example, in this item it is presented the results of the design of a grounding system installed to control the step and touch voltages in a structure located in an urban area. This is the grounding system of the 40<sup>th</sup> structure of a 138 kV transmission line.

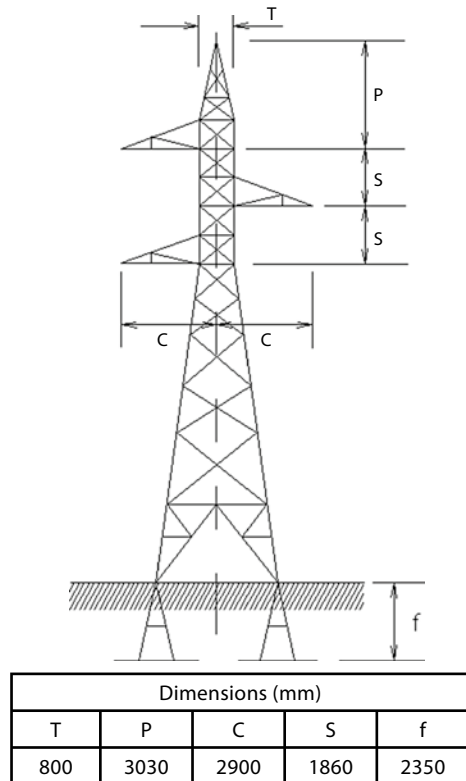
- Transmission line data:
  - Nominal voltage = 138 kV
  - Length = 60 km
  - Typical span = 400 m
  - Number of structures = 149
  - Conductor = ACSR 176.9 MCM - Linnet
  - Ground wire = ACSR 101.8 MCM - Petrel
  - Typical tower = see the following figure
  - Average grounding resistance of structures = 15  $\Omega$
  - Base of structure 40 = 5 m  $\times$  5 m
  - Distance between structure 40 and the substation at the beginning of line = 16 km.
- Electrical system data:
  - Symmetrical ground fault current in both substations of the line = 15 kA
  - Total ground fault clearing time = 1 s
  - Resistance of the substation ground mats = 1  $\Omega$
- Soil stratification in structure n<sup>o</sup> 40:
  - $\rho_1 = 500 \Omega\text{m}$
  - $\rho_2 = 1000 \Omega\text{m}$
  - $d_1 = 3 \text{ m}$ .

The designed grounding system is shown in Figure 4.29. Its grounding resistance was estimated in 29.3  $\Omega$  (Figure 4.30).

Also, it was recommended to cover the natural soil around the tower with granite stones (parallelepiped) with sides, at least, 10 cm in length.

In the design process of tower 40 grounding system, it was necessary to calculate the current distribution in the ground wire and towers of the line, for a ground fault in tower 40 (Figure 4.31). The ground potential rise of tower 40 was estimated in 6.03 kV. The current distribution calculation was made with a software developed

**Figure 4.29** Typical tower of the line.



specifically for this purpose (the ATP – Alternative Transients Program could also be used). The resistance of the grounding system in design was considered in the results shown here.

In points inside the covered area, the limits of step and touch voltages were estimated considering:

- $\rho_s = 5000 \Omega\text{m}$  (wet granite stones)
- $h_s = 0.1 \text{ m}$
- $\rho_1 = 500 \Omega\text{m}$

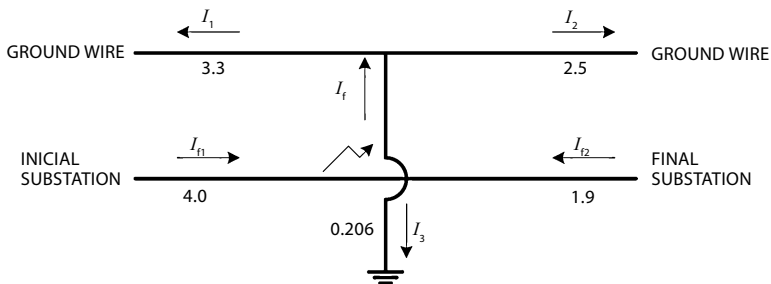
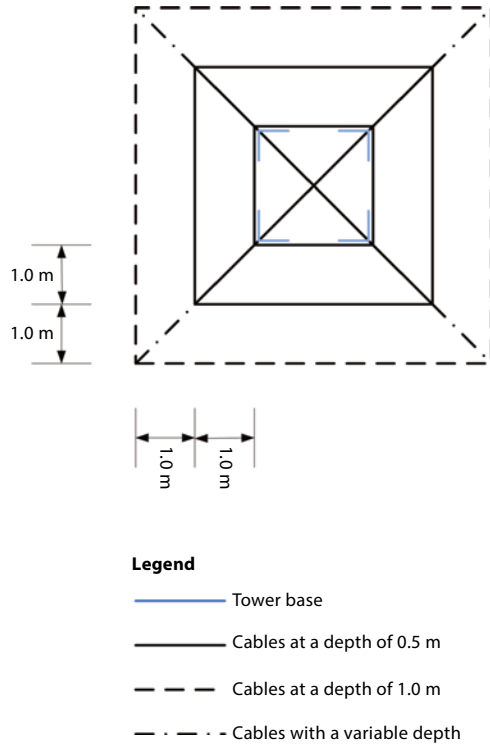
With these parameters,  $C_s$  is equal to 0.72.

Then:

$$R_{2Fs} = 6.0 \cdot 0.72 \cdot 5000 = 21600 \Omega$$

$$R_{2Fp} = 1.5 \cdot 0.72 \cdot 5000 = 5400 \Omega$$

**Figure 4.30** Grounding system of tower 40.



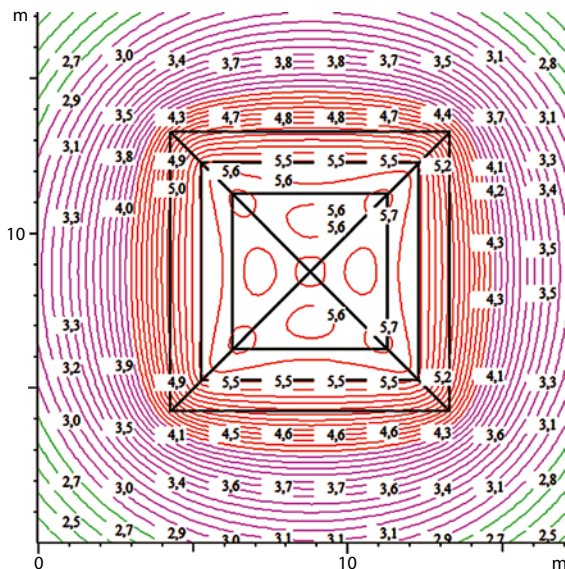
**Figure 4.31** Current distribution near tower 40, in kA, for a ground fault on it.

and the limits are:

$$V_{\max\_step} = (1000 + 21600) \frac{0,116}{\sqrt{I}} = 2621 \text{ V}$$

$$V_{\max\_touch} = (1000 + 5400) \frac{0,116}{\sqrt{I}} = 742 \text{ V}$$

**Figure 4.32** Equipotential curves on the surface of the soil near the structure n° 40. Values in kV.



In a point outside the covered area, the limits are:

$$V_{\max\_step\_adm} = (1000 + 6 \times 500) \frac{0,116}{\sqrt{l}} = 464 \text{ V}$$

$$V_{\max\_touch\_adm} = (1000 + 1,5 \times 500) \frac{0,116}{\sqrt{l}} = 203 \text{ V}$$

Figure 4.32 shows an equipotential map near tower 40.

The curve in red indicates the points where the generated touch voltage is equal to the allowable limit for this voltage. Points inside this curve have generated touch voltage less than the limit.

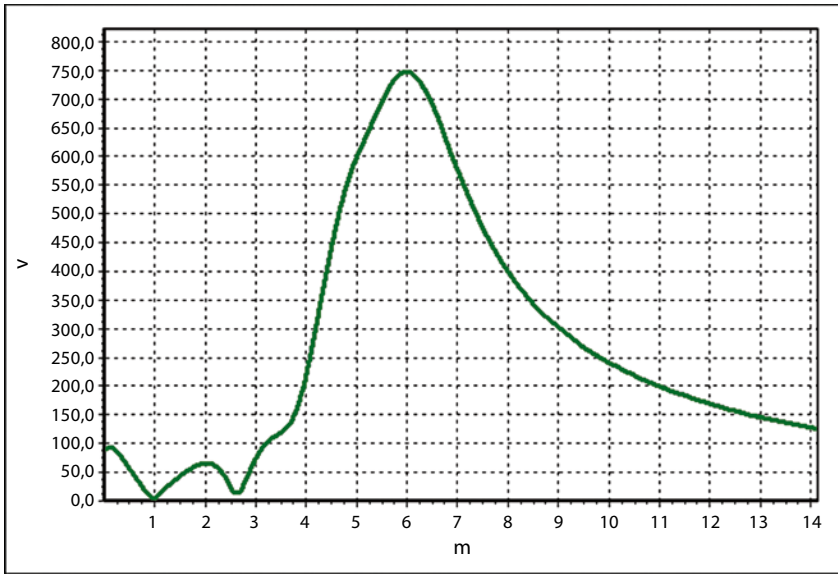
Figure 4.33 shows graphs of the calculated step voltages.

Table 4.15 lists the maximum values of the generated step and touch voltages with the respective limit. As it can be seen, the step and touch voltages are controlled.

### 4.10.2 Temporary (Sustained) Overvoltage

They are of sinusoidal type and defined by its magnitude and duration. They affect the insulation withstand of the clearances (gaps) and other insulation and are defined by test with an amplitude with duration of one minute. They are also important for examining the surge arrester behavior and its energy absorption. The surge arrester rating is chosen not to conduct significant current during these overvoltages.

The origins of temporary overvoltages are: earth faults; load rejection; line/equipment switching; resonances (IEC 71-2).



**Figure 4.33** Generated step voltage at 45 degree direction.

**Table 4.15** Comparison between limits and the generated step and touch voltages (for tower n°40)

Soil with thin layer of granite stones				Natural soil	
Limits (V)		Generated voltages (V)		Step voltage limit (V)	Step voltage generated (V)
$V_{touch}$	$V_{step}$	$V_{touch}$	$V_{step}$		
742	2621	513	748	464	428

**4.10.2.1 Earth Faults**

These overvoltages are related to phase-to-ground faults location and the system neutral earthing. For ungrounded earthing system the phase-to-ground overvoltage may reach values close to the phase-to-phase voltage. For grounded neutral impedance or solidly grounded system these overvoltages are much smaller.

**4.10.2.2 Load Rejection**

For long line systems, after load rejection overvoltages appear due to Ferranti effect, they are bigger in the line opened end.

Shunt reactors connected to the lines reduce these overvoltages.

The condition may become worse if load rejection is combined with pre existing, or post occurring phase-to-ground faults.

**4.10.2.3 Line/Equipment Switching**

Energization/reclosing of lines lead to temporary overvoltages due to Ferranti effect. Shunt reactors reduce the overvoltage.

Capacitor switching in is also a cause of temporary overvoltages.

#### 4.10.2.4 Resonances

Temporary overvoltages may be originated by resonances, and may be mitigated by detuning the system circuit.

Transformer energization and ferro-resonance should be of concern.

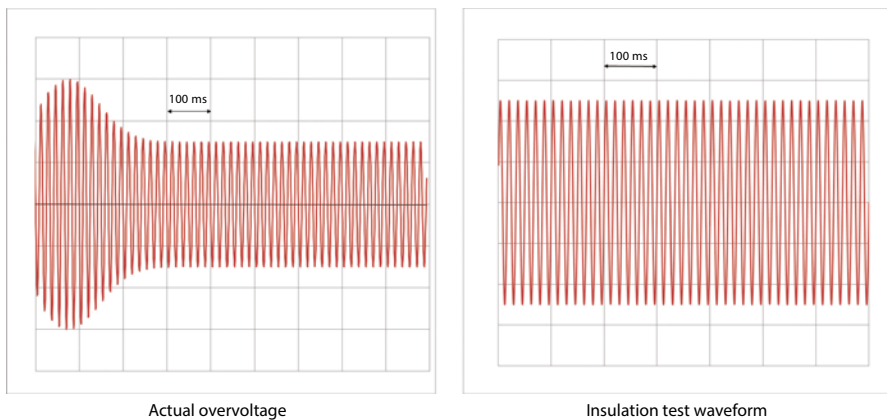
An example of sustained transient overvoltage due to load rejection is shown in Figure 4.34.

#### 4.10.3 Slow-Front Overvoltages (Switching Surges)

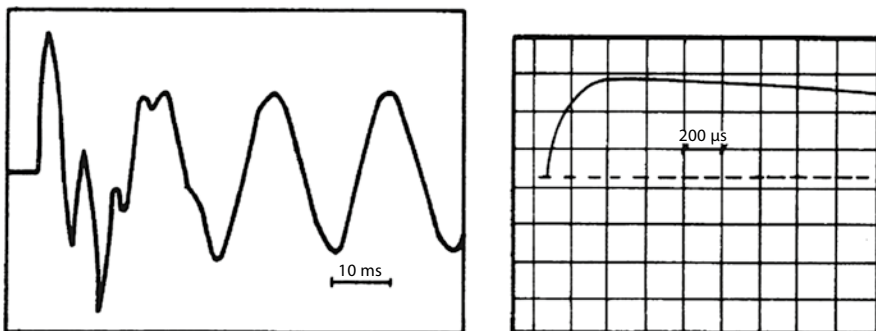
Slow front overvoltages are of oscillatory nature fast damped. They are represented in laboratory test by a wave with time-to-peak of 250  $\mu\text{s}$  and time to half-value in the tail 2500  $\mu\text{s}$  (Figure 4.35).

The switching surge overvoltages arise from:

- line energization
- line reclosing (re-energization)



**Figure 4.34** Sustained overvoltage – load rejection.



**Figure 4.35** Slow front overvoltage (actual on left and laboratory test on right).

- fault inception
- fault clearing
- load rejection
- capacitive switching in
- inductive load switching out.

#### 4.10.3.1 Line Energization

During line energization, a slow-front overvoltage occurs superimposed to the power frequency overvoltage. When the breaker closes, a travelling wave move along the line, originating a slow-front overvoltage (after some reflections/refractions).

The peak value of the overvoltage depends on the point-on-wave switching instant, and the Ferranti effect influenced by the presence of shunt reactors.

The overvoltage may be mitigated by synchronized switching or by the use of pre-insertion resistor.

When pre-insertion resistor is present, the transient phenomenon has two components: one when the resistor is inserted; and another when it is bypassed.

The resistor insertion time average value is specified (about 10 ms) but there is a random variation of few milliseconds (2-4 ms). Synchronized switching has also a random behavior as related to closing instant.

These energization overvoltages are determined by simulation with electromagnetic transient model software running a set of 100-200 cases (shots) characterized by the switching closing instant in the three phases.

It is assumed that the resistor insertion instant follows a Gaussian distribution defined by a mean value and standard deviation. As result, the maximum value of the overvoltage is determined (and the corresponding switching closing instants) and a set of voltages values in the sending, receiving and some intermediate distance of the line.

The values are used to define a statistical distribution of overvoltage (Gaussian or Weibull) through a mean, a standard deviation, and a truncated maximum value.

There are two ways for establishing the distribution of overvoltage: called “phase-peak” and “case-peak” methods. In the former for each shot, for one location, the peak value of the three phases are included in the distribution; in the latter, only the highest of the three phase peaks only is included in the distribution. Therefore they should be considered in different ways when designing the insulation.

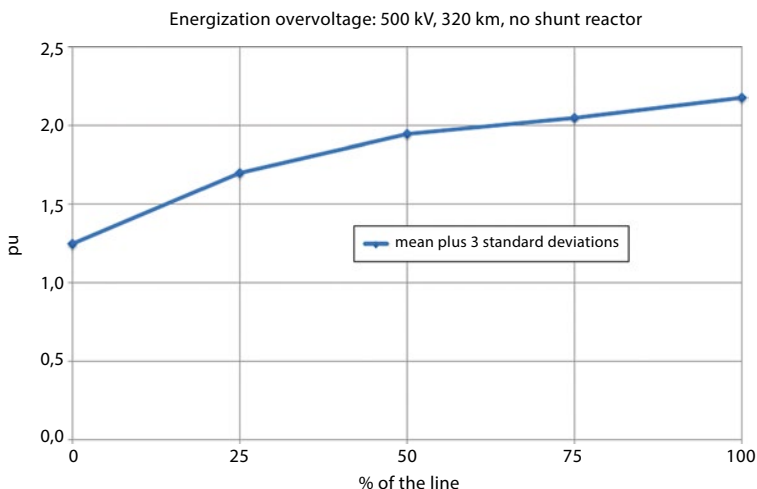
Energization over an existing phase-to-ground fault may lead to higher overvoltage; however they are not used for line insulation design but only to checking surge arrester performance.

It should be noted that the phase-to-ground and phase-to-phase overvoltage distribution shall be obtained for insulation design.

A graph with the mean plus three standard deviation values of phase-to-ground overvoltage along a line is depicted in Figure 4.36.

#### 4.10.3.2 Reclosing

After line opening, one or more tentative of reenergization may occur automatically. When the line is disconnected a trap charge is kept in the line (in the line capacitance) so the reclosing is an energization over the residual voltage of the line; this should lead to higher show-front overvoltage than for energization.



**Figure 4.36** Expected maximum switching surge overvoltage during line energization.

For lines without shunt-connected reactor the trap charge is a DC voltage with certain damping (due to line conductance).

For line with shunt-reactor the line voltage is of oscillatory nature (with two frequencies superimposed, a combination due to the natural line frequency and the operating voltage frequency). In the studies, the worst instant of breaker contact closing shall be searched. After that, a statistical calculation around this worst position is done (random contact closing instant).

The reclosing overvoltages are mitigated by using pre-insertion resistor in the breakers or synchronized closing system. The trap charge can be controlled through: open resistor in the breaker; shunt reactor; inductive potential transformer, and by closing/opening a line to ground fast switch.

The phase-to-ground and phase-to-phase over-voltage distributions are searched to be used in the insulation coordination, in a similar way as for the energization overvoltage.

Figure 4.37 depicts a trap charge in a reactor shunt compensated line.

#### 4.10.3.3 Load Rejection

Apart from the sustained overvoltage in the initial cycles there may occurs low-front overvoltages, in general lower than those for energization/reclosing.

Load rejection with phase-to-ground fault (before or after breaker operation) may be critical event for surge arrester performance.

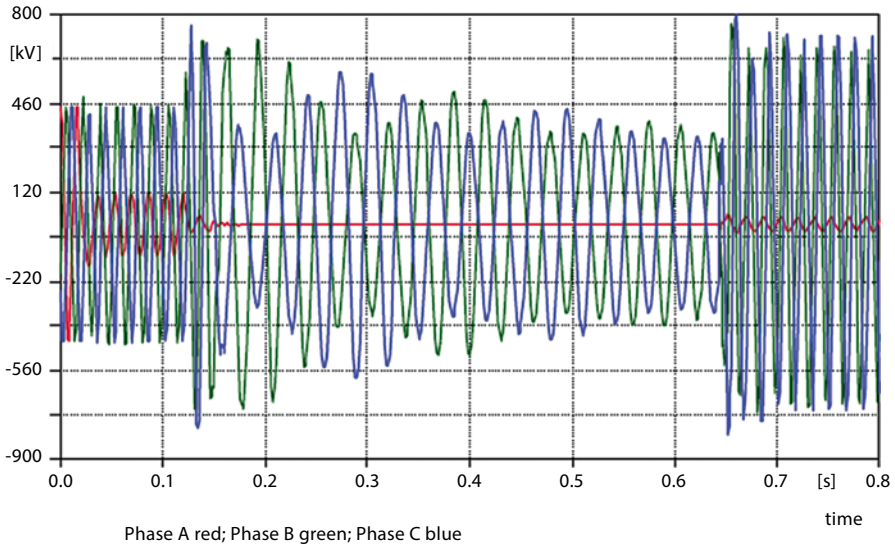
#### 4.10.3.4 Fault Application

When a fault occurs a travelling wave goes in the line and may cause high overvoltage in points of discontinuities (different surge impedances) or when summing up waves from different pass.

In general this overvoltage has short shape and is discharged by surge arrester without any high energy content.

Sometimes they are treated as fast-front surge.





**Figure 4.37** Trapped charge (500 kV system) from 0.12 to 0.65 s; unsuccessful reclosing (fault at phase A).

#### 4.10.3.5 Fault Clearing

They are in general lower than energization/reclosing overvoltages and they depend on the type and distance of the fault, breaker sequence of opening, and prior network condition. Opening resistor may be used to mitigate them.

#### 4.10.3.6 Inductive and Capacitive Load Switching

Capacitive load switching off does not lead to overvoltage; overcurrent during switching in is therefore of concern.

Inductive load switching off may cause local overvoltage when the breaker forces the current to zero before natural zero crossing.

Transformer energization may cause high inrush current that could lead to resonance in points of the system.

This type of overvoltage, in general, does not influence line design but substation design. Mitigation is obtained with closing/opening resistor or synchronized switching.

## 4.11 Insulation Coordination

### 4.11.1 General

When a low voltage stress is applied in insulation there is no flow of current. When this stress is increased to a sufficiently level, the resistivity along the pass through the insulation changes to a low value, conducting current (breakdown).

A number of factors influence the dielectric strength of the insulation (IEC 71-2):

- The magnitude, shape, duration, polarity of the voltage applied
- The electric field distribution in the insulation
- The type of insulation: air, liquid, solid, gas
- The physical state of the insulation (including ambient conditions).

Breakdown in air insulation is strongly dependent on gap configuration and polarity and on the wave shape of the voltage stress.

This withstand capability of insulation is determined through standard test:

- Sustained overvoltage sinusoidal wave
- Fast-front 1 min 1.2/50  $\mu$ s waveform
- Slow-front 250/2500  $\mu$ s waveform

Withstand capability is different depending on the wave polarity.

The insulation withstand depends on the ambient conditions, and it is referred to “standard atmospheric conditions”.

- Temperature 20 ° C
- Pressure 101.3 kPa (1013 mbar)
- Absolute humidity 11 g/m<sup>3</sup>.

#### 4.11.2 Statistical Behavior of the Insulation

First of all it should be noted that some insulations are non regenerative (oil, paper in a transformer for instance) and others are auto-regenerative like the air. In the latter case the statistical behavior is discussed here-in-after.

When a certain number of shots, with the same wave, are applied in an insulation the breakdown may occur by some of them only.

Due to this, the insulation withstand is defined by a probability function (Gaussian or Weibull) (Figure 4.38).

##### Gaussian (Normal) Distribution

$$P(U) = \frac{1}{\sqrt{2\pi}} \int_{-\infty}^x e^{-\frac{1}{2}y^2} dy \quad (4.123)$$

Where

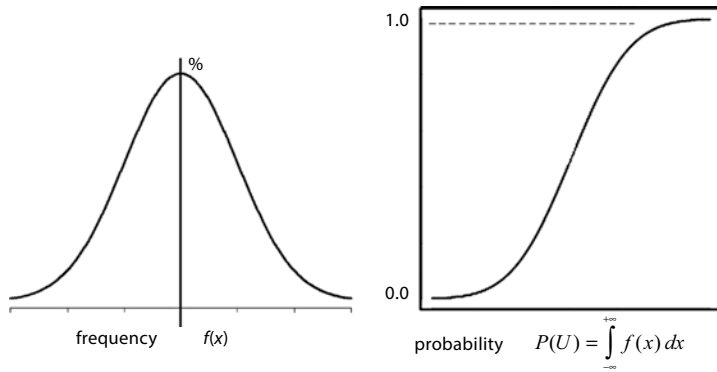
$$X = (U - U_{50}) / Z$$

$U_{50}$  being the 50% discharge voltage ( $P(U_{50})=0,5$ ), and Z being the conventional deviation.

Table 4.16 shows some values.

$P(y)$ =probability of not being exceeded

$[1-P(y)]$ =probability of being exceeded



**Figure 4.38** Gaussian distribution (frequency and probability).

**Table 4.16** Frequency and probability

y	P(y) Rounded values	1 - P(y)
-3	0.001	0.999
-2	0.02	0.98
-1.34	0.10	0.9
-1	0.16	0.84
0	0.50	0.5
1	0.84	0.16
1.34	0.90	0.1
2	0.98	0.02
3	0.999	10 <sup>-3</sup>
4	0.999968	0.3 10 <sup>-4</sup>
5	0.9999997	0.3 10 <sup>-6</sup>

**Weibull Distribution**

The equations are:

$$P(U) = 1 - e^{-\left(\frac{U-\delta}{\beta}\right)^\gamma} \tag{4.124}$$

Where  $\delta$  is the truncation value,  $\beta$  is the scale parameter and  $\gamma$  is the shape parameter.

$$\delta = U_{50} - NZ \tag{4.125}$$

$$\beta = NZ (\ln 2)^{-\frac{1}{\gamma}} \tag{4.126}$$

This leads to the modified Weibull

$$P(U) = 1 - 0,5^{\left(1 + \frac{U-U_{50}}{ZN}\right)^\gamma} \tag{4.127}$$

$N$ =number of conventional deviations

The exponents determined by

$$(P(U_{50} - Z) = 0,16) \quad (4.128)$$

$$\gamma = \frac{\ln \left[ \frac{\ln(1 - 0,16)}{\ln 0,5} \right]}{\ln(1 - (1/N))} \quad (4.129)$$

With truncation at ( $U_0 = U_{50} - 4Z$ ),  $N=4$ , results  $\gamma \approx 5.0$  and finally

$$(x = (U - U_{50}) / Z) \quad (4.130)$$

$$P(U) = 1 - 0,5^{\left(1 + \frac{x}{4}\right)^5} \quad (4.131)$$

### **Characterization of the Insulation Withstand**

The statistical behavior of the insulation (as a Gaussian distribution) is defined provided two values are known for instance, the mean  $U_{50}$ , and the standard deviation  $Z = U_{50} - U_{16}$ . Sometimes the value  $U_{50}$  is substituted by  $U_{10}$  or  $U_2$ .

When the Weibull distribution is used, the truncation value is also defined in terms of  $N$  conventional deviations (ex:  $N=4$ ).

The conventional deviation of the insulation can be assumed as:

- For fast-front (lightning)  $Z=0.03 U_{50}$
- For slow-front (switching surge)  $Z=0.06 U_{50}$

IEC 71-2 considers the value  $U_{10} = (U_{50} - 1.3 Z)$ , to define the withstand capability of equipment insulation.

## **4.11.3 Insulation Coordination Procedure**

### **4.11.3.1 Continuous (Power Frequency) Voltage and Temporary Overvoltage**

The coordination is set based in the maximum voltage peak value phase-to-ground that is the phase-to-phase voltage divided by  $\sqrt{3}$ .

Insulation withstand of the insulator string varies depending on the pollution level.

Table 4.17 contains the specific creepage (mm/kV), to set the recommended distance depending on the pollution level. The distance referred is the contour of the insulator (creepage distance).

**Table 4.17** Recommended creepage distance (IEC 71-2)

Pollution level	Examples of typical environments	Minimum nominal specific creepage distance mm/kV <sup>1</sup>
I Light	<ul style="list-style-type: none"> <li>- Areas without industries and with low density of houses equipped with heating plants</li> <li>- Areas with low density of industries or houses but subjected to frequent winds and/or rainfall</li> <li>- Agricultural areas<sup>2</sup></li> <li>- Mountainous areas</li> <li>- All these areas shall be situated at least 10 km to 20 km from the sea and shall not be exposed to winds directly from the sea<sup>3</sup></li> </ul>	16.0
II Medium	<ul style="list-style-type: none"> <li>- Areas with industries not producing particularly polluting smoke and/or with average density of houses equipped with heating plants</li> <li>- Areas with high density of houses and/or industries but subjected to frequent winds and/or rainfall</li> <li>- Areas exposed to wind from the sea but not too close coasts (at least several kilometres distant)<sup>3</sup></li> </ul>	20.0
III Heavy	<ul style="list-style-type: none"> <li>- Areas with high density of industries and suburbs of large cities with high density of heating plants producing pollution</li> <li>- Areas close to the sea or in any cases exposed to relatively strong winds from the sea<sup>3</sup></li> </ul>	25.0
IV Very Heavy	<ul style="list-style-type: none"> <li>- Areas generally of moderate extent, subjected to conductive dust and to industrial smoke producing particularly thick conductive deposits</li> <li>- Areas generally of moderate extent, very close to the coast and exposed to sea-spray or to very strong and polluting winds from the sea</li> <li>- Desert areas, characterized by no rain for long periods, exposed to strong winds carrying sand and salt, and subjected to regular condensation</li> </ul>	31.0

NOTE - This table should be applied only to glass or porcelain insulation and does not cover some environmental situations such as snow and ice in heavy pollution, heavy rain, arid areas, etc.

<sup>1</sup>According to IEC 815, minimum creepage distance of insulators between phase and earth related to the highest system voltage (phase-to-phase)

<sup>2</sup>Use of fertilizers by spraying, or the burning of crop residues can lead to a higher pollution level due to dispersal by wind

<sup>3</sup>Distances from sea coast depend on the topography of the coastal area and on the extreme wind conditions

**4.11.3.2 Slow-Front (Switching Surge)**

There are two methods: deterministic; and statistical approaches.

In the deterministic approach a statistical value of the overvoltage is set equal to a statistical value of the withstand (both with certain probability)

$$U_{S50} + N_S Z_S = U_{W50} - N_W Z_W \tag{4.132}$$

$U_{S50}$ ,  $U_{W50}$  are the means of the overvoltage and withstand capability

$Z_S, Z_W$  are the standard deviations (overvoltage-withstand)

$N_S, N_W$ =number corresponding to a desired probability (form instance  $N_S=3; N_W=4$ ), or the truncation points.

In the statistical approach the risk of failure is evaluated. The following assumptions are established:

- Peaks other than the highest are disregarded
- Shape is taken as identical to the standard waveform
- All overvoltage of the same polarity (the worst).

The risk is than calculated as

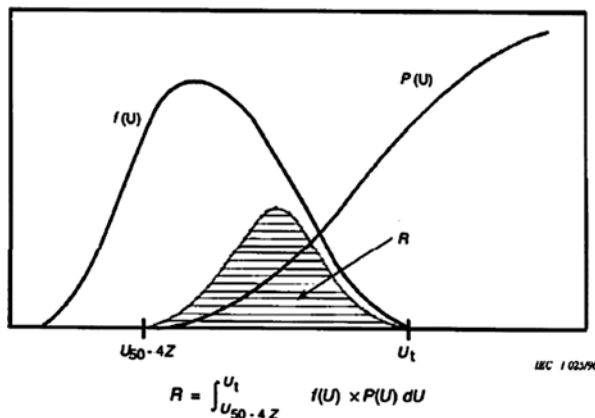
$$R = \int_{U_1}^{U_2} f(u)P(u)du \tag{4.133}$$

where:

- $f(u)$ =probability density of the overvoltage
- $P(u)$ =discharge probability of the insulation
- $U_1$ =truncation point of the discharge probability
- $U_2$ =truncation point of the overvoltage

Figure 4.39 shows the procedure.

A simplified approach consists in the assumption that the overvoltage ( $U_{S50}, Z_S$ ) and discharge voltage ( $U_{W50}, Z_W$ ) are Gaussian curves.



$f(u)$  = probability density of the overvoltage occurrence described by a truncated Gaussian or a Weibull function  
 $P(u)$  = discharge probability of the insulation described by a modified Weibull function  
 $U_t$  = truncation value of the overvoltage probability distribution  
 $U'_{50} - 4Z$  = truncation value of the discharge probability distribution

**Figure 4.39** Evaluation of the risk of failure.

Failure occurs when overvoltage is greater than withstand. The combination is also a Gaussian distribution in which the mean ( $R_{50}$ ) and the standard deviation ( $Z_R$ ) are:

$$R_{50} = U_{S50} - U_{W50} \quad (4.134)$$

$$Z_R = \sqrt{Z_S^2 + Z_W^2} \quad (4.135)$$

$$\text{Risk} = 1 - \frac{1}{\sqrt{2\pi}} \int_{-\infty}^0 e^{-\frac{1}{2}(x^2)} \quad (4.136)$$

$$X = \frac{x - R_{50}}{Z_R} \quad (4.137)$$

Example: Calculate the risk of failure for:

$$U_{S50} = 820 \text{ kV} \quad Z_S = 82 \text{ kV or } 10\% \quad (4.138)$$

$$U_{W50} = 1125 \text{ kV} \quad Z_W = 45 \text{ kV or } 4\% \quad (4.139)$$

$$R_{50} = 820 - 1125 = -305 \quad (4.140)$$

$$Z_R = \sqrt{82^2 + 45^2} = 93.5 \text{ kV} \quad (4.141)$$

$$X = \frac{0 - (-305)}{93.5} = 3.2 \quad (4.142)$$

From Gaussian table values  $X=3.2$ :

$$R = (1 - 0.99931) = 0.0007.$$

When there are  $n$  equal insulations stressed by the same overvoltage, the risk of failure  $R$ , of at least one insulation breakdown is:

$$R = 1 - (1 - R_1)^n \quad (4.143)$$

Where  $R_1$  is the individual risk

Therefore for calculating the risk in the case of:

- energization overvoltage, once known distribution at sending, middle and receiving ends, calculation is made as “quasi-peak” method.

The following steps shall be followed:

- set one insulation defined by  $U_{W50}$ ,  $Z_W$
- calculate the risks  $R_s$ ,  $R_m$ ,  $R_r$  (at sending, middle and receiving end points)
- assume that  $N_s$  insulations are stressed by the sending overvoltage,  $N_m$  and  $N_r$  by middle and receiving overvoltage.

The total risk of a failure will be:

$$R = 1 - (1 - R_s)^{N_s} (1 - R_m)^{N_m} (1 - R_r)^{N_r} \quad (4.144)$$

Note: If the distributions were determined as “phase–peak”, then, the three phases risk has to be considered as for instance.

$$R_r = 1 - (1 - R_{r\text{ ph}})^3 \quad (4.145)$$

$R_{r\text{1ph}}$  is the risk in one phase

### 4.11.3.3 Fast-Front (Lightning Surge)

The same concepts applied above for slow-front are valid for fast-front overvoltages.

### 4.11.3.4 Influence of Atmospheric Conditions

The air pressure, temperature, and humidity affect the withstand capability of an air gap or insulator.

Assuming that the effect of temperature and humidity cancel it other [1], than only the effect of air pressure (altitude) is present and the correction factor  $K_a$  is applied to the withstand capability of the insulation.

$$K_a = e^{m \left( \frac{H}{8150} \right)} \quad (4.146)$$

Where

$H$  is the altitude above sea level (in meters) and the value of  $m$  is as follows:

$m = 1.0$  for co-ordination lightning impulse withstand voltages;

$m$  according to Figure 4.40 for co-ordination switching impulse withstand voltages;

$m = 1.0$  for short-duration power-frequency withstand voltages of air-clearances and clean insulators.

*Note:* The exponent  $m$  depends on various parameters including minimum discharge path which is generally unknown at the specification stage. However, for the insulation co-ordination purposes, the conservative estimates of  $m$  shown in (Figure 4.146) may be used for the correction of the co-ordination switching impulse withstand voltages. The determination of the exponent  $m$  is based on IEC 60-1 in which the given relations are obtained from measurements at altitudes up to 2000 m. In addition, for all types of insulation response, conservative gap factor values have been used.

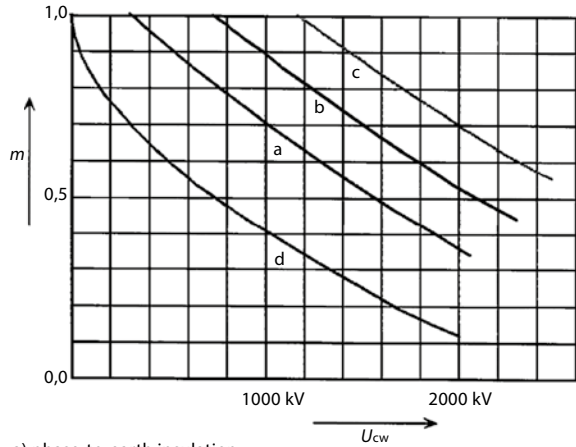
For polluted insulators, the value of the exponent  $m$  is tentative. For the purposes of the long-duration test and, if required, the short-duration power-frequency withstand voltage of polluted insulators,  $m$  may be as low as 0.5 for normal insulators and as high as 0.8 for anti-fog design.

The values of  $m$  are shown in Figure 4.40.

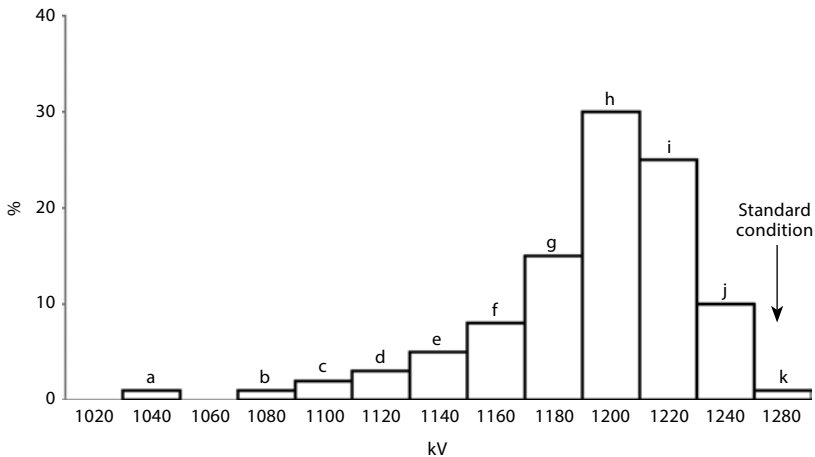
In Figure 4.41 the distribution of withstand value of an example of insulation affected by atmospheric conditions is shown.



**Figure 4.40** Dependence of  $m$  on the switching surge withstand voltage.



a) phase-to-earth insulation  
 b) longitudinal insulation  
 c) phase-to-phase insulation  
 d) rod-plane gap (reference gap)  
 For voltages consisting of two components, the voltage value is the sum of the components.



**Figure 4.41** Distribution of 50% withstand value of an insulation affected by atmospheric conditions.

The effect of atmospheric condition is then considered in the risk of one insulation by applying the overvoltage distribution in the withstand capability affected, in each interval, and then calculating the weight average of the values of risk.

### 4.11.4 Withstand Capability of Self Restoring Insulation

The air gaps, filled or not with insulators, are of the self-restoring type. The geometrical configuration of the gap influences its withstand capability.

The critical flashover value ( $U_{50}$ ), in kV, for “standard atmospheric condition”, can be estimated as function of the gap distance (d) in m by:

For slow-front

$$U_{50} = k500d^{0.6} \quad 2 < d < 5 \quad (4.147)$$

$$\text{or } U_{50} = k \frac{3400}{1 + \frac{d}{8}} \quad 5 < d < 15 \quad (4.148)$$

$k$  being the gap factor as shown in Figure 4.42.

Phase-to-phase insulation (see Figure 4.43) is also influenced by the factor  $\alpha$ , defined as the ratio of the negative peak and the sum of the positive and negative peaks.

Table 4.18 shows the gap factors to be considered for  $\alpha$  equal to 0.5 and 0.33.

- for fast-front overvoltages

$$U_{50} = k^+ 500 d \quad (4.149)$$

$$k^+ = 0,74 + 0,26 k \quad (4.150)$$

$K$  is the gap factor for slow-front overvoltages

For positive polarity and/or insulator strings in order to evaluate effect of lightning impinging the substation:

$$U_{50} = 700 d$$

- for sustained overvoltages

The withstand characteristic is shown Figure 4.44.

Finally in a tower there are many gaps subjected to the same overvoltage: conductor-tower (arm); conductor-guy wire; conductor-tower (lateral); conductor-to-ground; insulator string. The risk of failure in one tower  $R_i$  shall be estimated by:






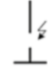
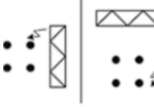
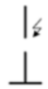
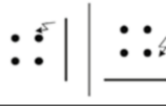




$$R_i = 1 - (1 - R_{g1})(1 - R_{g2}) \dots (1 - R_{gk}) \quad (4.151)$$

$R_{gk}$  is the risk of insulation gap  $k$ .

---

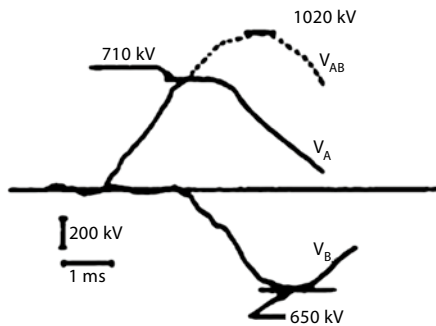
## 4.12 Electric and Magnetic Fields, Corona Effect

Ground level electric and magnetic field effects of overhead power lines have become of increasing concern as transmission voltages are increased. The electric fields are especially important because their effects on human beings and animals

Gap type	Insulator	Factor k	
		Without	With
rod-plane		1.0	1.0
rod-structure (below)		1.05	
conductor-plane		1.15	
conductor-window		1.20	1.15
conductor-structure (below)		1.30	
rod-rod (3m below)		1.30	
conductor-structure		1.35	1.30
rod-rod (6m)		1.40	1.30
conductor-guy wire		1.40	
conductor-tower arm		1.55	1.50
conductor rod (3 m)		1.65	
conductor rod (6 m)		1.90	
conductor-rod (above)		1.90	1.75

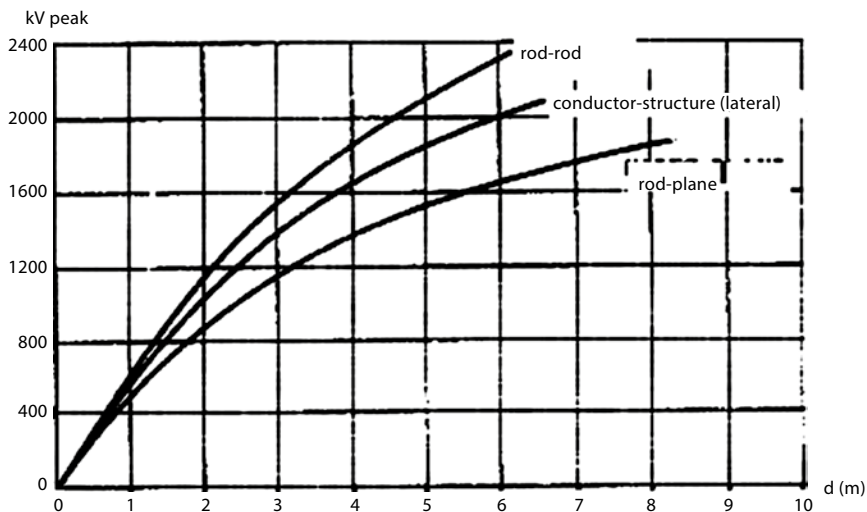
**Figure 4.42** Gap factor for slow-front overvoltages with and without insulator string.

**Figure 4.43** Phase-to-phase overvoltage.



**Table 4.18** Gap factor phase-to-phase insulation

Configuration	$\alpha=0.5$	$\alpha=0.33$
Ring-ring or large smooth electrodes	1.80	1.70
Crossed conductors	1.65	1.53
Rod-rod or conductor-conductor (along the span)	1.62	1.52
Supported busbars (fittings)	1.50	1.40
Asymmetrical geometries	1.45	1.36



**Figure 4.44** Withstand characteristic of gap (power frequency).

have been a concern in the last decades. Serious views still exist that prolonged exposure to electric and magnetic fields could be associated with adverse health effects or with increased risks. However, it is not appropriate to consider unlikely conditions when setting and applying electric field safety criteria because of possible consequences; thus statistical considerations are necessary.

The resultant electric and magnetic fields in proximity to a transmission line are the superposition of the fields due to the three-phase conductors. Usually some limitations, originated from the practice or researches are imposed to the maximum electric field at the edge of the right-of-way.

The evaluation of the electric and magnetic fields across the right-of-way of overhead transmission line can nowadays be made with high accuracy so that the possible health effects of such fields over humans, animals and plants can be evaluated.

Although there is no evidence of harmful effects of the magnetic fields over humans or animals, there are certain limitations imposed by the practice and by the good sense. International organizations like Cigré and ICNIRP have undertaken extensive investigations on such issue.

The range of maximum values expected and accepted as the usual field intensities of electric and magnetic fields are shown in Tables 4.19 and 4.20 below:

Although medical examinations in linesmen, performed in various countries, have so far failed to scientifically prove health problems directly attributed to electric and magnetic fields produced by overhead lines, some conventional limit values have been established for exposures from which the numbers given in Table 4.21 below gives an indication.

In general, limitations are according to Table 4.21, by ICNIRP, according to them maximum values for general public are set for the right-of-way border, while other values are established for occupational people.

**Table 4.19** Range of maximum allowable electric and magnetic fields below overhead lines of any voltage (example)

Exposure Type	Electric Field Limit(kV/m)	Magnetic Field Limit ( $\mu$ T)
Difficult Terrain	20	125
Non-populated Areas	15-20	100-125
Road Crossings	10-12	50-100
Frequent Pedestrian.	5	50
Circulation		

**Table 4.20** Range of maximum expected electric and magnetic fields below overhead lines as a function of line voltage

TL voltage (kV)	Electric field at ground level (kV/m)	Magnetic field at ground level ( $\mu$ T)
765	8-13	5
500	5-9	3
345	4-6	3
230	2-3.5	2
161	2-3	2
138	2-3	2
115	1-2	1.5
69	1-1.5	1

**Table 4.21** Maximum electric and magnetic field values set by ICNIRP (ICNIRP 1997)

Limit values	General public	Occupational
Electric field kV/m	250/f	500/f
Magnetic field $\mu$ T	5000/f	25000/f

According to ICNIRP new limits have been introduced as Guidelines for limiting Exposure to time-varying electric, magnetic, and electromagnetic fields (up to 300 GHz); the limit values for “general public” and “occupational workers” are established as below:

where  $f$  it is the frequency in Hz.

Regarding the maximum acceptable limits for the magnetic fields, there are no universally definitive numbers as some controversy is still worldwide existent especially about their real effects on the health of human beings and animals. While in some countries the regulations are more permissible, in others severe rules have been established.

Other two types of unwanted disturbances caused by overhead transmission lines on the environment are also of importance, namely:

Radio Noise or Radio Interference (RI) that is a disturbance within the radio frequency band, such as undesired electric waves in any transmission channel or device. The generality of the term becomes even more evident in the frequency band of 500 kHz to 1500 kHz (AM band). The frequency of 1000 kHz (1 MHz) is usually taken as reference for RI calculation.

Audible Noise (AN) produced by Corona of transmission line conductors has emerged as a matter of concern of late. In dry conditions the conductors usually operate below the Corona-inception level and very few Corona sources are present. Audible noise from AC transmission lines occurs primarily in foul weather. However, in general, it can be said that transmission systems contribute very little as compared with the audible noises produced by other sources. In the case of rural lines, the importance of the Audible Noise (AN) as well as of the Radio-Interference (RI) may be still lower, as the population density beside the line is generally too small.

#### 4.12.1 Corona Effects

When a set of voltages are applied on the conductors of a transmission line an electric field or voltage gradient appears on its surface (conductor surface gradient). If this surface gradient is above a certain limit (Peek gradient or critical Corona or set gradient) the Corona discharges initiate.

Electric discharge phenomena produce various effects (power loss, high frequency electromagnetic fields, acoustic and luminous emission, ions and ozone generation).

High frequency electromagnetic fields interfere with radio or TV signals in the proximity of the lines.

A person standing near an overhead line whose conductors and/or assemblies are under Corona can sometimes hear a special noise: frying, crackling and hissing sounds and low frequency hum.

These effects are influenced by the transmission line characteristics (conductor size, bundle configuration, phase/pole spacing, conductor height to ground), conductor surface gradient and atmospheric condition (temperature, pressure, rain, snow, etc) the last ones a statistical behavior to the phenomenon is assigned.

The phenomenon presents different aspects if AC or DC line is under consideration.

Corona considerations in the design of transmission lines have been discussed in the Cigré TB 61 (1996) and Cigré TB 20 (1974). This publication includes discussion of Corona losses (CL), radio interference (RI) and audible noise (AN).

Factors influencing the choice of conductor bundles are discussed below. This section provides basis for selection of the conductor bundle.

### 4.12.1.1 Conductor Surface Gradient

Consider the case of two conductors above soil.

For AC or DC lines, the relationship between charge ( $Q$ ) and voltage ( $V$ ) on the conductors or shield wires is given by:

$$[V] = [H][Q] \tag{4.152}$$

$H_{ij}$  are the Maxwell potential coefficients (refer to Figure 4.45):

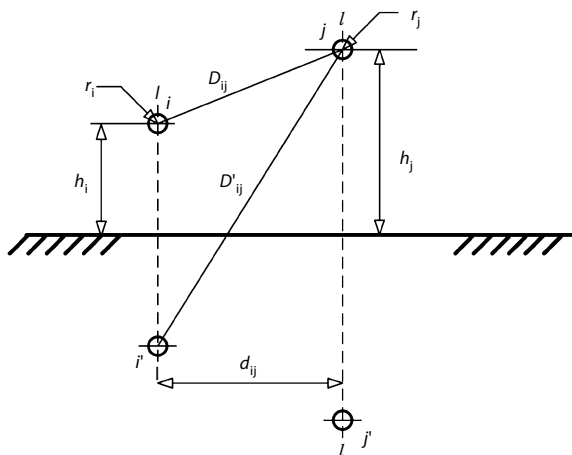
$$H_{ii} = \frac{1}{2 \pi \epsilon_0} \ln \frac{2 h_i}{r_{eqi}} \tag{4.153}$$

$$H_{ij} = H_{ji} = \frac{1}{2 \pi \epsilon_0} \ln \frac{D_{ij}}{D_{ij}} \tag{4.154}$$

where:

$r_i$  = single conductor (sub index c) or shield wire (sub index sw) radius;

**Figure 4.45** Symbols for  $\lambda_{ij}$  calculation.



$$r_{eq} = R \sqrt[n]{\frac{nr_i}{R}} = \text{equivalent radius of the bundle;}$$

$n$  = number of sub-conductors in the bundle;

$R$  = radius of the bundle;

$$R = \frac{a}{2 \sin(\pi / n)}$$

for a regular bundle with a distance between adjacent subconductors;

$$h_{ij} = h_{\min} + \frac{1}{3} s = \text{average height of the conductor or shield wire;}$$

$h_{\min}$  = minimum distance of the conductor or shield wire to ground;

$s$  = sag of the conductor or shield wire;

Equation above can be divided into:

$$\begin{bmatrix} V_c \\ V_{sw} \end{bmatrix} = \begin{bmatrix} H_{c-c} & H_{c-sw} \\ H_{sw-c} & H_{sw-sw} \end{bmatrix} \begin{bmatrix} Q_c \\ Q_{sw} \end{bmatrix} \quad (4.155)$$

If the shield wires are grounded, then  $V_{sw} = 0$  and the above equation system is reduced to:

$$[V_c] = \left( [H_{c-c}] - [H_{c-sw}] [H_{sw-sw}]^{-1} [H_{sw-c}] \right) [Q_c] \quad (4.156)$$

If the shield wires are isolated from ground then the corresponding equations can be deleted. In both cases the set of equations reduces to:

$$[V_c] = [H'_{c-c}] [Q_c] \quad (4.157)$$

The number of lines and rows of the matrix  $[\lambda'_{c-c}]$  is equal to the number of phases of an AC line or poles of a DC line. The charges are then calculated by:

$$[Q_c] = [H'_{c-c}]^{-1} [V_c] \quad (4.158)$$

Since it is assumed that the total charge of the bundle is equally distributed on the  $n$  subconductors, the mean gradient of a conductor in a bundle is given by:

$$g_a = \frac{1}{n} \frac{Q}{2 \pi \epsilon_0 r} \quad (4.159)$$

The average maximum gradient of the subconductors is defined by:

$$g = g_a \left[ 1 + \frac{(n-1) r}{R} \right] \quad (4.160)$$

The critical Corona onset gradient is given by:

$$g_c = g_o \delta m \left[ 1 + \frac{k}{\sqrt{\delta r}} \right] \quad (4.161)$$



where:

- $g_c$  = critical Corona onset gradient (kV/cm);
- $g_o$  = Corona onset gradient (normal ambient conditions: 25 °C, 76 cm Hg) (kV/cm);
- $r$  = radius of the conductor (cm);
- $k = 0.308$  for AC or DC (both polarities);
- $m$  = surface factor;
- $m = 1$  smooth and polished surface
- $m = 0.6$  to  $0.8$  actual dry weather service conductor
- $m = 0.3$  to  $0.6$  raindrops, snowflakes, extreme pollution
- $m = 0.25$  heavy rain
- $\delta$  = relative air density (RAD);

$$\delta = K_d \frac{P}{273 + t}$$

$P$  = pressure of the ambient air (cm Hg or Pa);

$t$  = temperature of the ambient air (°C);

$K_d$  as in Table 4.22.

In the line design the conductor surface gradient should be smaller than the Peek gradient and including a safety factor (ex:  $g < 0.95 g_c$ ). This gradient is also the key factor in the interferences that the line may cause (radio, audible).

#### 4.12.1.2 Corona Loss

AC transmission Corona losses (in dB) can be calculated based on equations presented in the references (Chartier 1983; Maruvada 2000)

$$P(dB) = 14.2 + 65 \log \frac{E}{18.8} + 40 \log \frac{d}{3.51} + K_1 \log \frac{n}{4} + K_2 + \frac{A}{300} \quad (4.162)$$

Where:

- $n$  = number of subconductors
- $d$  = diameter of subconductors, cm
- $K_1 = 13$  for  $n \leq 4$  and  $19$  for  $n > 4$

**Table 4.22** Values of  $K_d$

	$K_d$
Normal conditions (25 °C, 76 cm Hg)	
°C and cm Hg	3.921
°C and Pa	0.00294
IEC normal conditions (20 °C, 76 cm Hg)	
°C and cm Hg	3.855
°C and Pa	0.00289

$E$  = maximum conductor surface gradient, kV/cm

$A$  = altitude, m

$$K_2 = 10 \log \frac{I}{1.676} \quad \text{for } I \leq 3.6 \text{ mm/h}$$

$$K_2 = 3.3 + 3.5 \log \frac{I}{3.6} \quad \text{for } I > 3.6 \text{ mm/h}$$

$I$  = rain rate, in mm/h

A distribution of fair and rainy weather has to be established.

#### 4.12.1.3 Radio Interference

Radio interference (RI) is any effect on the reception of wanted radio signals due to any unwanted disturbance within the radio frequency spectrum. Radio interference is a concern only with amplitude modulation (AM) radio reception because frequency-modulated (FM) radio is inherently less sensitive to disturbances. Radio interference is evaluated by comparing the noise level with the radio signal, i.e. the signal-to-noise ratio (SNR), at the edge of the servitude or right-of-way, and for a frequency of normally 0.5 or 1 MHz using a quasi-peak detector with a bandwidth of 5 or 9 kHz according to CISPR or ANSI standards, respectively (1974; 1996). The RI level is expressed in dB above 1  $\mu$ V/m.

Since RI and AN are caused by the same phenomenon, i.e. streamer discharges appearing on the positive conductor or during the positive half-cycle, the variation of RI with the weather conditions is essentially the same as for AN. Thus, the RI level is the highest in rain for AC lines, but lower in rain for DC lines

As RI is dependent on the weather conditions, it is appropriate to represent the RI level in statistical terms for each weather condition, such as the  $L_5$  and  $L_{50}$  levels in fair weather or rain.

*Note:*  $L_x$  is termed the exceedence level; this is defined as the level that is exceeded  $x\%$  of the time. For example  $L_{50}$  is the level that is exceeded 50% of the time and  $L_{90}$  is exceeded 90% of the time. The value  $x$  and the cumulative frequency are complementary to one another, i.e.  $x\% = 100\% - \text{cumulative frequency } (\%)$ .

Alternatively, the results may be presented as an “all weather” curve considering average climate conditions.

Cigré TB 61 (1996) reports “empirical” formulae for the radio interference level at the reference frequency of 0.5 MHz or 1 MHz, at a given distance from a three-phase line, for three basic weather categories (mean fair weather, mean foul weather and heavy rain), as a function of the main influencing parameters (conductor surface gradient, diameter of the subconductors, number of subconductors in the bundle, frequency, etc.). These formulae were based on the results of direct measurements of radio interference levels performed on operating and experimental lines with system voltages of up to 800 kV and bundles of up to four subconductors.

Sometimes “empirical” equations are given considering two approaches: BPA and Cigré TB 61. To compare the results of the two methods, the following characteristics of the two measuring standards have to be considered (Table 4.23).

For comparison of measurements performed using different receivers:

Value (CISPR) = Value (ANSI) – 2 dB

**Table 4.23** Basic characteristics of CISPR and ANSI radio interference measurement standards.

	Receiver		Measuring Frequency
	Pass band	Charge/discharge constant	
CISPR	9 kHz	1 ms/160 ms	0.5 MHz
ANSI	5 kHz	1 ms/600 ms	1.0 MHz

For correction of measuring frequency:

Value (CISPR) = Value (ANSI) + 5.1 dB

Cigré approach consider (CISPR specification: QP: 9 kHz – 0.5 MHz) and the “heavy rain” RI in dB is:

$$RI_{hr} = -10 + 3.5g + 6d - 33 \log\left(\frac{D}{20}\right)$$

where

$g$  = maximum surface gradient (function of the mean height)

$D$  = radial distance from the phase to the point

$d$  = subconductor diameter

With:  $10 \text{ m} < D < 60 \text{ m}$ , and the term  $6d$  is valid for  $1 \text{ cm} < d < 2.5 \text{ cm}$  only.

It should be noted that (see Figure 4.46):

- from the heavy rain value subtract 24 dB to get mean fair weather value
- from the heavy rain value subtract 7 dB to get “mean foul weather”
- from the heavy rain value subtract 3.5 dB to get “mean stable rain”.

The equation applies for all phases, however the total RI can be calculated by:

$$E_i = 20 \log \sqrt{\sum_{k=1}^3 E_{ki}^2} \tag{4.163}$$

$$E_{kj} = 10^{\frac{RI_{kj}}{20}} \tag{4.164}$$

Ranking of the phase-fields:

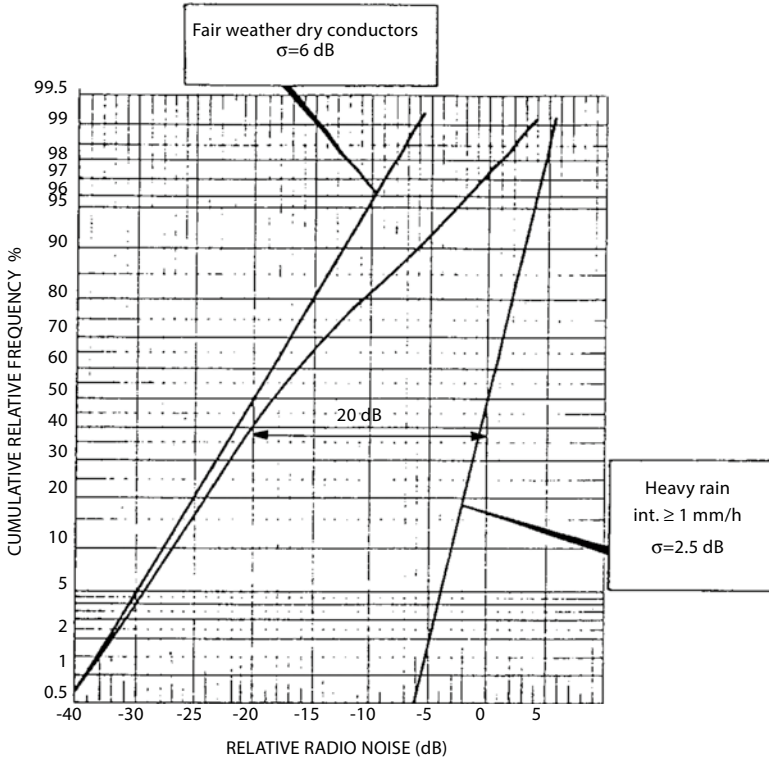
$$RI_a \geq RI_b \geq RI_c \tag{4.165}$$

(dB (1  $\mu$ V/m))

$$\text{If } RI_a - RI_b \geq 3 \text{ dB: } RI = RI_a \tag{4.166}$$

$$\text{If } RI_a - RI_b < 3 \text{ dB: } RI = \frac{RI_a + RI_b}{2} + 1.5 \tag{4.167}$$

Design criteria for RI from transmission lines are generally based on signal to noise ratios (SNR) for acceptable AM radio reception. Studies carried out on Corona-generated RI from AC and DC transmission lines indicate that the SNRs for acceptable radio reception are in the Table 4.24.



**Figure 4.46** RI and weather.

**Table 4.24** Quality of radio reception

Signal noise ratio Logarithmic (dB)	Code	Reception quality Subjective impression
30	5	Interference not audible
24	4	Interference just perceptible
18	3	Interference audible but speech perfectly received
12	2	Unacceptable for music music but speech intelligible
6	1	Speech understandable only with great concentration
0	0	Spoken word unintelligible: noise swamps speech totally

Minimum radio station signal requirement in many countries (ex: Brazil) is 66 dB for cities with population from 2500 to 10000 inhabitants. Similar condition probably applies to other countries and is used here as part of the criteria.

At present, there are no established design criteria for RI from DC transmission lines; so the tentative guidelines are for limiting the RI at the edge of the right of way to  $(66-18)=48$  dB or to keep a reception code 3 at the reception. The SNR above may be referred to average fair weather noise. For more stringent criteria, the noise shall be below  $48-6=42$  dB for 85% probability of not being exceeded (in fair weather), meaning that in 15% of the time the reception will be classified as between the code 2 (in fair weather). The reference frequency is considered here as 0.5 MHz, if 1 MHz is considered the noise is 6 dB lower.

### 4.12.1.4 Television Interference

Investigations regarding conductor Corona interference above 30 MHz are not as extensive as for RI in the frequency range up to 30 MHz. In practice, interferences to television reception (TVI) are more often caused by microgap discharges on power line hardware or by polluted insulators than by conductor Corona. Because of the higher frequency range, attenuation along a power line as well as that away from the line is considerably larger. Consequently, effects of local noise sources are much more pronounced for TVI. There are no indications that TVI should be of special concern to AC or DC lines; therefore, if a line has an acceptable RI level, then TVI need not be considered, and is not further discussed here (1974).

### 4.12.1.5 Audible Noise

The audible noise emanates from the air pressure variations that are caused by the Corona discharges, more specifically the streamer discharges created under positive DC voltage or during the positive half-cycle of the AC voltage. The audible noise is the result of numerous uncorrelated Corona discharges, resulting in a broadband noise spectrum covering the entire range of audible frequencies. AN from AC lines also contain a hum component (100 or 120 Hz) caused by space charge movement close to the conductor, correlated with the power frequency.

The human ear has a different response to each of these frequencies; therefore weighting filter networks are used for measuring the human response. The most common is the A-weighting network, in which case the audible noise level is stated as dBA above 20 μPa.

For the AC conductors, (1996) presents empirical formulas for direct calculation of AN from different sources. A Cigré formula for AN L<sub>5</sub> levels, derived from the original formulas, is also given. A formula developed by BPA formula is also presented and will be used here.

For “wet conductor” the average excitation function is:

$$\Gamma A_{50} = K_1 + 120 \log g + K_2 \log n + 55 \log d + \frac{q}{300} \tag{4.168}$$

	K <sub>1</sub>	K <sub>2</sub>
n < 3	-169.7	0
n ≥ 3	-182.7	26.4

For average fair-weather subtract 25 dBA

Range of validity: 230 – 1500 kV, n ≤ 16, 2 ≤ d ≤ 6.5 cm

The AN level in dBA is:

$$LA = \Gamma A + 54.3 - 11.4 \log D \tag{4.169}$$

$$\Gamma A_5 = \Gamma A_{50} + 3.5 \tag{4.170}$$

The sum of the individual pressure values from all phases results in the total sound pressure at the point:

$$L_{ATot} = 10 \log \sum_{i=1}^3 10^{\frac{LA_i}{10}} \tag{4.171}$$

Note: The hum component of Corona is usually low, but might be taken into consideration separately in special “foul weather” conditions with large Corona loss.

The AC lines design criteria are defined based on subjective evaluation obtained from group of people.

Low complaints :< 52 dBA (equivalent to business office noise)

Moderate: (some) complaints = 52-58 dBA

Many complaints: >58 dBA

Moreover the weather condition has to be established and in some countries it is defined as maximum noise not to be exceeded at average rain = 42 dBA (average). This level corresponds to suburban living room noise ([EPRI Transmission](#)).

## 4.1.2.2 Fields

### 4.1.2.2.1 Electric Field

For the calculation of the electric fields close to the ground, first the V-Q-Maxwell potential coefficient are used ([EPRI Transmission](#)).

The charges in all phases and eventually grounded shield wires ( $Q$ ) are calculated by:

$$[Q] = [H]^{-1} [V] \quad (4.172)$$

It should be noted that  $V = (V_r + j V_i)$  is a complex number and so  $Q = (q_r + j q_i)$

The electric field in a point N with coordinates  $(x_N, y_N)$  due to the charge  $q_a$  and its image  $q_a$  is:

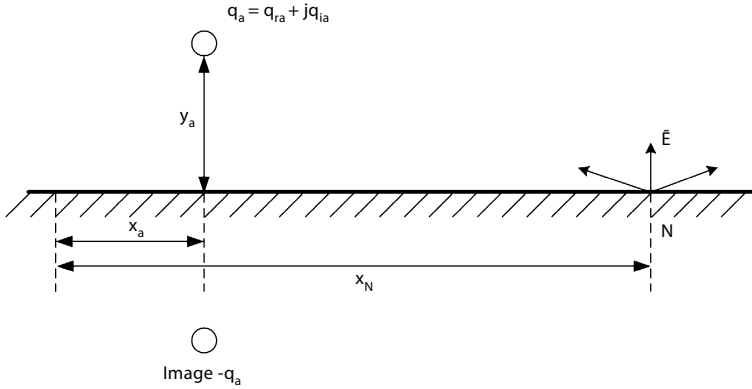
$$\vec{E}_a = \tilde{E}_{x,a} \vec{u}_x + \tilde{E}_{y,a} \vec{u}_y \quad (4.173)$$

Where  $\vec{u}_x$  and  $\vec{u}_y$  are the unit vectors along the horizontal and vertical axes and  $\tilde{E}_{x,a}$  and  $\tilde{E}_{y,a}$  are given by:

$$\begin{aligned} \tilde{E}_{x,a} &= \frac{(q_{ra} + jq_{ia})(x_N - x_a)}{2\pi\epsilon \left[ (x_a - x_N)^2 + (y_a - y_N)^2 \right]} - \\ &\frac{(q_{ra} + jq_{ia}v)(x_N - x_a)}{2\pi\epsilon \left[ (x_a - x_N)^2 + (y_a + y_N)^2 \right]} \end{aligned} \quad (4.174)$$

And

$$\begin{aligned} \tilde{E}_{y,a} &= \frac{(q_{ra} + jq_{ia})(y_N - y_a)}{2\pi\epsilon \left[ (x_a - x_N)^2 + (y_a - y_N)^2 \right]} - \\ &\frac{(q_{ra} + jq_{ia})(y_N + y_a)}{2\pi\epsilon \left[ (x_a - x_N)^2 + (y_a + y_N)^2 \right]} \end{aligned} \quad (4.175)$$



**Figure 4.47** Calculation of the electric field at ground level.

The horizontal and vertical components,  $\tilde{E}_x$  and  $\tilde{E}_y$  of the electric field are calculated by adding the contributions of all the conductors (a,b,...):

$$\tilde{E}_x = \tilde{E}_{x,a} + \tilde{E}_{x,b} + \dots \tag{4.176}$$

$$\tilde{E}_y = \tilde{E}_{y,a} + \tilde{E}_{y,b} + \dots \tag{4.177}$$

The results is an equation where there are the real and imaginary parts of the charge and components in the x and y axis. To find the maximum values an specific calculation is needed ([EPRI Transmission](#)); one way is tabulating  $\tilde{E}_x, \tilde{E}_y$ , and  $E_t = \sqrt{E_x^2 + E_y^2}$  as function of the time and getting the maximum value of  $E_t$ .

For the electric field at ground level the x axis components of a charge and its image cancel themselves (Figure 4.47).

The equation is then:

$$E_{y,a} = \frac{q_a}{\pi \epsilon_0} \frac{y_a}{(x_a - x_N)^2 + y_a^2} \tag{4.178}$$

Similar equations apply to other phases and the total field becomes:

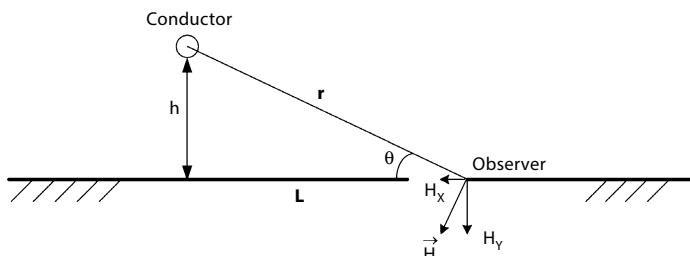
$$E_t = E_{y,a} + E_{y,b} + \dots \tag{4.179}$$

### 4.12.2.2 Magnetic Field

The phenomena and calculation procedure are presented in ([EPRI Transmission](#)) and is summarized here-in-after (Figure 4.48).

The variables to be considered are the flux density B and the magnetic field H. They are related by the equation

$$\begin{aligned} B &= \mu H \\ \mu &= \mu_0 \mu_r \end{aligned} \tag{4.180}$$



**Figure 4.48** Magnetic flux at ground level.

The permeability of the free space is  $\mu_0 = 4\pi \cdot 10^{-7}$  and  $\mu_r$  the relative permeability is unity for all except ferromagnetic materials.

Assuming a circle in a plane perpendicular to the conductor whose center is on the conductor, the magnetic field along the circle is a constant given by:

$$H = \frac{i}{2\pi r} \quad (4.181)$$

$$B = \frac{\mu i}{2\pi r}$$

Where  $i$  is the current and  $r$  the radius of the circle.

Simplified calculation of the magnetic field at ground level is given by:

$$H = \frac{i}{2\pi\sqrt{h^2 + L^2}} = \frac{B}{\mu} \quad (4.182)$$

$$H_x = H \sin(\theta) = H \frac{h}{r}$$

and

$$H_y = H \cos(\theta) = H \frac{L}{r} \quad (4.183)$$

For multi-conductor the superposition applies in a similar way presented for electric field. The maximum value has to be searched taking into consideration also that the current has real and imaginary parcels.

Another consideration relates to the image of conductors, they have to be located at great depth  $d$  that in a first approximation (being  $\rho$  the soil resistivity and  $f$  the frequency)  $d$  is given by:

$$d \cong 660 \sqrt{\frac{\rho}{f}} \quad (4.184)$$

Accurate calculation may call for the use of Carson's equations. However for many purposes the earth current may be disregarded.



## 4.13 Overvoltages and Insulation Coordination

First, the reader shall realize that the line constants consideration are included in the section related to AC lines (Section 4.1.7) and is not repeated here reason why this section starts with overvoltages.

The selection of the optimum transmission line (bipole) alternatives encompasses the different components of the line, so that a global optimization can be achieved. The optimum choice only has a real meaning when electrical, mechanical, civil and environmental aspects are taken into account as a whole set, for which a satisfactory performance and reasonable costs are simultaneously looked for (Cigré TB 388 2009).

Regarding the transmission line itself, its design includes at first the electrical requirements such as power transfer capability and voltage which are specified from which the tower-top geometry, the electric field effects, the Corona effects, the overvoltage and insulation coordination and the required right-of-way are established. Then the mechanical design of the towers and foundations, the determination of conductors and shield wires stresses are carried out; finally the economics including direct costs, cost of losses, operation and maintenance cost along line life, are evaluated.

The design process is iterative as the electrical parameters can be met with a variety of solutions. The optimum solution is derived from interaction with planners and designers.

*Note:* this text is based on (Cigré TB 388 2009) that may be consulted if more details are necessary. See also Chapter 7 and for electrical constants details Section 4.1.7 (that includes AC and DC line constants).

### 4.13.1 Overvoltages

#### 4.13.1.1 Types of Overvoltages

The definition of the insulation levels is dependent on different voltage stresses that reach the air-gaps and are so chosen as to result in the best compromise between a satisfactory electrical performance and reasonable costs.

To define the tower-top-geometry of the towers, in the case of a DC line, the following voltage stresses are considered: sustained due to operating voltage, and transient due to lightning and switching surge overvoltages. Therefore, the scope of this clause is an evaluation of the overvoltages in the HVDC system aiming at the DC line insulation design required.

The switching-surge overvoltages in a HVDC system occur in the DC as well as in the AC part of the system.

In the latter one, overvoltages are the result of the following switching operations: line energization; line reclosing, load rejection, fault application, fault clearing and reactive load switching, and all should be evaluated.

As related to HVDC system, the above mentioned overvoltages are also considered for the converter station insulation design; by the use of surge arresters, the overvoltages are limited to values corresponding to the arrester Maximum Switching and Lightning Surge Voltage Levels. The surge discharge capability of the arrester needs to be verified as part of the overvoltage studies for equipment specification.

Regarding switching surges fault application is the only one type of overvoltage to be considered because of the intrinsic process of the HVDC system. For line energization and reclosing, the DC voltage is ramped up smoothly from zero, and in the reclosing process the line de-energization process eliminates the trapped charge.

As for load rejection, it generally does not transfer overvoltages to the DC side. DC filter switching does not cause overvoltages.

Lightning overvoltages may start a fault in the DC line, however its effect is smaller as compared with AC system faults due to the fact that the fault current will be limited by HVDC station controls, the line voltage is ramped down and after a sufficient time for the trapped charge discharge, the voltage is ramped up to the nominal value or to a reduced voltage value (around 80% for example).

Shield wires are normally installed in the lines for reducing the number of faults, by providing appropriate shielding. The major point in the design is then to locate the shield wires in the right position. Shield wires may also be used as a communication medium for control of the converters, their design needs to take both functions into account.

Sustained overvoltages in the DC side of HVDC systems do not occur due to the intrinsic control process of the HVDC operation. It should be noted that overvoltages in the DC side may appear due to harmonic/filter/smoothing reactor resonance. It is considered here that this is a problem to be solved by the design of appropriate elements, and so such kind of stresses will not be considered herein for the insulation design of the DC line.

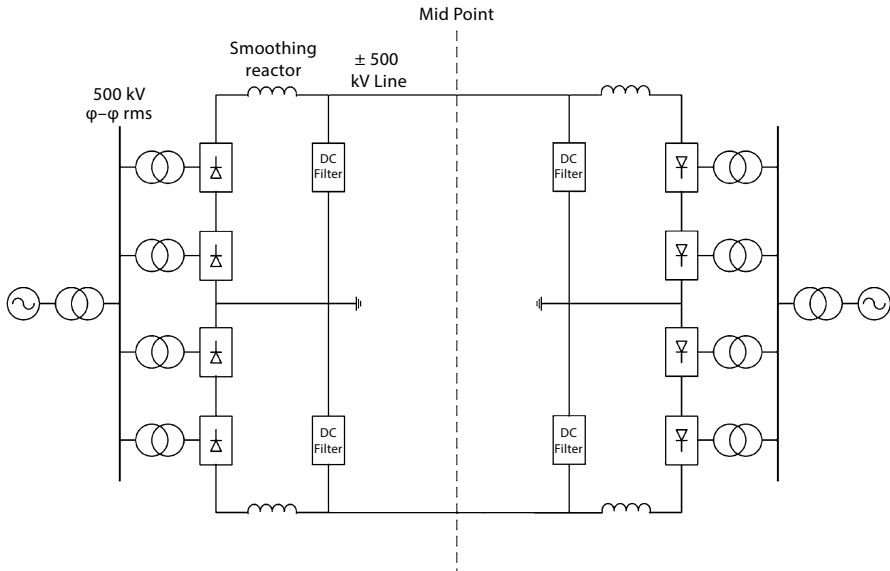
### ***Determination of Switching Surge Overvoltage (Fault Application)***

Switching surge due to fault application in a DC line, being the most important voltage stress to be applied to its insulation, will be evaluated hereafter.

#### **MODELING**

The overvoltages hereinafter are calculated with PSCAD/EMTP (Electromagnetic Transient Program) using models such as the one shown on Figure 4.49. The data of the Base Case are here also represented.

- Generator/receiving system  
They are modeled as a short circuit power, providing enough power as required. The short-circuit capacities used are: 9400MVA for single-phase short-circuit and also for three-phase short-circuit.
- The converter transformers of both terminals are specified in this model as:  
Two transformers per pole herein modeled with the following characteristics:  
Power=400 MVA each



**Figure 4.49** HVDC system modeling for fault application calculation (1300 MW).

Reactance  $x_{cc} = 18\%$

Turn ratio = 500/199 kV at rectifier or 194 kV at inverter

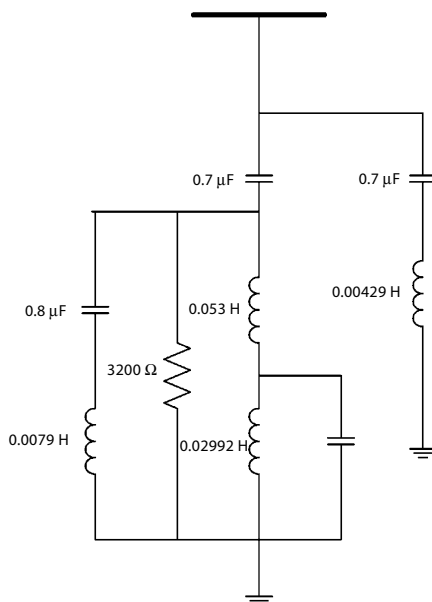
- DC filters/smoothing reactor  
The values used here are (EPRI EL 3892 1985):  
Smoothing reactor of 200 mH;  
DC filter as below (Figure 4.50)
- Simulation time step = 5  $\mu$ s
- Converter stations

They are modeled using PSCAD/EMTP blocks. Converter control system are modeled according to (Szechtman et al. 1991)

There is a system voltage control in the inverter ( $\gamma_{min}$  = extinction angle control), line current control at rectifier ( $\alpha$  = firing angle control). At fault inception in the HVDC line the current tends to increase and the control acts reducing the line current (different from HVAC systems). Also the line protection sensing the fault change  $\alpha$ ,  $\gamma$ , to values above  $90^\circ$  and the current goes to zero.

- DC line  
The line model is composed of eight sections, each one modeled as lossless line traveling wave equations. Line losses (resistance) are represented in the model at section end. Electrical parameters (resistance and inductance) are modeled as frequency dependent or constant. For more detailed analysis see Section 4.1.7.

**Figure 4.50** DC filter parameters.



#### FAULT APPLICATION PHENOMENA

For the initiation of the fault in the negative pole, a positive surge of value equal to the pre-fault voltage is injected in the fault point, and the resulting surge travels in both line directions, reflecting in the line end and coming back to the fault point. The traveling wave is coupled to the positive pole resulting in an overvoltage which values are due to the composition of the forwarded and of the reflected waves.

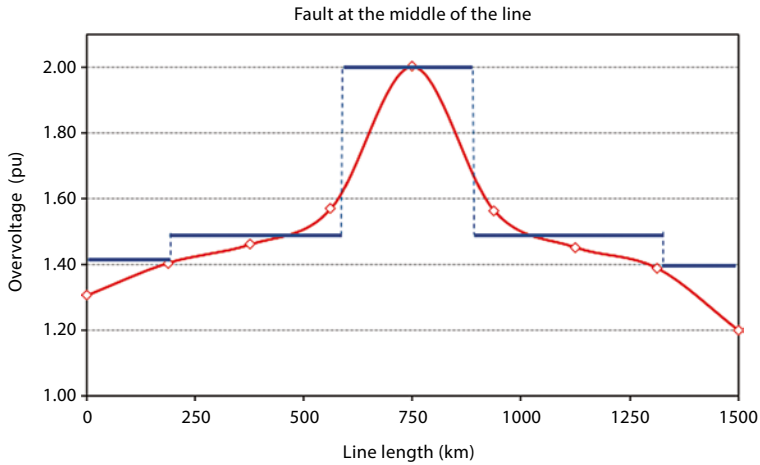
The maximum overvoltage occurs for a fault initiated in the middle of the line, within a time close to the travel time to the line end and back to the mid point of the first reflections. Faults in other locations produce smaller overvoltages. Due to this, the overvoltage profiles down the line are similar for every line length, as will be shown later. Line end equipment (filters, smoothing reactor and source) play an important role, as they define the traveling wave reflection coefficients.

#### CALCULATION RESULTS

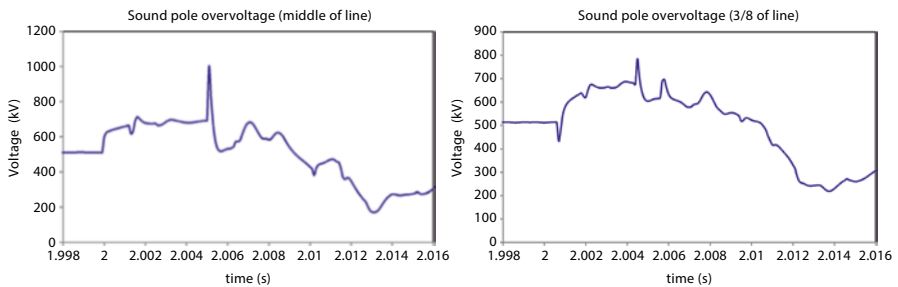
For the Base Case calculation, the following points were taken into account: a line 1500 km long; equal sources at both ends (rectifier and inverter) and line parameters variable with the frequency.

Figure 4.51 shows the maximum overvoltage profile in the sound pole for a fault initiated at mid point of the other pole, and Figure 4.52 the voltage versus time in the mid/end point of the sound pole.

The maximum overvoltage reaches 2.0 pu, however the overvoltages are below 1.6 pu (20% lower) at 1/4 of the line. Standard deviation for insulation switching surge withstand is 6%, this means that the overvoltage in the major part of the line does not contribute to the risk of failure and therefore the line is designed considering mainly the maximum value (2.0 pu in this case). As example in the insulation coordination calculation the envelope shown in blue in the Figure 4.51 may be used to address risk of failure.



**Figure 4.51** Overvoltage profile along the sound pole for a fault initiated at midpoint of the other pole.



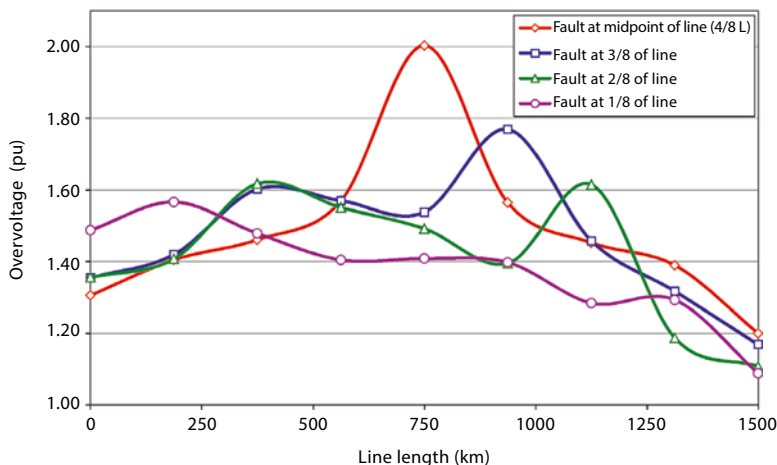
**Figure 4.52** Fault at mid point, overvoltage in the sound pole (middle and 3/8 of l) (1,500 km line).

From here on, the line is split in several segments, identified as a fraction of its length (1/8, 1/4, 3/8 and so on). Figure 4.53 shows the overvoltage profile for fault initiated at other line positions. It can be seen that all values are below 1.8 pu and so do not contribute so much to the risk of failure.

### 4.13.2 Insulation Coordination

This section aims at designing the clearances and at defining the number and type of insulators to be used in the insulator strings.

The number of insulators is initially selected based on the maximum DC voltage withstand and on the assumption of a certain pollution level. The number of insulators obtained by these criteria is then verified by considering the overvoltage values. The clearances to be determined are: conductor-to-tower cross-arm, conductor-to-tower or objects (lateral), conductor-to-ground or objects (at the ground), and conductor to guy wires.



**Figure 4.53** Overvoltage profiles, Base Case, fault in different positions.

**Table 4.25** Clearances for operating voltages (m)

Operating Voltage (kV)	Clearance (m)
+500	1.20
+800	1.90

They are calculated for switching surge overvoltage withstand. However, the clearance to tower and guy wires as well as to edge of right-of-way shall be verified in the condition of insulation string swing due to wind in order to prevent flashovers and the touch of objects (such as trees) at the border of the right-of-way.

#### 4.13.2.1 Operating Voltage Withstand

##### *Air Clearances*

For determining the minimum necessary conductor-structure clearances for operating voltage insulation, the following premises are considered:

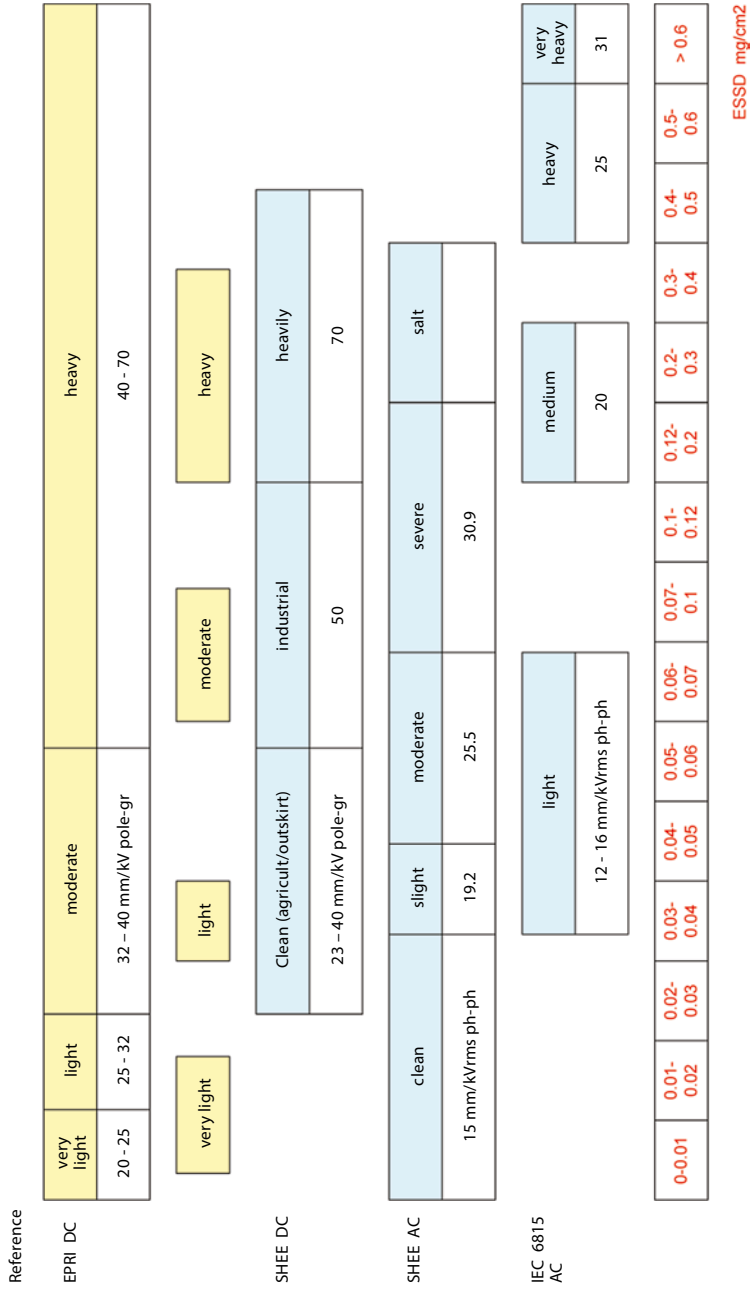
- Withstand voltage regarding the most unfavorable condition: positive polarity, conductor-to-structure;
- Maximum operating voltage and correction for the atmospheric conditions: 1.15 pu.

The distances conductor-to-structure were obtained according (EPRI 1977) and are shown on Table 4.25.

##### *Number of Insulators*

In AC or DC system the number of insulators in a string is determined by adopting an environmental condition (pollution, air density) and choosing a creepage distance criterion for AC or for DC (Figure 4.54).

As example, by using a creepage distance (pole-to-ground) equal 30 mm/kV, the number of insulators and the respective insulator string lengths are determined and



**Figure 4.54** Creepage design criteria.

**Table 4.26** Number of Insulator and String Length

Operating Voltage (kV)	Creepage distance Number of Insulators	30 mm/kV String Length (m) (*)
± 500	30	5.20
± 800	48	8.17

Notes:

The following type of insulator was considered:

- Anti-fog insulator, pitch of 165 mm and leakage distance of 508 mm
- Hardware length: 0.25 m
- Porcelain type or glass. Composite can be used in any area and is robust against vandalism and pollution.

It should be noted that the suitability of the insulator string length is verified considering switching surge and the gap conductor cross arm.

shown in Table 4.26. The creepage distances adopted are adequate with a good safety margin to zones with a pollution level classified as “light contamination”.

For agricultural areas and woodlands 23 mm/kV is recommended, and for outskirts of industrial areas 40 mm/kV is recommended. Some references recommend as acceptable even lower creepage distances down to 20 mm/kV (for area classified as with “very light pollution”); however a higher figure is here considered as more appropriate.

As a reference, the Itaipu lines (“light pollution - agricultural area”) were designed for 27 mm/kV and have shown adequate performance in more than 20 years of operation.

### **Insulator String Swing Angle**

The swing angle of the conductor due to wind, as example, was calculated according Cigré/IEC (Cigré TB 48 1995) recommendation, using the following data:

- Line altitude = 300 m
- Average temperature = 16 °C
- Minimum ratio of vertical/horizontal span = 0.7
- Wind return period = T = 50 years
- Mean value of the distribution (m/s) =  $\bar{V}$  = 18.39 (10 min integration)
- Standard deviation = 3.68 m/s
- Wind distribution with 30 years of measurements
- Terrain classification = B

Considering a Gumbel distribution (extreme values), the wind velocity to be considered, depending on the return period, is determined by:

$$V_i = \bar{V} + \frac{X}{C_1}(Y - C_2) \quad (4.185)$$

$$Y = -\ln\left(-\ln\left(1 - \frac{1}{T}\right)\right) \quad (4.186)$$



where:

$V_t$  = Wind velocity (m/s) with return period  $T$ .

$\bar{V}$  = Wind velocity - mean (m/s).

$S$  = Standard deviation (m/s).

$C_1 = 1.11237$  and  $C_2 = 0.53622$  are coefficients, for a sample of 30 years [35].

$T$  = return period (years).

It Results =  $V_t = 29.52$  m/s

The insulator string deflection is calculated by:

The swing angle of an insulator may be related to the wind velocity by:

$$\bar{\Phi} = \tan^{-1} \left[ \frac{(\rho / 2) V_R^2 k D L_w + F_{wi} / 2}{W_c + W_i / 2} \right] \quad (4.187)$$

In this formula the following symbols are used:

$\rho$  air density

$V_R$  reference wind speed

$k$  correction factor taking into account the effect of wind span

$D$  conductor diameter

$L_w$  wind span

$F_{wi}$  wind load insulator

$W_c$  effective conductor weight taking into account the differences in the level of conductor attachments

$W_i$  weight of insulator

$V_R = 1.05 V_t$  (5 min integration) = 30.99

$\rho = 1.18$  kg/m<sup>3</sup>

$k = 1.0$

$D = 0.0382$  m

$L_w = 450$  m

By disregarding insulators parameters:

$1.18 * 0.5 * (30.99)^2 * 1 * 450 * 0.0382 = 9748.5$  Newtons

$W_c = 2.671$  kg/m  $\times 450$  m  $\times 0.7$  (ratio  $L_p/L_w$ )  $\times 9.81 = 8253.8$  Newtons

$\varphi = 49.7^\circ$

The calculations were done based on (Cigré TB 48 1995) Cigré TB 48, for a set of ACSR-Aluminum Conductor Steel Reinforced conductors; the results are shown on Table 4.27.

#### 4.13.2.2 Switching Surge Withstand

##### *Calculation Procedure*

Once the switching surge overvoltages (as determined before) are known, the clearances are calculated based on the risk of failure considering the withstand capability of the gaps. This is estimated by:

**Table 4.27** Swing Angle to be used together with the respective Clearances for the Operating Voltage

Conductor code	Aluminum/steel mm <sup>2</sup> /mm <sup>2</sup>	Aluminum MCM*	Swing Angle (°)
Joree	1.274/70	2.515	44.5
Lapwing	806/57	1.590	49.7
Bluejay	564/40	1.113	53.4
Tern	403/29	795	56.7

\* 1 MCM=0.5067 mm<sup>2</sup>

Note: The conductor types and stranding taken as examples in this report can be further optimized in the case of a real project. There are cases where other conductor types (ASC Aluminum Conductor; AAC-Aluminum-Alloy Conductor, ACAR – Aluminum Conductor Aluminum-Alloy Reinforced; AACSR-Aluminum-Alloy Steel Reinforced) may be more adequate. These, however, will not be covered here. The entire methodology does however apply to them.

$$V_{50} = k \cdot 500 \cdot d^{0.6} \quad (4.188)$$

where:

$V_{50}$ =Insulation critical flashover (50% probability), (kV)

$d$ =gap distance (m)

$k$ =gap factor:

$k = 1.15$  conductor – plane

$k = 1.30$  conductor – structure under

$k = 1.35$  conductor – structure (lateral or above)

$k = 1.40$  conductor – guy wires

$k = 1.50$  conductor – cross arms (with insulator string)

*Note:* The standard deviation  $\sigma$  of the withstand capability is 6% of the mean.

The latter equation applies to Extra High Voltage System when  $2 < d < 5$  m.

An alternative equation when  $5 < d < 15$  m, is:

$$V_{50} = k \frac{3400}{1 + 8/d} \quad (4.189)$$

The clearances are determined based on the fault application overvoltage profiles, aiming at a certain flashover failure risk target (design criteria). It is proposed here a failure rate of 1 in 50 or 1 in 100 years. It will also be assumed, as design criteria, that 1 fault per 100 km per year (mainly due to lightning) can occur. The overvoltages shown on Figure 4.51 are used for this purpose. The following steps are carried out (together with an example):

- Select one line length and one rated voltage (Ex: 1500 km; 500 kV as the Base Case);
- Select one gap type and size (Ex: conductor-structure lateral=3.0 m);
- Select the overvoltage profiles in the sound pole for fault in the middle of the other pole (Ex: maximum value is  $2.0 \times 500 = 1000$  kV);
- Calculate the risk of flashover for the tower in the mid-point of the line for 1 gap (Ex: The critical flashover value of the gap is  $V_{50} = 1.35 \times 500 \times (3.0)^{0.6} = 1305$  kV) the

overvoltage 1000 kV is at  $(-1305 + 1000)/(0.06 * 1305) = -3.9 \sigma$ , hence corresponding to a risk of failure of  $5 \times 10^{-5}$  (see Gaussian probability (2-9));

- Calculate the flashover risk of failure in the central section (Ex: suppose 300 km, the envelope of Figure 2-3, or 600 gaps in parallel subjected to the same overvoltage of the tower in the mid-point of the line, leading to a risk of failure of  $600 * 5 \times 10^{-6} = 3 \times 10^{-3}$ );
- Extend the flashover risk calculation for parallel gaps (towers) for the whole overvoltage profile (Ex: 1.5 pu, see Figure 4.53 envelope, or 750 kV that is at  $(-1305 + 750)/(0.06 * 1305) = -7.0 \sigma$  and the risk  $< 1.0 \times 10^{-8}$ . Considering 800 km or 1600 towers the composite risk is  $< 1.6 \times 10^{-5}$ , therefore negligible contribution to the value on item V above. For the third step of figure 2-3 the overvoltage is 1.4 pu also not contributing to the risk of failure);
- Repeat calculation of the flashover risks of failure for the gap, for fault at other points: or send, or 1/8, or 3/8, or 5/8, or 7/8, or receiving end of the line (ex: disregard this parcels as very few overvoltage values are above 1.6 pu);
- Calculate the weighted flashover average risk of failure, considering that each profile represents fault occurring in a section of (1/8) of the length of the line except seeding/receiving end profiles that correspond to  $(1/2) \times (1/8)$  of the length. The total flashover risk R is then determined (Ex:  $(3.0/8) \times 10^{-3}$ );
- Consider the number of occurrences (faults) and determine the probability of flashover (Ex: 1 fault per 100 km per year or 15 faults per year). Check against 1 in 50 - 100 years (Ex:  $15 \times (3/8) \times 10^{-3} = 0.005$  or once in 200 yr); if the flashover risk is different, then select another gap size (Ex: 2.8 m as the risk can be increased) and go to step III above;
- Repeat for all gaps.

It should be noted that, if the line is designed with I-strings (as opposed to V-strings), then it is recommended to consider in the risk calculation the effect of possible winds simultaneously with the overvoltages.

There are two approaches for taking this point into account: first, by calculating the clearances for an established risk and admitting that such clearances shall be maintained with a certain swing due to wind (of about  $15^\circ$ ); or second, considering the simultaneous occurrence of wind and overvoltage, and finally calculating the composite risk (to lead to 1 failure in 50 years).

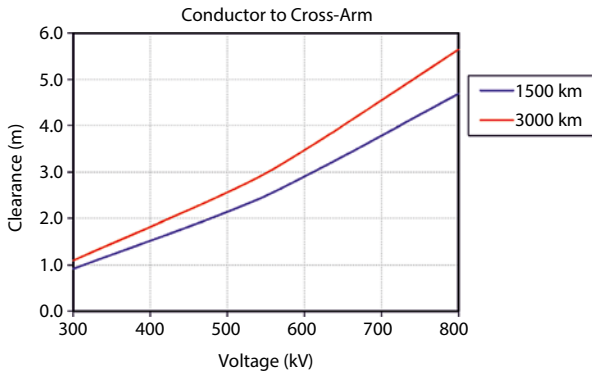
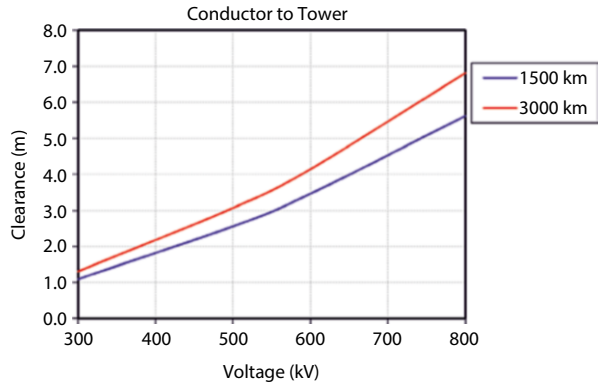
### **Clearances for an Established Flashover Risk of Failure**

The following Figures (4.55, 4.56, 4.57, and 4.58), taken from (Cigré TB 388 2009) in slight different conditions established here, show the clearances for the gaps above mentioned as a function of the line voltage. They were designed for a flashover risk of failure of 1/50 yr, no displacement due to wind, and the overvoltages were calculated using the J. Marti line model and the software EMTP-RV.

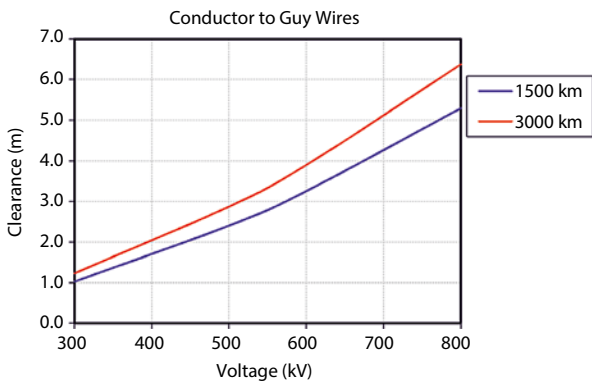
### **Switching Overvoltages with Conductor Displacement due to Wind**

Cigré TB 48 (Cigré TB 48 1995) recommends the adoption of a swing angle caused by a wind intensity corresponding to 1% probability of being exceeded in a year

**Figure 4.55** Conductor to tower clearances.

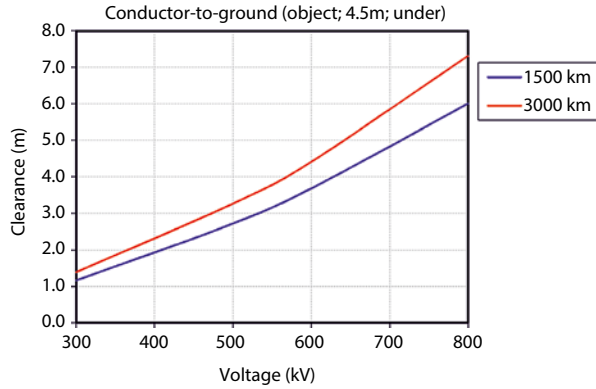


**Figure 4.56** Conductor to cross-arm clearance.



**Figure 4.57** Conductor to guy wires clearance.

**Figure 4.58** Conductor to object clearance (add 4.5 m to get Conductor-to-ground distance).



**Table 4.28** Swing angle to be used together with Switching Surge Clearances

ACSR Conductor code	MCM*	Swing Angle (°)
Joree	2.515	13.4
Lapwing	1.590	15.3
Bluejay	1.113	17.0
Tern	795	18.6

\* 1 MCM=0.5067 mm<sup>2</sup>

together with the occurrence of switching surge overvoltages. Using the wind distribution as per item 2.2.1, the wind intensity is 13.54 m/s.

The swing angles caused by this wind are shown on Table 4.28.

It should be noted that considering simultaneously: the conductor swing due to the wind with 1% probability of being exceeded in one year, and the clearances corresponding to a risk of 1/50 years; the final flashover risk will be much smaller than 1/50, therefore the stated criteria is conservative.

An alternative approach is to find a clearance considering the composite risk for overvoltage distribution and a swing due to the wind distribution.

Note: It should be alerted here that the results obtained in this example and others are applicable only to the parameters used, i.e. wind speed, probability functions, etc.

**Composite Risk Calculation**

Using this approach a swing angle lower than 8° is obtained.

**Atmospheric Conditions**

The calculations presented consider standard laboratory test conditions, however corrections should be considered if atmospheric conditions are different from standard one.

**Table 4.29** Values of  $K_d$ 

	$K_d$
Normal conditions (25 °C, 76 cm Hg)	----
°C and cm Hg	3.921
°C and Pa	0.00294
IEC normal conditions (20 °C, 76 cm Hg)	----
°C and cm Hg	3.855
°C and Pa	0.00289

$$V_{correct} = V_{standard} \left( \frac{\delta}{H} \right)^n \quad (4.190)$$

where:

$\delta$  is the relative air density (RAD);

$$\delta = K_d \frac{p}{273 + t} \quad (4.191)$$

$p$  = pressure of the ambient air (cm Hg or Pa);

$t$  = temperature of the ambient air (°C);

$K_d$  = as in Table 4.29;

$H$  is the humidity correction; factor function of steam pressure that is calculated using maximum saturated steam pressure, humid bulb temperature, air pressure, and dry bulb temperature (also a correction curve is needed).

$n$  = exponent function of the gap length

Atmospheric correction has a statistical behavior and this shall be taken into consideration in the risk of failure calculation. This can be simplified by changing  $V_{50}$  by the average value of the correction or by changing the gap withstand capability standard deviation ( $\sigma$ ) by composite standard deviation that includes the standard deviation of the correction factor.

## 4.14 Pole Spacing Determination

The pole spacing requirements are determined considering the use of  $I$ - or  $V$ -strings.

### 4.14.1 Case of I-Strings

For the pole spacing evaluation, the swing angles of the insulator strings as determined before will be used.

#### 4.14.1.1 Pole Spacing Required for Operating Voltage

The minimum pole spacing  $DP_{TO}$  is:

**Table 4.30** Assumed Tower Widths

Operating Voltage (kV)	Tower Width (m)
±500	1.7
±800	2.5

**Table 4.31** Pole Spacing (m) for Operating Voltage/strings

ACSR Conductor	Cross Section (MCM)*	Pole Spacing (m)	
		±500 kV	±800 kV
Joree	2.515	12.5	18.8
Lapwing	1.590	13.1	19.8
Bluejay	1.113	13.6	20.6
Tern	795	14.0	21.1

\*1 MCM=0.5067 mm<sup>2</sup>

$$DP_{TO} = (R + d_{min} + (L + R)\sin(\theta))2 + w \tag{4.192}$$

where:

dmin=Operating voltage clearance;

R=bundle radius  $R = \frac{a}{2 \sin(\pi / N)}$

a=subconductor spacing (as general rule, 45 cm is adopted);

N=number of subconductors in the bundle (N=4 is adopted for all calculations here), leading to R=0.32 m;

L=insulator string length;

θ=swing angle for the maximum wind speed with 50 year return period;

w=tower width at conductor level, as per Table 4.30.

The pole spacing values are shown on Table 4.31.

**4.14.1.2 Pole Spacing Required for Switching Surges**

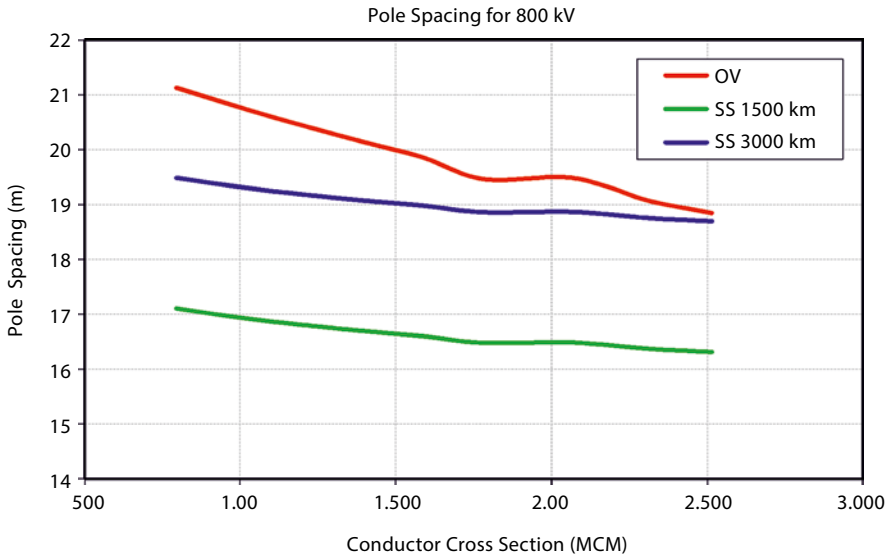
The minimum pole spacing required for switching surges is calculated in a similar manner as before, except that the swing angles are those from Table 4.28. The results for ±800 kV bipole lines are shown on Figure 4.59.

It can be seen that the operating voltage criteria governs the pole spacing for ±800 kV voltages and of course for the other voltages as well.

Therefore, the values of Table 4.31 shall be used as pole spacing for I-string configurations.

**4.14.2 Case of V-Strings**

In this case there will be no swing angles due to wind at the towers the clearance requirements for switching surges will determine the pole spacing. However, the



**Figure 4.59** Pole Spacing ( $\pm 800$  kV, 750 to 3000 km). Nomenclature: OV  $\rightarrow$  Operating Voltage; SS  $\rightarrow$  Switching Surge.

V-strings having length ( $L$ ) shall be inserted in the tower, meaning that the minimum pole spacing ( $PS_{\min}$ ) for installation will be:

$$PS_{\min} = 2L \cos(45^\circ) + w \quad (4.193)$$

where:

$w$  = tower width;

It is assumed here that the V-string angle is 90 degrees, however this opening can be reduced.

The pole spacing requirement is otherwise calculated by:

$$DP_{TO} = (d_{\min} + R) 2 + w \quad (4.194)$$

(provided that  $DP_{TO} > PS_{\min}$ )

The results are shown on Table 4.32.

In summary the pole spacing distances are:

- $\pm 500$  kV  $\Rightarrow$  9.3 m
- $\pm 800$  kV  $\Rightarrow$  14.4 m for line length
  - 15.6 for line length equal to  $< 2250$  km
  - 16.8 for line length equal to 3000 km

It should be noted that clearances for insulation is not the only criteria to choose between I- or V-strings, for instance I-string offers less surface for pollution from



**Table 4.32** Pole spacing requirements

Operating Voltage (kV)	Clearance Conductor Structure (m)			Bundle Radius (m)	Tower Width (m)	Pole Spacing (m)			
	1500 km	2250 km	3000 km			1500 km	2250 km	3000 km	PSmin
±500	2.55	2.83	3.06	0.32	1.70	7.4	8.0	8.5	9.3
±800	5.62	6.25	6.81	0.32	2.50	14.4	15.6	16.8	14.3

birds excretion, the Corona protection rings are simpler, and of course are less expensive as they have less insulators.

## 4.15 Conductor Current Carrying Capability and Sags

The current carrying capability of ACSR conductors were calculated based on Cigré recommendation (TB 207), that relates to AC current. It should be noted that the DC current has a lower heating effect than AC current due to the absence of the transformer and eddy current effects, however this will not be considered here. Therefore, the methodology of calculation can be considered as the same for both AC and DC lines.

The following assumptions are considered:

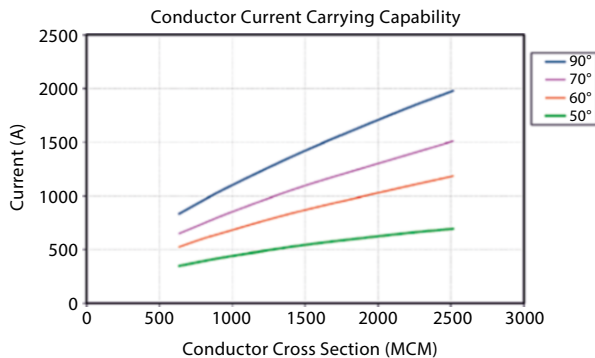
- Wind speed (lowest) 1 m/s
- Wind angle related to the line 45 degree
- Ambient temperature 35 °C
- Height above sea level 300 to 1000 m
- Solar emissivity of surface 0.5
- Cond. solar absorption coefficient 0.5
- Global solar radiation 1000 W/m<sup>2</sup>

The maximum temperature of the conductor will be limited here to 90 °C (as design criteria commonly used in many countries) for steady state and in emergency or short duration conditions, although it could be accepted temperatures even above 100 °C for non-special conductors (Thermal Resistant Conductors may withstand a higher temperature in the steady state condition). However, the conductor is selected based on economic criteria (cost of line plus losses) leading to a maximum operating temperature in normal conditions much lower (~55 to 60 °C). Therefore 90 °C will eventually apply to pole conductors at abnormal conditions as well as to electrode lines and metallic return conductors. Figure 4.60 shows the current capability for some conductors, so that the corresponding values for intermediate sizes can be interpolated.

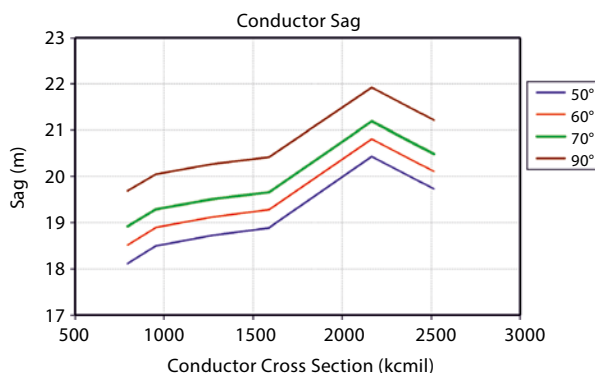
The sags are presented on Figure 4.61 for conductor temperatures in the range from 50 to 90 °C. The sag calculation was based on the following conditions:

- Span=450 m
- EDS=Every Day Stress condition

**Figure 4.60** Conductor Current Carrying Capability for alternatives maximum temperature criteria.



**Figure 4.61** Conductor sags.



- Tension of 20% of the RTS (this is a simplification - ideally the EDS should be selected based on fixed H/w horizontal-tension/weight, the catenary’s parameter);
- Temperature: 20 °C.

It can be seen that the sags vary from 18 to 22 meters, depending on the conductor temperature and type of conductor. It should be noted that the conductors considered in this graph are those of the tables shown before. Conductors with the same aluminum but different steel contents will have different sags.

### 4.16 Tower Height

The following distances are defined hereunder.

The conductor height at the tower ( $h_p$ ) is:

$$h_p = C_s + sc + Ext + R \tag{4.195}$$

where:

$h_p$  = distance from the center of the bundle to ground at tower;

$C_s$  = clearance to ground at mid-span = 12.5 and 19.5 m for ±500 and ±800 kV, respectively, determined by electric field criteria;

**Table 4.33** Conductor and shield wire heights at tallest tower (Two shield wires; for one add 2.5 m to hg)

Voltage (kV)	hp (m)	hg (m)
±500	42.8	50.8
±800	50.8	61.8

sc=conductor sag at 90 ° C (criteria adopted), as per Figure 4.61 (22 m adopted for all conductors in this clause);

$R$ =bundle radius;

Ext=tower extensions up to  $3 \times 3 \text{ m} = 9 \text{ m}$

The shield wire height ( $h_g$ ) at the tower is:

$$h_g = h_p + R + dis + D_G \quad (4.196)$$

where:

dis=insulator string and hardware length: 5.2 and 8.17 m for ±500 and ±800 kV, respectively;

The assumed values for shield wire to cross arm distance  $D_G$  are:

$D_G = 2.5 \text{ m}$  (for the case of two shield wires),

or

$D_G = 5 \text{ m}$  (for the case of only one shield wire).

Table 4.33 shows the values to be used in the calculations which follow.

## 4.17 Lightning Performance

In order to get a good performance under lightning strokes, the design of HVDC lines should include the use of shield wires (one or two).

The shield wires reduce the direct strokes to the conductors. For the strokes that hit the shield wires, there will be an overvoltage that is coupled to the pole conductors and can cause flashovers or not.

To set a good design, some conditions shall be considered:

- The current of the stroke that hit the pole conductors should not produce an overvoltage greater than the insulation withstand of the line.
- The closer are the shield wires to the pole conductor, the better will be the performance due to strokes hitting the shield wires.
- The tower footing resistance and the corresponding tower footing surge impedance should be low, therefore requiring the use of an adequate grounding system, generally counterpoises at the towers.

In regions with ice, the second condition may be conflicting with the requirements of keeping a safety distance from the shield wire to the pole conductors during icing events.

The clearances at the tower are designed to withstand switching overvoltages with a pre-established risk of failure, or the operating voltage.

Once defined the required clearances, the Critical Impulse Flashover Capability  $E$  of the insulation (50% probability) for lightning surges (fast front overvoltages) are known.

With  $E$ ,  $V_{op}$ - the operating voltage- and the conductor surge impedance  $Z$ , the critical “threshold current”  $I_{oc}$ , into the conductor for which a flashover will start is determined by:

$$I_{oc} = \frac{2(E - V_{op})}{Z} \quad (4.197)$$

The striking distance  $r_{sc}$  is a function of  $I_{oc}$  and is calculated by:

$$r_{sc} = k \cdot 6.7 \cdot I_{oc}^{0.8} \quad (4.198)$$

where:

$$r_{sc} = \text{in (m)}$$

$$I_{oc} = \text{in (kA)}$$

$k$  is a factor different from 1 eventually adopted for shield wires or ground.

The horizontal distance  $X$  between conductor and shield wire is:

$$X = r_{sc} \left( \sqrt{1 - (k - T)^2} - \sqrt{1 - (k - R)^2} \right) \quad (4.199)$$

where:

$$r_{sc} = \text{striking distance (m)}$$

$$k = \text{factor}$$

$$T = h_g^* / r_{sc}$$

$$R = h_p^* / r_{sc}$$

$$h_g^* = \text{average shield wire height (m)}$$

$$h_p^* = \text{average conductor height (m)}$$

Three types of terrain may be considered, namely:

- Flat: in this case the following parameters are used in the equations above.

$$h_p^* = h_p - S_c \quad (2/3) \quad (4.200)$$

$$h_g^* = h_g - S_g \quad (2/3) \quad (4.201)$$

$h_p$ ,  $h_g$  are conductor or shield wire heights at tower; and  $S_c$ ,  $S_g$  are the conductors and shield wire sags.

- Rolling: in this case:

$$h_p^* = h_p \quad (4.202)$$

$$b^* = (h_g - h_p) + (S_c - S_g) \quad (2/3) \quad (4.203)$$

$$h_g^* = h_p^* + b^* \quad (4.204)$$

- Mountainous

$$h_p^* = 2 h_p \quad (4.205)$$

**Table 4.34** Protection for direct strokes

Voltage (kV)	$E$ (kV)	$hg^*$ (m)	$hp^*$ (m)	2 shield wires			
				$I_{oc}$ (kA)	$r_{sc}$ (m)	$X$ (m)	$\theta$ (°)
±500	3000	55.2	42.8	14.3	56.2	1.6	11.5
±800	4850	66.2	50.8	23.1	82.7	4.7	23.3

$h_p^*$ ,  $h_g^*$  as in the rolling case.

In this report the evaluations will be done considering rolling terrain, average tower (no extensions) and  $k=1$ .

The protection angle  $\theta$  is then:

$$\theta = \arctan \left( \frac{X}{h_g - h_p} \right) \quad (4.206)$$

The line surge impedance  $Z$  is assumed here as 350  $\Omega$ .

When the lightning activities are low (and on icing regions where it is desired that the shield wires should not be in the same vertical line as the conductors), one shield wire may be a preferable design for economical reasons.

From Table 4.34 it can be seen that the minimum protection angle  $\theta$  can be set at values from 11 to 23 degrees. The closer are shield wires to the conductors, the better is the lightning performance for back flashovers due the higher coupling factor.

As a consequence, the protection angle can be adopted as 10 degrees, when using two shield wires.

Note: Only EHS steel wire is considered for shielding purpose. However other material or characteristics may be used if one intend for instance to provide dual function: lightning shielding and communication (carrier or fiber optics).

## 4.18 Right-of-Way Requirements for Insulation

The Right-of-Way width (ROW) is defined considering the following aspects: Conductor swing and clearances to objects at the border of ROW, Corona and field effects. At this point, only the first condition is examined and the results will be partial.

In the ROW determination, clearances for operating voltage and I-type insulator string length are used.

The swing angles are calculated using the same parameters as clauses before, except that the ratio vertical to horizontal span is equal 1.0, and the span length should not exceed 600 m. It should be reminded that the wind intensity corresponds to 50 year return period. The swing angles are shown on Table 4.35.

The conductor sags (Table 4.36) were obtained by starting from EDS conditions and considering the wind load with the coincident temperature.

**Table 4.35** Swing angles for ROW width definition

Conductor		Swing Angle (degree)
ACSR Code	Section (MCM)*	
Joree	2515	34.1
Lapwing	1590	39.1
Bluejay	1113	43.5
Tern	795	47.5

\* 1 MCM=0.5067 mm<sup>2</sup>**Table 4.36** Sags for ROW width definition

Conductor		Sag (m)
ACSR Code	Section (MCM)*	
Joree	2515	36.5
Lapwing	1590	34.9
Bluejay	1113	34.5
Tern	795	33.6

\* 1 MCM=0.5067 mm<sup>2</sup>**Table 4.37** Right Of Way (I-strings) in (m)

Conductor		±500 kV	±800 kV
ACSR Code	Section (MCM)*		
Joree	2515	62.1	73.2
Lapwing	1590	66.7	78.5
Bluejay	1113	71.3	83.8
Tern	795	74.3	87.2

\* 1 MCM=0.5067 mm<sup>2</sup>

### 4.18.1 Line with I-Strings

The minimum ROW when using I-strings is determined by:

$$ROW = \left[ (R + L + S) \sin \theta + d_{\min} \right] 2 + PS \quad (4.207)$$

Where:

$d_{\min}$  = operating voltage clearance

$R$  = bundle's radius (m)

$L$  = insulators string length

$S$  = conductor sag

$\theta$  = swing angle due to wind (50 year return period)

$PS$  = pole spacing

Table 4.37 shows the ROW width as function of the conductor type.

### 4.18.2 Line with V-Strings

The minimum ROW widths ("V strings") are calculated according to the same equation before but disregarding insulator string length. The results are shown in Table 4.38.

**Table 4.38** Right of Way (V-Strings)

ACSR Conductor CODE	SECTION (MCM)*	±500 kV 750 to 3,000 Km	±800 kV <2,250 km	2,250 km	3,000 km
Joree	2515	53.2	59.6	60.7	61.8
Lapwing	1590	56.3	62.7	63.8	65.0
Bluejay	1113	59.9	66.3	67.4	68.5
Tern	795	61.9	68.4	69.5	70.6

\*1 MCM=0.5067 mm<sup>2</sup>

Note that the results (for I- or V-strings) are partial as Corona effects were not yet considered. Also note that only horizontal design is considered (vertical design will lead to smaller ROW).

## 4.19 Corona effects

### 4.19.1 Conductor Surface Gradient and onset Gradient

#### 4.19.1.1 Conductor Surface Gradient

The parameter that has the most important influence on Corona performance is the conductor surface electric field or conductor surface gradient. Electrostatic principles are used to calculate the electric field on the conductors of a transmission line.

The procedure of calculation may be the same indicated for AC lines. However for DC lines simplified approach can also be used.

When bundled conductors are used, the electric field around the sub-conductors of the bundle is distributed non-uniformly, with maximum and minimum gradients occurring at diametrically opposite points and the average gradient at a point in between. Using the method known as Markt and Mengele's method, the average and maximum bundle gradients of a bipolar HVDC line, with  $n$ -conductor bundles on each pole, are given as (Maruvada 2000).

$$E_a = \frac{V}{n r \ln \left( 2H / \left( r_{eq} \sqrt{\left( \frac{2H}{S} \right)^2 + 1} \right) \right)} \quad (4.208)$$

where:

$V$ =voltage applied (actually  $\pm V$ ) to the conductors of the line, kV

$r$ =conductor radius, cm

$H$ =conductor height, cm

$S$ =pole spacing, cm

$$E_m = E_a \left[ 1 + (n-1) \frac{r}{R} \right] \quad (4.209)$$

Where:

$r$ =sub-conductor radius, cm

$R$ =bundle radius, cm

$r_{eq}$  = equivalent bundle radius, cm

$$R = \frac{a}{2 \sin (\pi / N)} \quad (4.210)$$

$$r_{eq} = R \left[ \frac{n r}{R} \right]^{1/n} \quad (4.211)$$

$a$  = distance between adjacent subconductors, cm

Equations above give reasonably accurate results for the maximum bundle gradient, for  $n \leq 4$  and for normal values of  $H$  and  $S$ .

Consider the line geometry indicated below as Base Case example for calculations in this session.

Voltage	$\pm 500$ kV
Conductor MCM	$3 \times 1590$
Code	Lapwing
Diameter	3.822 cm
Bundle spacing	45 cm
Pole spacing	13.0 m
Minimum conductor-ground clearance	12.5 m

The conductor surface gradient (conductor considered parallel to ground at minimum height).

$$R = \frac{45}{2 \sin (\pi / 3)} = 26 \text{ cm} \quad (4.212)$$

$$r_{eq} = 26 \left[ \frac{31.911}{26} \right]^{1/3} = 15.7 \text{ cm} \quad (4.213)$$

$$E_a = \frac{500}{31.911 \ln \frac{21250}{15.7 \sqrt{\left( \frac{2 * 1250}{1300} \right)^2 + 1}}} \quad (4.214)$$

$$= 20.297 \text{ kV / cm}$$

$$E_m = 20.297 \left[ 1 + (3-1) \frac{1.911}{26} \right] = 23.28 \text{ kV / cm} \quad (4.215)$$

As a general formulation the equations of the electrostatic phenomena described in Section 4.1 can be used. The charge-voltage equation in the matrix form is:

$$[V] = [H][Q] \quad (4.216)$$



where:

$V$  = voltages on the conductors and shield wires [kV]

$Q$  = charges [kV\*F/km]

$H$  = Maxwell's potential coefficients [km/F]

The inverse equation is:

$$[Q] = [C][V] \quad (4.217)$$

Where:

$C$  = the admittance coefficient (F/km).

Once known the charge in a bundle  $Q_b$  the average charge in one sub conductor is  $Q_b/n$  and the average field is

$$E_a = \frac{Q_b / n}{2 \pi \epsilon r_c} \quad (4.218)$$

$r_c$  = sub conductor wire radius

The maximum electric field  $E_m$  is then calculated by the equation above.

When looking for the electric field in the shield wires the procedure used is as follows.

If the shield-wires are grounded at the towers, their voltages are zero and their charges are calculated by:

$$Q_{SW1} = C_{SW1-C1} V_+ + C_{SW1-C2} V_- \quad (4.219)$$

Where  $C_{SW1-C1}$  is the mutual coefficient between shield wire 1 and pole 1 (positive) and  $C_{SW1-C2}$  from shield-wire 1 and pole 2 (negative).

The electric field in the shield wire surface is:

$$E_{SW1} = \frac{Q_{SW1}}{2 \pi \epsilon r} \quad (4.220)$$

where:

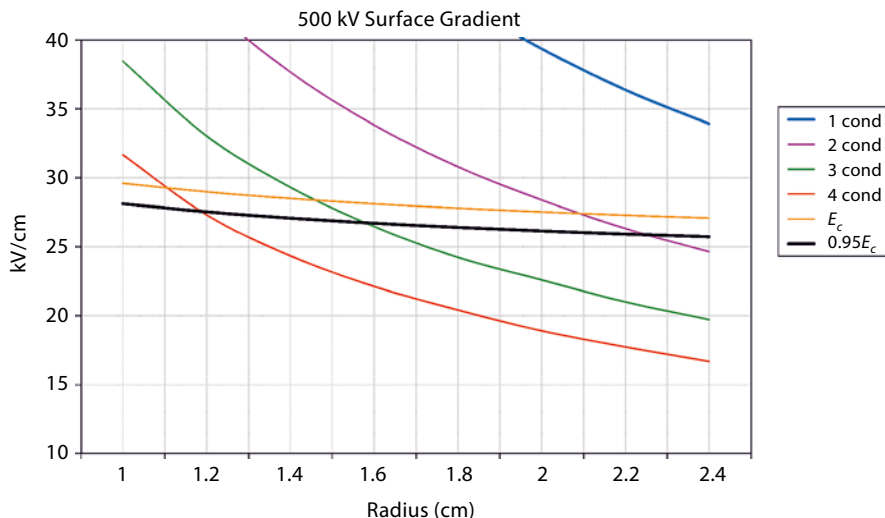
$r$  = shield wire radius

$$\epsilon = \frac{1}{36\pi} 10^{-9} \text{ F / m } \text{ or } \frac{1}{36\pi} 10^{-6} \text{ F / km}$$

In reference (Cigré TB 388 2009) it is found a calculation of shield wire surface gradient  $E_{SW}$  for a  $\pm 800$  kV two twelve pulse converter per pole. In normal operation condition, for both poles at 800 kV,  $E_{SW} = 13.7$  kV considering the shield wires and conductors position as it is in the tower. However,  $E_{SW} = 13.7$  kV, if the calculation is carried with the position as it is in the mid-span. When in one pole the voltage is 800 kV and in the other 400 kV (emergency of one converter)  $E_{SW} = 18.9$  kV and with 800 kV and zero is the other pole  $E_{SW} = 24.1$  kV (conductors and shield wire position as they are in the tower).

#### 4.19.1.2 Corona Onset Gradient

When the electric field at the surface of a transmission line conductor exceeds a certain value, partial electrical breakdown of the surrounding air takes place, giving rise to Corona discharges.



**Figure 4.62** Conductor Surface Gradients for  $\pm 500$  kV.

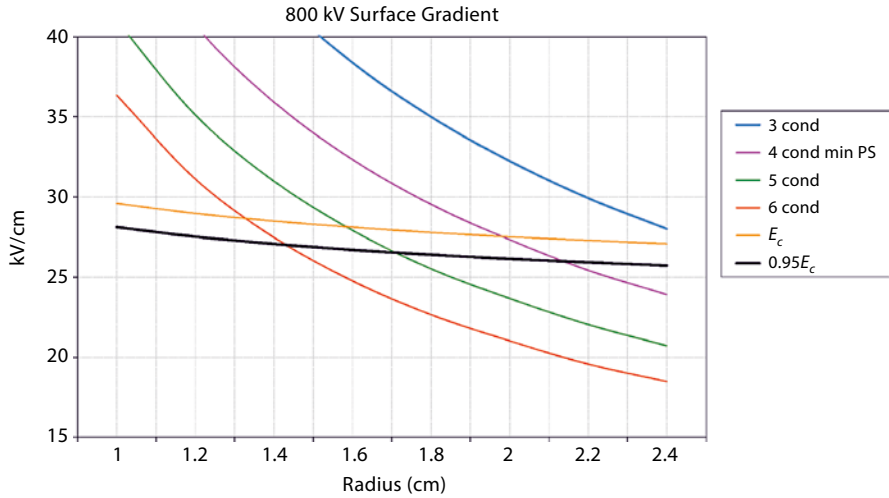
For the Base Case example in this session,  $3 \times 1590$  MCM conductor Lapwing ( $1 \text{ MCM} = 0.5067 \text{ mm}^2$ ) and assuming  $m = 0.82$ ;  $\delta = 0.915$ ;  $r = 1.911 \text{ cm}$ , the critical gradient is:

$$E_c = 30 \cdot 0.82 \cdot 0.915 \cdot \left[ 1 + \frac{0.301}{\sqrt{0.915 \cdot 1.911}} \right] = 27.6 \text{ kV/cm} \quad (4.221)$$

Reference (Cigré TB 388 2009) shows graphs indicating conductor surface gradient (kV/cm) and critical gradient  $E_c$  as function of conductor radius. The figures for 500 and 800 kV are reproduced here (Figures 4.62 and 4.63).

### 4.19.2 Corona Loss

Corona losses on both AC and DC transmission lines occur due to the movement of both positive and negative ions created by Corona. However, there are basic differences between the physical mechanisms involved in AC and DC Corona loss (Maruvada 2000; Cigré TB 1974). On AC lines, the positive and negative ions created by Corona are subject to an oscillatory movement in the alternating electric field present near the conductors and are, therefore, confined to a very narrow region around the conductors. On DC lines, however, ions having the same polarity as the conductor move away from it, while ions of opposite polarity are attracted towards the conductor and are neutralized on contact with it. Thus, the positive conductor in Corona acts as a source of positive ions which fill the entire space between the conductor and ground, and vice-versa, for the negative conductor.



**Figure 4.63** Conductor Surface Gradients for  $\pm 800$  kV.

The case more widely used is the bipolar HVDC transmission line, the positive and negative conductors in Corona emissions having the same polarity as the respective conductor. Unipolar space charges fill the space between each pole and ground while ions of both polarities mix in the bipolar region between the two poles and are subject to some amount of recombination.

Theoretical calculation of Corona losses from HVDC transmission lines requires analysis of the complex electric field and space charge environment in the unipolar and bipolar regions. Such an analysis determines in the first step the electric field and ion current distributions on the surface of the conductors and ground plane and then evaluating Corona losses of the line. Ambient weather conditions have a large influence on Corona losses from the line. The losses are lower under fair weather conditions than under foul weather conditions such as rain, snow etc. However, the ratio of foul weather to fair weather Corona losses on a DC line is much lower than in the case of an AC line.

Because of the complexity of theoretical calculations and the large number of factors influencing Corona on practical HVDC transmission lines, it is often preferable to obtain empirical formulas derived from a large amount of data on long-term Corona loss measurements made on experimental lines with different conductor bundles and under different weather conditions. However, the amount of data available for CL from DC lines is much more limited than in the case of AC lines and, consequently, the accuracy and applicability of empirical formulas may be limited.

For unipolar DC lines, Corona losses may be calculated using an empirical formula derived from measurements made on an experimental line in Sweden (Knudsen et al. 1974), which is given as:

$$P = V_u k_c n r_c 2^{0.25(g-g_0)} 10^{-3} \tag{4.222}$$

where:

$P$  = Corona loss, kW/km

$V_u$  = line voltage, kV

$n$  = number of sub-conductors in the bundle

$r_c$  = sub-conductor radius, cm

$g$  = maximum bundle gradient, kV/cm

$g_0$  = reference value of  $g$ , and  $k_c$  is an empirical constant

The reference value is given as  $g_0 = 22 \delta$  kV/cm, where  $\delta$  is the relative air density. The empirical constant is given as  $k_c = 0.15$  for clean and smooth conductors,  $k_c = 0.35$  for conductors with surface irregularities and  $k_c = 2.5$  for the calculation of all-weather Corona losses.

For bipolar DC transmission lines, some empirical formulas have been developed for Corona losses in different seasons of the year and under different weather conditions. However, the following empirical formulas are recommended since they are derived using available experimental data from a number of different studies (Corbellini et al. 1996), for evaluating fair and foul-weather Corona losses of bipolar HVDC transmission lines:

$$P_{\text{fair}} = P_0 + 50 \log\left(\frac{g}{g_0}\right) + 30 \log\left(\frac{d}{d_0}\right) + 20 \log\left(\frac{n}{n_0}\right) - 10 \log\left(\frac{H S}{H_0 S_0}\right) \quad (4.223)$$

$$P_{\text{foul}} = P_0 + 40 \log\left(\frac{g}{g_0}\right) + 20 \log\left(\frac{d}{d_0}\right) + 15 \log\left(\frac{n}{n_0}\right) - 10 \log\left(\frac{H S}{H_0 S_0}\right) \quad (4.224)$$

Where  $P$  is the bipole Corona loss in dB above 1 W/m,  $d$  is conductor diameter in cm and the line parameters  $g$  (conductor surface gradient),  $n$  (number of conductors),  $H$  (height) and  $S$  (pole spacing) have the same significance as described above. The reference values assumed are  $g_0 = 25$  kV/cm,  $d_0 = 3.05$  cm,  $n_0 = 3$ ,  $H_0 = 15$  m and  $S_0 = 15$  m. The corresponding reference values of  $P_0$  were obtained by regression analysis to minimize the arithmetic average of the differences between the calculated and measured losses. The values obtained are  $P_0 = 2.9$  dB for fair weather and  $P_0 = 11$  dB for foul weather.

$$P(\text{W/m}) = 10^{P(\text{dB})/10} \quad \text{bipole losses in W/m}$$

In the economic evaluation it will be considered 80% of time fair-weather and 20% as foul-weather.

For the Base Case example:

$$\begin{aligned}
 P_{\text{fair}} &= 2.9 + 50 \log\left(\frac{23.28}{25}\right) + 30 \log\left(\frac{3.822}{3.05}\right) \\
 &+ 20 \log\left(\frac{3}{3}\right) - 10 \log\left(\frac{12.513}{15 \cdot 15}\right) = 5.7 \\
 P_{\text{fair}} \text{ (W / m)} &= 10^{5.7/10} = 3.7 \text{ W / m}
 \end{aligned}$$

Similarly:  $P_{\text{foul}} \text{ (W/m)} = 20.6 \text{ W/m}$  and  $P_{\text{tot}} = 0.8 \cdot 3.7 + 0.2 \cdot 20.6 = 7.1 \text{ W/m}$ .

### 4.19.3 Radio Interference and Audible Noise

While Corona losses occur due to the creation and movement of ions by Corona on conductors, radio interference and audible noise are generated by the pulse modes of Corona discharges. The current pulses induced in the conductors and propagating along the line produce RI, while the acoustic pulses generated by these modes of Corona and propagating in ambient air produce AN.

The characteristics of Corona-generated RI and AN on DC transmission lines differ significantly from those on AC lines. Firstly, while all three phases of an AC line contribute to the overall RI and AN of the line, only the positive pole of a DC line contributes to the RI and AN level. Secondly, the RI and AN levels of DC transmission lines under foul weather conditions such as rain etc., which produce rain drops on conductors, are lower than those under fair weather conditions. This is contrary to the case of AC lines on which foul weather conditions produce the highest levels of RI and AN, much higher than in fair weather. These two distinguishing features play important roles in predicting the RI and AN performance of DC transmission lines and in establishing the design criteria necessary for conductor selection.

#### 4.19.3.1 Radio Interference

Both analytical and empirical methods may be used for calculating the RI level of DC transmission lines.

Some empirical methods have been developed for predicting the RI level of DC transmission lines under different weather conditions. Based on data obtained on experimental as well as operating lines, a simple empirical formula (for the bipole-as negative pole contribution can be neglected) has been developed (Cigré TB 1974; Chartier et al. 1983) for predicting the average fair weather RI level for bipolar HVDC transmission lines as:

$$\begin{aligned}
 \text{RI} &= 51.7 + 86 \log \frac{g}{g_0} + 40 \log \frac{d}{d_0} + \\
 &10 \left[ 1 - \log^2 (10 f) \right] + 40 \log \frac{19.9}{D} + \frac{q}{300}
 \end{aligned} \tag{4.225}$$

Where:

$RI$  = radio interference level measured at a distance  $D$  from the positive pole with a CISPR instrument, dB above  $1 \mu\text{V/m}$

$g$  = maximum bundle gradient, kV/cm

$d$  = conductor diameter, cm

$f$  = frequency, MHz

$D$  = radial distance from positive pole, m

The contribution of the negative pole is 4 dB lower. The noise under foul weather is 3 dB lower

The reference values are  $g_0 = 25.6 \text{ kV/cm}$  and  $d_0 = 4.62 \text{ cm}$ .

Adequate statistical information is not presently available to determine the difference in the RI level between the average and maximum fair-weather values or between the fair and foul-weather values.

However, based on the results of some long-term studies (Maruvada 2000), the maximum fair weather RI may be obtained by adding 6 dB and the average foul weather RI may be obtained by subtracting 5 dB from the average fair-weather value.

Design criteria for RI from transmission lines are generally based on signal-to-noise ratios (SNR) for acceptable AM radio reception, similarly as presented for AC line (Section 4.1).

For the Base example the following value is obtained:

$$RI = 51.7 + 86 \log \frac{23.28}{25.6} + 40 \log \frac{3.822}{4.62} + 10 \left[ 1 - \log^2 (10 \cdot 1) \right] + 40 \log \frac{19.9}{30} + \frac{600}{300} = 41.8 \text{ dB}$$

Note that it was assumed:  $f = 1 \text{ MHz}$ ;  $D = 30 \text{ m}$ ;  $q = 600 \text{ m}$ .

#### 4.19.3.2 Audible Noise

As in the case of RI, analytical treatment of AN from transmission lines requires knowledge of a quantity known as generated acoustic power density, which can be obtained only through extensive measurements on an experimental line using a number of conductor bundles and carried out in different weather conditions.

Based on measurements made on experimental as well as operating DC lines and the general characteristics of Corona-generated AN, an empirical formula has been developed (Chartier et al. 1981) for the mean fair weather AN, in dBA, from a DC line as:

$$AN = AN_0 + 86 \log(g) + k \log(n) + 40 \log(d) - 11.4 \log(R) + \frac{q}{300} \quad (4.226)$$

where:

$g$  = average maximum bundle gradient, kV/cm

$n$  = number of sub-conductors

$d$  = conductor diameter, cm

$R$  = radial distance from the positive conductor to the point of observation

The empirical constants  $k$  and  $AN_0$  are given as:

$$\begin{aligned} k &= 25.6 && \text{for } n > 2 \\ k &= 0 && \text{for } n = 1, 2 \\ AN_0 &= -100.62 && \text{for } n > 2 \\ AN_0 &= -93.4 && \text{for } n = 1, 2 \end{aligned}$$

The maximum fair-weather AN (probability 10% of not being exceeded) is calculated by adding 5 dBA to the mean fair weather value obtained above, while the mean AN during rain is calculated by subtracting 6 dBA from the mean fair weather AN.

As in the case of RI, there are presently no regulations for AN from HVDC transmission lines. The Environmental Protection Agency (EPA) in the US recommends that the day-night average sound level  $L_{dn}$  (U.S. EPA 1974) be limited to 55 dBA outdoors. The level  $L_{dn}$  is defined as:

$$L_{dn} = 10 \log \left\{ \frac{1}{24} \left[ 15 \cdot 10^{\frac{L_d}{10}} + 9 \cdot 10^{\frac{L_n+10}{10}} \right] \right\} \quad (4.227)$$

where  $L_d$  and  $L_n$  are the day and night time sound levels, respectively. However, since the highest level of AN from DC lines occurs in fair weather, it may be prudent to limit the  $L_{dn}$  (10%) of AN from HVDC transmission lines to 55 dBA, and this corresponds to 50 dBA for  $L_{dn}$ (50%). Reference (Chartier et al. 1981) indicates that the night and the all time distribution are close together by 1.5 dBA. Therefore assuming  $L_d=L_n=42$  to 44 dBA, it results  $L_{dn} \sim 50$  dBA.

As a conclusion, the AN calculated by the equation above (average value) shall be limited to  $\sim 42$  dBA at the edge of the right-of-way.

For the Base Case example the following value is obtained:

$$\begin{aligned} AN &= -100.62 + 86 \log(23.28) + 25.6 \log(3) + \\ &40 \log(3.822) - 11.4 \log(\sqrt{12.5^2 + (30 - 6.5)^2}) + \frac{600}{300} \end{aligned}$$

AN = 38.2 dBA

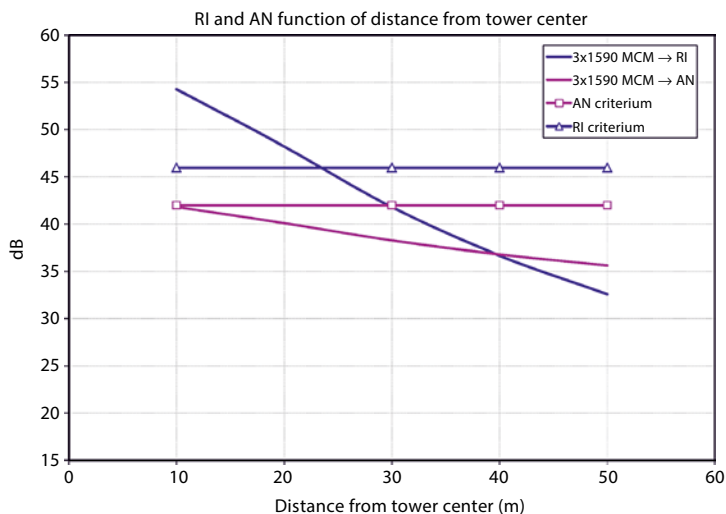
Note that:  $D=30$  m;  $q=600$  m

In the Figure 4.64 the values of AN and RI as function of the lateral distance are shown.

It can be seen that RI will govern the right-of-way width requirements. It should be remembered that the conductor position in the calculations were those in the mid-span. Sometimes the equivalent distance to ground (minimum distance plus 1/3 of the sag) may be used.

#### 4.19.3.3 Final ROW Width

The final right-of-way of a HVDC line is chosen as the largest requirements for insulation coordination and Corona effect.



**Figure 4.64** RI and AN values for the Base Case example and criteria.

Figure 4.65 (from (Cigré TB 388 2009)) illustrates what defines the (1/2 ROW) for  $\pm 500$  kV, 3 conductors per pole. In this case, RI governs for conductors larger than 1400 MCM (insulation requirements are always smaller in this case).

## 4.20 Electric and Magnetic Field

### 4.20.1 Ground-Level Electric Field and Ion Current

#### 4.20.1.1 Introduction

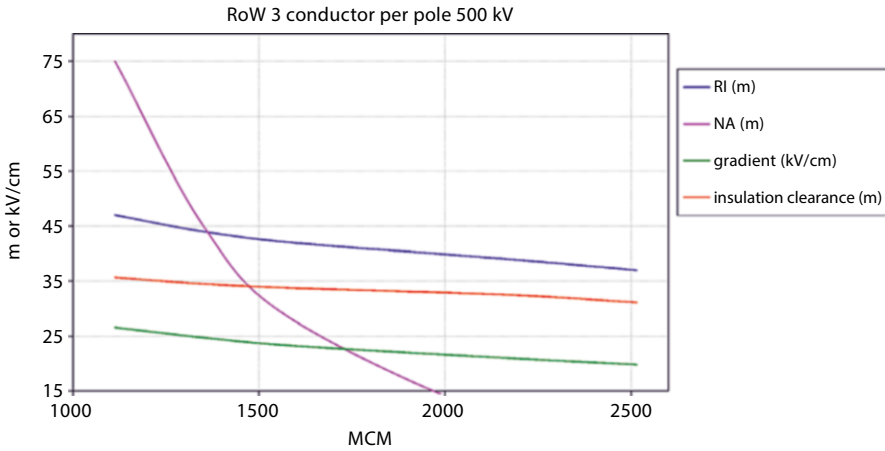
Induction effects under AC transmission lines are defined mainly in terms of the magnitude and frequency of the alternating electric fields at the ground level. In the case of DC transmission lines, however, the magnitudes of both the electric field and the Corona-generated ion currents at ground level are required to characterize any induction effects.

Corona-generated ion space charge fills the entire space between the conductors and the ground plane. In the cases of both unipolar and bipolar DC transmission lines, only positive or negative unipolar space charge exists at ground level. The combined presence of DC electric field and ion space charge is generally known as space charge field (Maruvada 2000).

Both unipolar and bipolar space charge fields are defined in terms of a set of coupled non-linear partial differential equations. Solution of these equations, with appropriate boundary conditions, provides a description of the electric field, space charge density and ion current density at every point and, consequently, at the surface of the ground plane.

Unipolar DC space charge fields are defined by the following equations:





**Figure 4.65** Half ROW requirements and gradient for ±500 kV (bipole having three conductors per pole).

$$\nabla E = \frac{\rho}{\epsilon_0} \tag{4.228}$$

$$\mathbf{J} = \mu \rho \mathbf{E} \tag{4.229}$$

$$\nabla \mathbf{J} = 0 \tag{4.230}$$

where  $\mathbf{E}$  and  $\mathbf{J}$  are the electric field and current density vectors at any point in space,  $\rho$  is the space charge density,  $\mu$  is the ionic mobility and  $\epsilon_0$  is the permittivity of free space. The first is Poisson’s equation, the second defines the relationship between the current density and electric field vectors, and the third is the continuity equation for ions. Solution of these equations, along with appropriate boundary conditions, for the conductor-ground-plane geometry of the HVDC transmission line, determines the ground-level electric field and ion current distributions (Maruvada 2000).

Corona activity on the conductors and the resulting space charge field are influenced, in addition to the line voltage and geometry, by ambient weather conditions such as temperature, pressure, humidity, precipitation and wind velocity as well as by the presence of any aerosols and atmospheric pollution. It is difficult, if not impossible, to take all these factors into account in any analytical treatment of space charge fields. Information on the Corona onset gradients of conductors, which is an essential input in the analytical determination of electric field and ion current environment, is also difficult to obtain under practical operating conditions. For these reasons, it is necessary to use analytical methods in combination with accurate long-term measurements of ground-level electric field and ion current distributions under experimental as well as operating HVDC transmission lines, in order to develop prediction methods.

#### 4.20.1.2 Calculation Methods

- The first method for solving equations above for multiconductor dc transmission line configurations was developed by Maruvada and Janischewskyj (Maruvada 2000). The method, originally developed to calculate Corona loss currents, involves the complete solution of the unipolar space charge modified fields and, consequently, the determination of the ground-level electric field and ion current density distributions. The method of analysis does not include the influence of wind.

The method of analysis is based on the following assumptions:

- The space charge affects only the magnitude and not the direction of the electric field
- For voltages above Corona onset, the magnitude of the electric field at the surface of the conductor in Corona remains constant at the onset value.

The first assumption, often referred to as Deutsch's assumption, implies that the geometric pattern of the electric field distribution is unaffected by the presence of the space charge and that the flux lines are unchanged while the equipotential lines are shifted. Since HVDC transmission lines are generally designed to operate at conductor surface gradients which are only slightly above Corona onset values, Corona on the conductors generates low-density space charge and the ions may be assumed to flow along the flux lines of the space-charge-free electric field. This assumption is much more valid for dc transmission lines than for electrostatic precipitators where Corona intensity and space charge densities are very high.

The second assumption, which was also implied in Townsend's analysis, has been justified from theoretical as well as experimental points of view.

- Gela and Janischewskyj (Janischewsky et al. 1979) developed the first Finite Element Method (FEM) for solving the unipolar space charge modified field problem without recourse to Deutsch's assumption. This method has been used and improved by many authors. However the method is quite complex and difficult to be used for line designers
- A simplified method of analysis was developed at the Bonneville Power Administration (BPA) for determining the ground-level electric field and current density under unipolar and bipolar dc transmission lines. In addition to the two assumptions mentioned, other simplifying assumptions were made to develop the computer program ANYPOLE which was made available in the public domain. One of the simplifying assumptions made in this program was the replacement of bundled conductors by an equivalent single conductor.

The input data and the results of calculation for the Base Case example follows (Figures 4.66 and 4.67).

According to (Chartier et al. 1981) the values obtained using the default values for Corona and Ion information lead to results with 90% probability of not being exceeded.

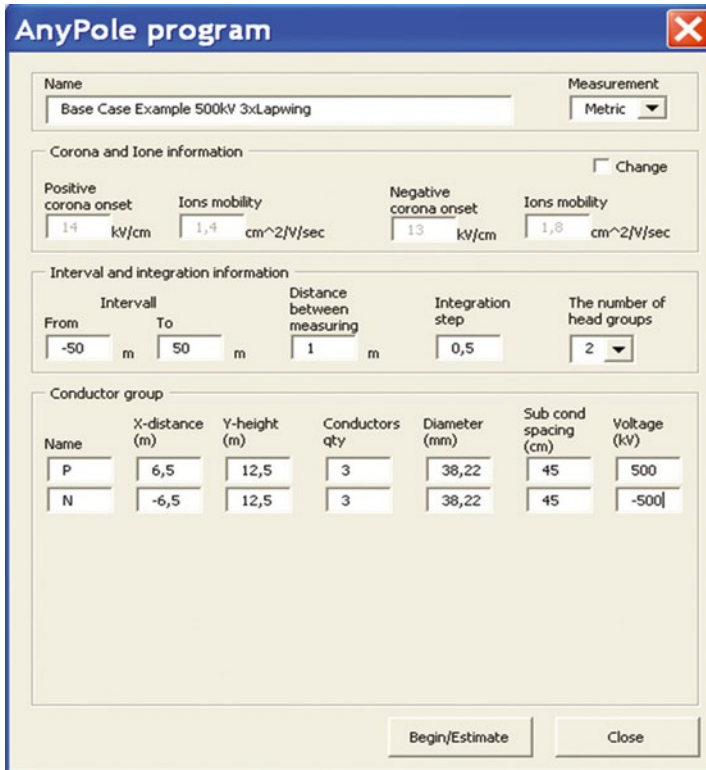


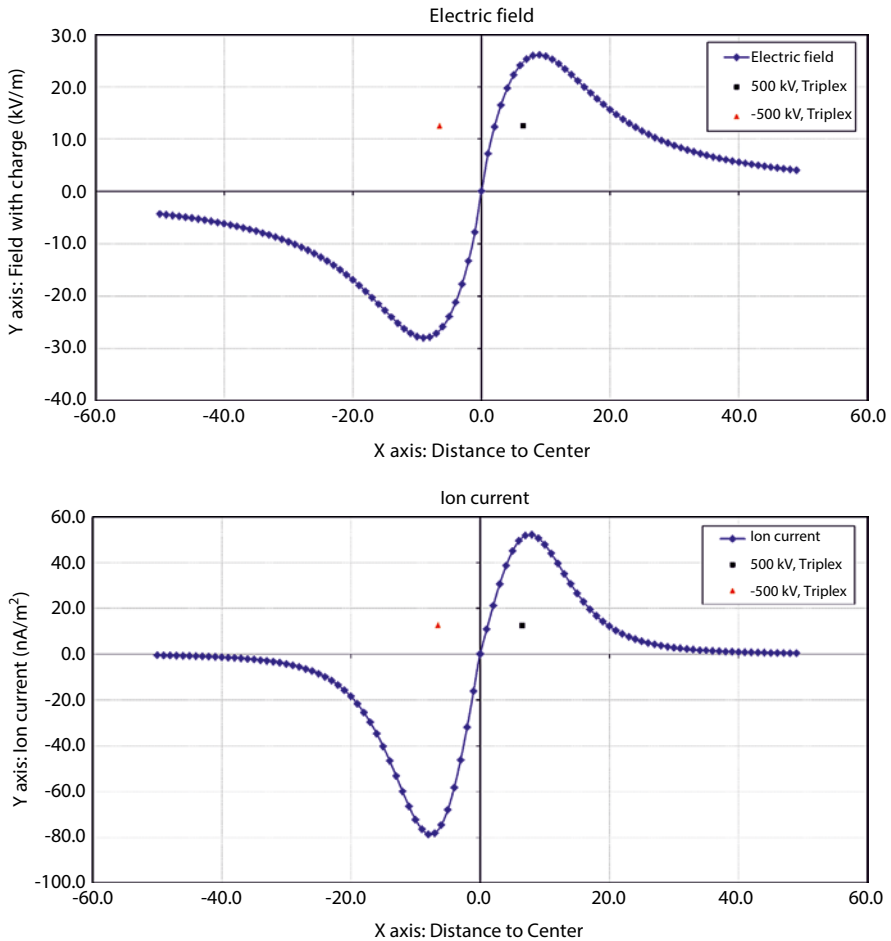
Figure 4.66 Input data Base Case example.

- Empirical methods are generally derived from extensive experimental data obtained preferably on operating HVDC transmission lines, but also on full-scale test lines. In order to derive valid and accurate methods, the experimental data should be obtained for lines of different voltages and configurations with a wide range of values for parameters such as conductor bundle, conductor height and pole spacing in the case of bipolar lines. The validity is usually restricted to the range of values of line parameters for which the experimental data, used to derive the empirical method, was obtained.

A semi-empirical method, called the “degree of Corona saturation” method, was proposed (Johnson et al. 1987) for calculating ground-level electric fields and ion currents under bipolar dc lines. The basic principle of the method is given by the equation,

$$Q = Q_e + S(Q_s - Q_e) \tag{4.231}$$

where  $Q_e$  is the electrostatic value of any parameter (electric field, ion current density or space charge density),  $Q_s$  is the saturated value of the parameter and  $S$  is the degree of saturation. The electrostatic value  $Q_e$  of the parameter can be calculated



**Figure 4.67** Results of calculation for the Base Case example.

using the well-established electrostatic field theory. It should be noted that the electrostatic values of current density and charge density are zero.

Equations were derived for the saturated values of  $Q_s$  of the electric field, ion current density and charge density, based on laboratory tests on reduced-scale models with thin wires of unipolar and bipolar dc line configurations. The degree of Corona saturation factor  $S$  was derived from full-scale tests carried out on a number of bipolar dc line configurations.

The reference (Johnson et al. 1987) presents the equations and parameters to carry on the calculations and are reproduced here

- *Maximum saturated values (positive or negative), within right of way (in the ground, close to conductors, bipolar lines) [4.6].*

$$E = 1.31(1 - e^{-1.7P/H}) V / H \quad (4.232)$$

$$J_+ = 1.65 \times 10^{-15} (1 - e^{-0.7P/H}) V^2 / H^3 \quad (4.233)$$

$$J_- = 2.15 \times 10^{-15} (1 - e^{-0.07P/H}) V^2 / H^3 \quad (4.234)$$

$P$  = pole spacing (m)

$H$  = conductor height (m)

$V$  = Voltage (kV)

$E$  = Electric field (kV/m)

$J$  = Ion flow (A/m<sup>2</sup>)

- Maximum saturated values in the ground, at any distance “ $x$ ” from the tower center provided that  $1 < (x - P/2)/H < 4$

$$E = 1.46 [1 - e^{-2.5 P/H}] \cdot e^{-0.7(x - P/2)/H} V / H \quad (4.235)$$

$$J_+ = 1.54 \cdot 10^{-15} [1 - e^{-1.5 P/H}] \cdot e^{-1.75(x - P/2)/H} V^2 / H^3 \quad (4.236)$$

$$J_- = 2 \cdot 10^{-15} [1 - e^{-1.5 P/H}] \cdot e^{-1.75(x - P/2)/H} V^2 / H^3 \quad (4.237)$$

- Electrical Field without space charge

$$E = \frac{2VH}{\ell n \left( \frac{4H}{D_{eq}} \right) - \frac{1}{2} \ell n \left[ \frac{4H^2 + P^2}{P^2} \right]} \left[ \frac{1}{H^2 + (x - P/2)^2} - \frac{1}{H^2 + (x + P/2)^2} \right] \quad (4.238)$$

- Saturation factor

$$S = 1 - e^{-k(G - G_0)} \quad (4.239)$$

$k$  = empirical coefficient

$G$  = surface gradient (kV/cm)

$G_0$  = empirical coefficient

- Values considering the degree of saturation

**Table 4.39** Parameters Go and k for the weather conditions

		summer fair	spring fair	fall fair	summer humidity fog	summer rain	snow
	Go	9	14.5	12	7.5	6	12
positive 50%	K	0.037	0.041	0.039	0.06	0.058	0.03
	Go	3	11	10	3	6	11
positive 95%	K	0.067	0.086	0.092	0.086	0.087	0.045
	Go	9	14.5	12	8.5	6	12
negative 50%	K	0.015	0.021	0.017	0.045	0.058	0.03
	Go	3	11	11	3	6	11
negative 95%	K	0.032	0.065	0.07	0.063	0.087	0.045

$$Q = Q_e + S(Q_s - Q_e) \quad (4.240)$$

$Q$  = value of a quantity (electrical field, ion flow, etc.)

$Q_s$  = saturated value

$Q_e$  = electrostatic value

$S$  = degree of saturation

Information obtained from field tests (Johnson et al. 1987), parameters for the calculation considering the effect of weather, are shown in Table 4.39.

Moderate weather can be represented by “fall-fair” and extreme by “summer high humidity and fog”.

Below the results (with intermediate calculation values) for the Base Case example are shown (Tables 4.40 and 4.41).

### 4.20.1.3 Design Criteria

Reference (Cigré TB 473 reports the analysis done by Cigré JWG B4/C3/B2.50 related to electric fields near HVDC lines and concluded:

“None of the scientific weight-of-evidence reviews conducted to date concluded that any adverse health effects of exposure are likely but micro-shocks under some conditions under a DC transmission line could be annoying or provoke startle”.

In the absence of any significant induction effects and the lack of evidence linking exposure to dc electric fields and ion currents with any health hazards, perception thresholds for dc electric fields and ion currents are generally used as criteria for the design of dc transmission lines. Figure 4.68 summarizes the results of an investigation conducted to evaluate the perception of electric field.

From the figure it can be seeing that:

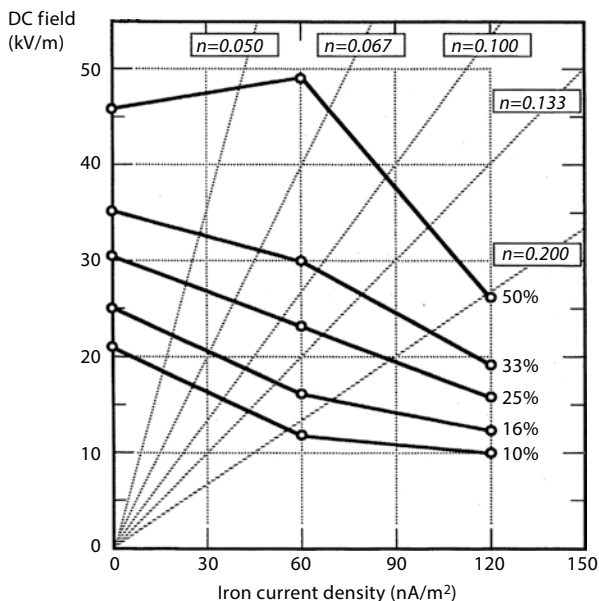
- for 25 kV/m and 100 nA/m<sup>2</sup>, 1/3 of the persons perceived the existence of the field
- for 15 kV/m and 15 nA/m<sup>2</sup>, less than 10% perceived the field

**Table 4.40** Data and intermediate values

	Worst value	at $X=20$ m
Voltage (kV)	+/-500	+/-500
Conductor diam (cm)	3.822	3.822
Number of cond.	3	3
Bundle spacing (cm)	45	45
Pole Spacing $P$ (m)	13	13
Height $H$ (m)	12.5	12.5
$X$ distance center (m)	10	20
$P/H$	1.04	1.04
$H/V$	0.025	0.025
$H/Deq$	39.81	39.81
$E_s$ maximum sat values	43.46	
$J_+$ $10^{-15}$ max sat values	109.21	
$J_-$ $10^{-15}$ max sat values	142.30	
$X - P/2$	3.5	13.5
$X + P/2$	16.5	26.5
$(X - P/2)/H$	0.28	1.08
$E_s$ sat at $X$		25.39
$J_+$ sat at $X$		19.26
$J_-$ sat at $X$		30.55
$G$ without space charge at $X$	10.5	5.2

**Table 4.41** Results:  $E$  (kV/m);  $J$  (nA/m<sup>2</sup>)

	Worst value	at $X=20$ m	Worst value	at $X=20$ m
	Spring	Spring	Summer high humidity/fog	Summer high humidity/fog
S 50% pos	0.302	0.302	0.612	0.612
S 95% pos	0.652	0.652	0.825	0.825
S 50% neg	0.168	0.168	0.486	0.486
S 95% neg	0.550	0.550	0.721	0.721
E 50% pos	20.4	11.3	30.7	17.6
E 95% pos	32.0	18.4	37.7	21.9
E 50% neg	16.0	8.6	26.5	15.0
E 95% neg	28.6	16.3	34.3	19.8
J 50% pos	33.0	5.8	66.8	11.8
J 95% pos	71.2	12.6	90.1	15.9
J 50% neg	24.0	5.1	69.1	14.8
J 95% neg	78.2	16.8	102.6	22.0



**Figure 4.68** DC field intensities and iron current densities detected by various of the more sensitive subjects.

- Therefore a pair  $E$  and  $J$  can be selected as design criteria associated with awe-ather condition, for example:
- in any place inside the ROW: 25 kV/m; 100 nA/m<sup>2</sup>, spring 50% values (average); or 40 kV/m; 90 nA/m<sup>2</sup> summer high humidity/fog
- at the ROW edge 10 to 15 kV/m; 10 to 15 nA/m<sup>2</sup>, summer high humidity/fog 95% values.

#### 4.20.2 Magnetic Field

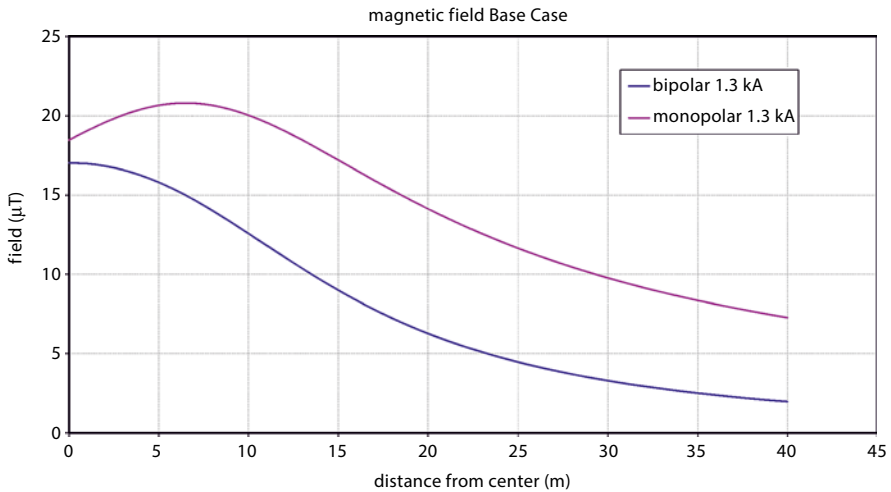
The magnetic field of transmission lines is calculated using two-dimensional analysis assuming conductors parallel over a flat terrain.

The magnetic field  $H_{ji}$  at a point  $(x_i, y_i)$  at a distance  $r_{ij}$  from the AC and DC conductor or shield wires with a current  $I_i$  (real part only) is calculated as if for AC lines.

Figure 4.69 shows the magnetic field for the Base Case example considering 1300 MW and  $\pm 500$  kV.

Note that the currents in the poles are of different polarity, therefore reducing the effect. For monopolar transmission the magnetic fields are higher. The magnetic field is of the order of the earth magnetic field  $\sim 50 \mu\text{T}$ .





**Figure 4.69** Magnetic Field.

## 4.21 Hybrid Corridor or Tower

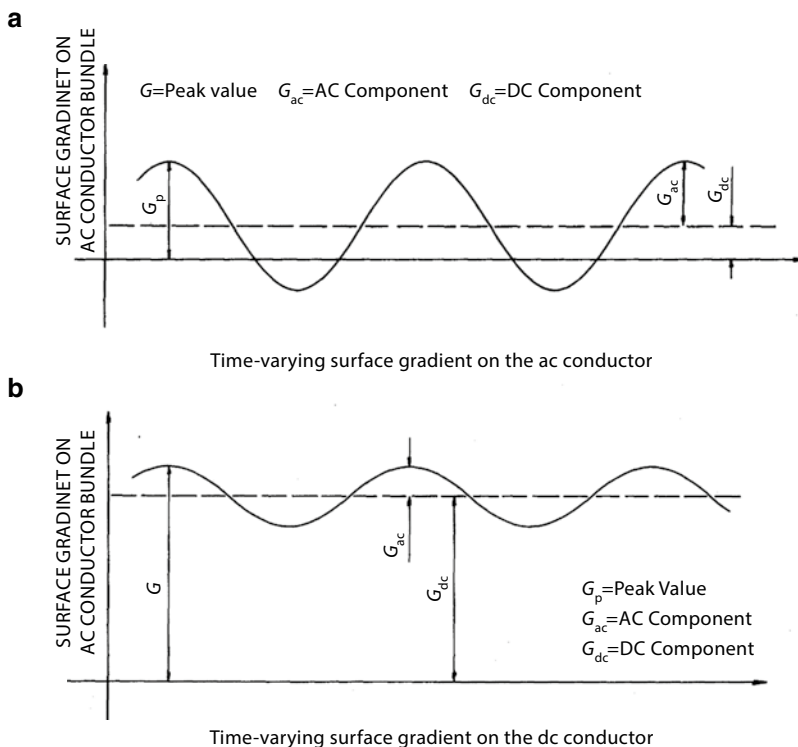
Today important discussion has been carried out related to conversion of AC to DC lines. In these cases there comes the possibility of having AC and DC line close together or in the same tower.

In this case there will be interaction of electric and magnetic field and change in the conductor surface gradient due to induction from one circuit to the other, therefore influencing the Corona phenomena.

It is well accepted practice that Corona and field effects need to be taken into account when designing new AC and DC power lines, when up-rating the voltage of an existing AC line, or when converting existing AC lines to DC operation. The aim of this item is therefore to give a sufficiently detailed description of the characteristics and prediction of DC Corona and field effects and how to integrate these into converted line designs. The various technical descriptions have also attempted to emphasize those aspects which relate specifically to the conversion of AC lines to DC operation (Cigré WG B2 41).

### 4.21.1 Conductor Surface Gradient

The calculation procedure shall include the concept that the AC conductor surface voltage gradients are biased by the presence of the DC conductors, while the DC conductor surface gradients include a ripple emanating from the presence of the AC conductors, as illustrated in Figure 4.70. The calculation procedure proposed covers only electrostatic effects; any influence of space charges on the electric fields on the surface of the AC conductors is tentatively disregarded.



**Figure 4.70** Conductor surface voltage gradients in hybrid configurations.

As discussed later, the Corona performance of a hybrid configuration can then be established by applying conventional calculation methods in the following way:

- Calculate the peak values of the combined AC and DC electric field distribution on the surfaces of the AC and DC conductors.
- The Corona performance of the AC conductors may be calculated as for conventional AC lines after dividing the peak values of the calculated conductor surface gradients by  $\sqrt{2}$ .
- The Corona performance of the DC conductors may be calculated using conventional DC empirical methods by applying the peak values of the conductor surface gradient.

#### 4.21.2 Radio Interference

The calculation of RI from hybrid configurations presents some peculiarities.

- RI levels from DC lines are higher in fair-weather than in rain, and therefore primarily considered as a fair-weather phenomenon. On the other hand, RI levels from AC

lines are considered as both a fair weather and a foul weather phenomenon. For hybrid configurations, it is therefore necessary to study both weather conditions.

- RI from AC conductors occurs around the peak of the positive half-cycle of the power frequency voltage, whereas RI from DC conductors for an equivalent gradient occurs all the time, primarily from the positive conductor.
- The nuisance value appears to be higher for AC than for DC.

The empirical formulas presented can be used to calculate the RI level of a hybrid configuration at any particular distance from each AC phase and DC pole conductor by applying the appropriate surface voltage gradients. With this information, the total RI level is determined by adequately adding those levels for the different weather conditions (Cigré WG B2 41).

Remind that:

For AC contribution: Foul weather RI=heavy rain-7 dB and fair=heavy rain -24 dB

For DC: fair negative weather RI=fair positive- 4 dB and foul =fair-3 dB.

### 4.21.3 Audible Noise

As with RI, the calculation of AN from hybrid configurations presents some peculiarities:

- AN levels from DC lines are higher in fair-weather than in rain, and therefore primarily considered as a fair-weather phenomenon. In contrast, AN levels from AC lines are much higher in rain and therefore considered as a foul weather phenomenon. For hybrid configurations, it is therefore necessary to study both weather conditions.
- AN from AC conductors occurs around the peak of the positive half cycle of the power frequency voltage, whereas RI from DC conductors for an equivalent gradient occurs all the time, and practically only from the positive conductor.

The empirical formulas presented can be used to calculate the AN level of a hybrid configuration at any particular distance from each AC phase and DC pole conductor by applying the appropriate surface voltage gradients. With this information, the total AN level is determined by adequately adding those levels for the different weather conditions.

Remind that:

For AC contribution: Fair weather AN=foul- 25 dB

For DC: foul weather AN positive=fair positive- 6 dB and foul negative=zero.

### 4.21.4 Corona Losses

Formulas for calculating Corona losses on AC lines and isolated DC lines are presented previously. However, due to the lack of full-scale test results there is no information available how to apply these formulas to hybrid configurations (one may use the concept of equivalent surface gradient as input in the presented equations for AC and DC lines.

### 4.21.5 Electric and Magnetic Fields

The AC electric field at ground is calculated by the conventional method described, with the DC conductors at zero potential. The result is an increase as compared with DC line only (Cigré WG B2).

The DC electric field and ion current density at ground level may be estimated in the same way as for isolated DC lines, with the AC conductors at zero potential.

The magnetic fields are calculated by the conventional method described. The AC and DC magnetic fields can be treated separately since the effects on humans are different (there are no induction effects from DC magnetic fields).

---

## References to 4.1–4.12

- Abramowitz, M., Stegun, I.A.: Handbook of Mathematical Functions. Dover Publication
- Aileman, A.R.: Insulation coordination for power systems. Marcel Dekker, New York (1999). 767 p
- Aluminum Association Handbook
- Anderson, R.B., Eriksson, A.J.: Lightning parameters for engineering application. *Electra* **69**, 65–102 (1980)
- Anderson, R.B., Eriksson, A.J., Kroninger, H., Meal, D.V., Smith, M.A.: Lightning and thunderstorm parameters. In: *Lightning and Power Systems*. London: IEE Conf. Publ. No. 236, 5 p (1984)
- Baba, Y., Rakov, V.A.: On the use of lumped sources in lightning return stroke models. *J. Geophys. Res.* **110**, D03101. doi:10.1029/2004JD005202
- Brown, G.W., Whitehead, E.R.: Field and analytical studies of transmission line shielding II. *IEEE PAS* **88**, 617–626 (1969)
- Chartier, V.L.: Empirical expressions for calculating high voltage transmission line Corona phenomena. First Annual Seminar Technical Program for Professionals Engineers, BPA (1983)
- Chartier, V.L., Stearns, R.D.: Formulas for predicting audible noise from overhead high voltage AC and DC lines. *IEEE Trans.* **PAS-100**(1), 121–130 (1981)
- Chartier, V.L., Sarkinen, S.H., Stearns, R.D., Burns, A.L.: Investigation of corona and field effects of AC/DC hybrid transmission lines. *IEEE PAS-100(1), 72–80 (1981)*
- Cigré TB 20: Interferences produced by corona effect of electric systems (1974)
- Cigré TB 20: Interferences produced by corona effect of electric systems; description of phenomena, practical guide for calculation (1974)
- Cigré TB 21: Electric and magnetic fields produced by transmission systems (1980)
- Cigré TB 48: Tower Top Geometry. WG 22-06 (1995)
- Cigré TB 61: Addendum to interferences produced by corona effect of electric systems (1996)
- Cigré TB 74: Electric power transmission and the environment. Field, noise and interference
- Cigré TB 299: Guide for weather parameters for bare conductors to use for the deterministic rating calculation
- Cigré TB 388: Impacts of HVDC lines in the economics of HVDC projects (2009)
- Cigré TB 440: Use of surge arresters for lightning protection of transmission lines
- Cigré TB 473: Electric field and ion current environment of HVDC overhead transmission lines
- Cigré TB 549: Working Group C4.407 – “Lightning Parameters for Engineering Applications” – Cigré TB 549, Aug (2013)
- Cigré TB No. 61: Addendum to Cigré Document No. 20 (1974). Chapter 7 (1996)
- Cigré WG 33-04, TB 63: Guide to Procedures for Estimating the Lightning Performance of Transmission Lines. Paris (1991)
- Cigré WG B2-41: Guide to the conversion of existing AC lines to DC operation
- Corbellini, U., Pelacchi, P.: Corona losses on HVDC bipolar lines. *IEEE Trans.* **PWRD-11**(3), 1475–1480 (1996)

- Dawalibi, F., Barbeito, N.: Measurements and computations of the performance of grounding systems buried in multilayer soils. *IEEE Trans. Power Deliv.* **6**(4), 1483–1490 (1991)
- Dommel, H.W.: Electromagnetic Transient Program – Reference Manual (EMTP Theory Book prepared for BPA) (1986)
- Douglass, D.: Alternating Current (AC) resistance of helically stranded conductors. Cigré TB 345 2008 SC B2 Overhead lines WG B2 12
- EPRI EL 3892: HVDC Converter Stations for voltages above 600 kV. Project 2115-4 (1985)
- EPRI Transmission line reference book 345 kV and above 2nd edition
- EPRI: Transmission line reference book HVDC to 600 kV. EPRI report (1977)
- Fernandes, J.H.M., et al.: Eletronorte and the challenge of long-distance transmission in Brazil. Cigré (2008)
- Fink, D.G., Beaty, H.W.: Standard Handbook for Electrical Engineering. McGraw-Hill, fourteen Ed., (SHEE)
- Happoldt, H., Oeding, D.: Elektrische Kraftwerke und Netze (Electrical Power Plants and Systems). Springer (1978)
- Heppel, R.J.: Computation of potential at surface above an energized grid or other electrode, allowing for non uniform current distribution. *IEEE PAS* **PAS-98** (1979)
- HVDC Reference Book, TR-102764 (EPRI DC) (1993)
- ICNIRP: Guidelines for limiting exposure to time varying electric, magnetic, and electromagnetic fields (1997)
- IEC 61815: Guide for the selection of insulators in respect to polluted conditions. (1986)
- IEC 62305: Protection against lightning – part 1: general principles
- IEC 71-2: Insulation coordination part 2: application guide (1996)
- IEEE Standard 1410: IEEE guide for improving the lightning performance of electric power overhead distribution lines (2010)
- IEEE Std 80: IEEE guide for safety in AC substation grounding (2000)
- IEEE Std 142: IEEE recommended practice for grounding of industrial and commercial power systems (1991)
- IEEE Std 1243: IEEE guide for improving the lightning performance of transmission lines (1997)
- Janischewsky, W., Grela, G.: Finite element solution for electric fields of coronating DC transmission lines. *IEEE PAS-98*(3) (1979)
- Johnson, G.B.: Degree of corona saturation for HVDC transmission lines. *IEEE PWRD-2*(2) (1987)
- Kiessling, F., et al.: Overhead Power Lines. Springer (2003)
- Knudsen, N., Ilceto, F.: Contribution to the electrical design of HVDC overhead lines. *IEEE Trans. PAS-93*(1), 233–239 (1974)
- MacGorman, D.R., Maier, M.W., Rust, W.D.: Lightning strike density for the contiguous United States from thunderstorm duration records, NUREG/CR-3759, Office of Nuclear Regulatory Research, U.S. Nuclear Regulatory Commission, Washington, DC, 44 p (1984)
- Maruvada, P.S.: Corona Performance of High-Voltage Transmission Lines. Research Studies Press, Baldock (2000)
- Mousa, A.M.: The soil ionization gradient associated with discharge of high current into concentrated electrodes. *IEEE PWRD* **9**(3), 1669–1677 (1994)
- Nolasco J.F., et al.: Assessment and Improvement of availability of overhead lines and components. Cigré B2 Session -n°-22-107 (2002)
- Nucci, C.A.: Survey on Cigré and IEEE procedure for the estimation of the lightning performance of overhead transmission and distribution lines. Asia-Pacific International Symposium on EMC (2010)
- Popolansky, F.: Frequency distribution of amplitudes of lightning currents. *Electra* **22**, 139–147 (1972)
- Sekioka, S., Sonoda, T., Ametani, A.: Experimental study of current-dependent grounding resistance of rod electrode. *IEEE Trans. Power Del.* **20**, 1569–1576 (2005)
- Stephen R.: The thermal behaviour of overhead conductors. Sections 1 and 2. Cigré SC:22 Overhead lines. *Electra*. No: 144 pp. 107–125 (1992)

- Stephen, R.: Probabilistic determination of conductor current rating – *Cigré Electra* **164**, 103–119 (1996)
- Stevenson, W.D.: *Elements of Power System Analysis* (1962)
- Szechtman, M., Wess, T., Thio, C.V.: First benchmark model for HVDC control studies. *Electra*, No. 135 (1991)
- TB 207: Thermal behavior of overhead conductors (2002)
- Tompson, E.M.: The dependance of lightning return stroke characteristics on latitude. *J. Geograph. Res.* **85** (1980)
- U.S. EPA., 550/9-74-004: Information on levels of environmental noise requisite to protect public health and welfare with an adequate margin of safety (1974)
- Visacro, S., Alípio, R.: Frequency dependence of soil parameters: experimental results, predicting formula and influence on the lightning response of grounding electrodes. *IEEE PWRD* **27**(2), 927–935 (2012)
- Visacro, R.: A comprehensive approach to the grounding response to lightning currents. *IEEE PWRD* **2**(2) (2007)
- Visacro, S., Alípio, R., Murta, M.H., Pereira, C.: The response of grounding electrodes to lightning currents: the effect of frequency-dependent soil resistivity and permittivity. *IEEE EMC* **52**(2), 401–406 (2011)
- Wagner, C.F.: The relation between stroke current and the velocity of the return stroke. *IEEE Trans. Power Syst.* **82**, 609–617 (1963)
- Young, F.S., Clayton, J.M., Hileman, A.R.: Shielding of transmission lines. *IEEE Trans.* **PAS 82**, 132–154 (1963)

---

## References to 4.13–4.21

- Abramowitz, M., Stegun, I.A.: *Handbook of Mathematical Functions*. Dover Publication
- Chartier, V.L., Stearns, R.D.: Formulas for Predicting Audible Noise from Overhead High Voltage AC and DC Lines. *IEEE Trans. PAS-100*(1), 121–130 (1981)
- Chartier, V.L.: Empirical Expressions for Calculating High Voltage Transmission Line Corona Phenomena. First Annual Seminar Technical Program for Professional Engineers, Bonneville Power Administration (BPA) (1983)
- Cigré TB 473: Electric Field and Ion Current Environment of HVDC Overhead Transmission Lines
- Cigré TB 20: Interferences Produced by Corona Effect of Electric Systems; Description of Phenomena, Practical Guide for Calculation (1974)
- Cigré TB 48: Tower Top Geometry. WG 22-06 (1995)
- Cigré TB No. 61: Addendum to Cigré Document No. 20 (1974). Chapter 7 (1996)
- Cigré TB 388: Impacts of HVDC lines in the economics of HVDC projects. (2009)
- Cigré WG B2-41: Guide to the conversion of existing AC lines to DC operation
- Corbellini, U., Pelacchi, P.: Corona Losses on HVDC Bipolar Lines. *IEEE Trans. PWRD-11*(3), 1475–1480 (1996)
- EPRI EL 3892: HVDC Converter Stations for voltages above 600 kV. Project 2115-4 (1985)
- EPRI: Transmission Line Reference Book HVDC to 600 kV. EPRI Report (1977)
- Fink, D.G., Beaty, H.W.: *Standard Handbook for Electrical Engineering*. McGraw-Hill, fourteen Ed., (SHEE)
- HVDC Reference Book, TR-102764 (EPRI DC) (1993)
- IEC 61815: Guide for the selection of insulators in respect to polluted conditions. (1986)
- Janischewsky, W., Grela, G.: Finite Element Solution for Electric Fields of Coronating DC Transmission Lines. *IEEE PAS-98*(3) (1979)

- Johnson, G.B.: Degree of Corona Saturation for HVDC Transmission Lines. IEEE PWRD-2(2) (1987)
- Knudsen, N., Iliceto, F.: Contribution to the Electrical Design of HVDC Overhead Lines. IEEE Trans. PAS-93(1), 233–239 (1974)
- Maruvada, P.S.: Corona Performance of High-Voltage Transmission Lines. Research Studies Press Ltd., Baldock (2000)
- Szechtman, M., Wess, T., Thio, C.V.: First Benchmark Model for HVDC Control Studies. Electra (135) (1991)
- TB 207: Thermal Behavior of Overhead Conductors (2002)
- U.S. EPA., 550/9-74-004: Information on Levels of Environmental Noise Requisite to Protect Public Health and Welfare with an Adequate Margin of Safety (1974)



**Joao F. Nolasco** graduated in Electric & Electronic Engineering and M.S. in Transmission Systems, as well as in Statistics in State University of Minas Gerais (UFMG), Brazil. Engineer in Siemens Brazil (Jan to June 1967) and then in Siemens Germany (1967-1969). Professor in the UFMG University (1968-1970), then started his career at the Electric Utility Cemig, where has been in sequence Planning Engineer, Design Engineer, Head of Electric Studies of T. Lines and finally Head of Transmission Line Department. From 1994 until today, he has acted as Consultant in both AC and DC Transmission Systems and Planning, providing services to several Utilities and private Transmission Companies in Brazil, Argentine, Chile, Peru, Bolivia, Suriname, Mexico, USA, South Africa etc. In Cigré he has been Member of SC B2 (Overhead Lines) - 1984 to 1998 -

and then Convener of some WG's and TF's covering AC & DC lines (1998-2014). Author of more than 100 papers, several technical reports and two Technical Brochures. One of the authors of the Book "Overhead Power Lines" (Springer Verlag, Germany - 1993). He wrote and provided courses on Transmission and Distribution Lines at the University of Cape Town in 1989 and in other countries afterwards.



**José Antonio Jardini** has received his B.Sc. degree from the Polytechnic School at the University of Sao Paulo (USP) in 1963. Subsequently, he obtained his M.Sc. and Ph.D. degrees in 1970 and 1973, all from the same institution. From 1964 to 1991 he worked at Themag Eng. Ltd (Engineering Company) in the area of Power Systems, Automation and Transmission Lines projects. Currently, he is Full Professor in the Department of Engineering of Energy and Electric Automation at University of São Paulo. He is a member of CIGRE and was the Brazilian representative in the SC38 of CIGRE and member of WG B4 (HVDC & FACTS power electronics). At IEEE he is Fellow Member and Distinguished Lecturer of PES/IEEE and was also for IAS/IEEE. He is one of the authors of several Cigré

Brochures on HVDC Lines Economics, Convener of JWG Electric of HVDC Transmission Lines, and Converter modelling. He had many volunteer activities at IEEE as: South Brazil section Chairman; region treasurer, IEEE Fellow Committee, nomination boards, Education Society Fellow Committee. Awards: IEEE HVDC Uno Lamm (2014); IEEE MGA Larry K Wilson(2010); IEEE innovation (2004); CIGRE B4 Technical (2011).



**Elilson E. Ribeiro** graduated in Electrical Engineering (1984) and M. S. in Electric Power Systems (1987) in State University of Minas Gerais (UFMG). Engineer of MF Consultoria (1987-1998). Professor in the Pontifical Catholic University of Minas Gerais (PUC Minas; from 1999 until today) and Director of NSA Consultoria. He has acted as Consultant, primarily, in the areas of electromagnetic and thermal modelling in equipment development (air core power reactors), grounding system design (for transmission lines, power substation and industrial installations), analysis of electromagnetic transients in electric power systems, analysis of electromagnetic interference from transmission lines and transmission line design.